antibiotics

MDPI

Review

Lipid-Centric Approaches in Combating Infectious Diseases: Antibacterials, Antifungals and Antivirals with Lipid-Associated Mechanisms of Action

Olga S. Ostroumova * and Svetlana S. Efimova

Laboratory of Membrane and Ion Channel Modeling, Institute of Cytology, Russian Academy of Sciences, Tikhoretsky Ave. 4, St. Petersburg 194064, Russia; efimova@incras.ru
* Correspondence: ostroumova@incras.ru

Abstract: One of the global challenges of the 21st century is the increase in mortality from infectious diseases against the backdrop of the spread of antibiotic-resistant pathogenic microorganisms. In this regard, it is worth targeting antibacterials towards the membranes of pathogens that are quite conservative and not amenable to elimination. This review is an attempt to critically analyze the possibilities of targeting antimicrobial agents towards enzymes involved in pathogen lipid biosynthesis or towards bacterial, fungal, and viral lipid membranes, to increase the permeability via pore formation and to modulate the membranes' properties in a manner that makes them incompatible with the pathogen's life cycle. This review discusses the advantages and disadvantages of each approach in the search for highly effective but nontoxic antimicrobial agents. Examples of compounds with a proven molecular mechanism of action are presented, and the types of the most promising pharmacophores for further research and the improvement of the characteristics of antibiotics are discussed. The strategies that pathogens use for survival in terms of modulating the lipid composition and physical properties of the membrane, achieving a balance between resistance to antibiotics and the ability to facilitate all necessary transport and signaling processes, are also considered.

Keywords: membrane; lipid biosynthesis; antimicrobials; antibiotics; drug resistance; pore formation; ion channels; membrane curvature stress

Citation: Ostroumova, O.S.; Efimova, S.S. Lipid-Centric Approaches in Combating Infectious Diseases: Antibacterials, Antifungals and Antivirals with Lipid-Associated Mechanisms of Action. *Antibiotics* **2023**, *12*, 1716. https://doi.org/10.3390/antibiotics12121716

Academic Editors: Philip W. Wertz, Doris Rušić and Josko Bozic

Received: 31 October 2023
Revised: 5 December 2023
Accepted: 8 December 2023
Published: 11 December 2023

1. Introduction

Here, we provide an overview of antibacterial, antifungal, and antiviral agents that target lipid biosynthesis and modulate the properties of pathogen membranes, including pore formation, the induction of curvature stress, and full disruption. Taking into account the emphasis on the lipid-associated mechanisms of action of potent antimicrobial drugs, to compare various agents that inhibit lipid biosynthesis, the concentrations causing a twofold decrease in the activity of appropriate enzymes are presented. The threshold concentration in the membrane bathing solution is chosen to quantitatively characterize the effectiveness of various pore-forming antibiotics. The modulation of the properties of the host cell plasma membranes, targeting enzymes engaged in the regulation of lipid metabolism and the biosynthesis of pathogens' cell wall components, are not reviewed.

2. Antibacterials with Lipid-Associated Mechanisms of Action

We focus on two modes of targeting antibacterial agents towards pathogen membranes: (i) indirect action via inhibition of the biosynthesis of membrane lipids; (ii) primary interaction with lipids, which results in the disruption of the functioning of bacterial membranes. These fundamentally different possibilities are considered below.

2.1. Inhibitors of Membrane Lipid Biosynthesis in Bacteria

Despite the fact that bacterial cell wall biosynthesis inhibitors, especially β-lactams and glycopeptide antibiotics, inhibiting the synthesis of the peptidoglycan layer, are the most effective and extensively used classes of antibiotics [1,2], they are not covered in this work, which focuses on targeting the lipid membrane. This part of the review concerns the key enzymes in the biosynthesis of membrane lipids in bacteria and their inhibitors. Possible ways to regulate the biosynthesis, transport, and degradation of lipids are not considered.

2.1.1. Biosynthesis of Fatty Acids of Bacterial Membrane Lipids

The search for selective inhibitors of enzymes participating in bacterial pathways for lipid biosynthesis is a good strategy to find novel antibiotics due to the fact that a certain lipid composition of the bacterial membrane is necessary for its proper functioning, and there is a difference in the principal organization of lipid biosynthesis in bacteria and mammals. In particular, the membrane's fatty acid composition is very important for metabolic plasticity and the growth rate of bacteria. Bacterial and mammalian fatty acid synthases (FAS) have various types. Bacterial and plant fatty acid synthases belong to type II (FASII), and each reaction is catalyzed by distinct single-functional small proteins. Type I fatty acid synthases (FASI), present in mammals and yeast, are composed of one polypeptide chain, and each stage of FAS is accomplished by a various functional domain of this multidomain protein. Figure 1 summarizes the information about the key enzymes of FASII in different bacteria. Due to another principal organization of mammalian FASI, the specific inhibitors of key enzymes of bacterial FASII are expected to be good candidates for the development of low-toxicity antibacterials. Molecules that effectively inhibit fatty acid synthesis in bacteria are discussed extensively in the text below. Table 1 provides information on some specific inhibitors of each known enzyme, as well as their inhibitory concentrations. A demonstration of the ability of the compound to inhibit the activity of the appropriate enzyme in in vitro tests can be considered as direct evidence in favor of a lipid synthesis-related mechanism of action and a specific molecular target. For this reason, the table presents only those inhibitors for which such information can be found in the available literature. The minimum inhibitory concentrations against various bacteria are not presented in Table 1 due to the high variability depending on the bacterial strain. Examples of the most common/known inhibitors are also shown in Figure 1 and marked with a black box. Next, we analyze the possibility of pharmacologically influencing this bacterial pathway and discuss more promising chemical scaffolds for further optimization. It should be taken into account that the therapeutic strategy, in addition to analyzing the inhibitory concentrations, must take into account the risks of developing resistance to the antibiotic and the side effects of its application.

Table 1. Major inhibitors of bacterial FASII.

Inhibitor	Structure	Enzyme	Origin	IC_{50}, μM	References
amino-oxazole dibenzylamide	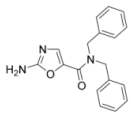	**AccC**	*E. coli*	0.125	[3]
(R)-2-(2-chlorobenzylamino)-1-(2,3-dihydro-1H-inden-1-yl)-1H-imidazo[4,5-b]pyridine-5-carboxamide	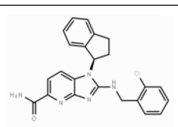	**AccC**	*E. coli*	0.02	[4]
moiramide B	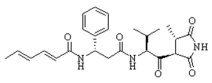	**AccAD**	*S. aureus*	0.096	[5]
			E. coli	0.006	[5]

Table 1. *Cont.*

Inhibitor	Structure	Enzyme	Origin	IC_{50}, μM	References
andrimid	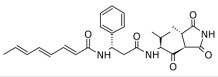	**AccAD**	*S. aureus*	0.091	[5]
			E. coli	0.004	[5]
thiolactomycin	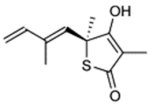	**FabH**	*S. pneumoniae*	7.9 ± 1.1	[6]
			H. influenzae	5.8 ± 1.6	[6]
			M. tuberculosis	24	[7]
			E. coli	32–110	[6,8]
		FabF	*E. coli*	6	[8]
		FabB	*E. coli*	2–25	[8,9]
SB418011	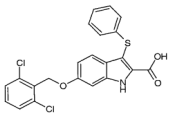	**FabH**	*S. pneumoniae*	0.016 ± 0.003	[6]
			H. influenzae	0.59 ± 0.05	[6]
			E. coli	1.20 ± 0.40	[6]
cerulenin	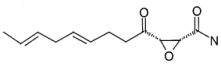	**FabF**	*E. coli*	20	[8]
		FabB	*E. coli*	3	[8]
platensimycin	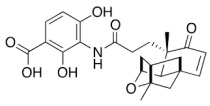	**FabF**	*S. aureus*	0.02–0.29	[10,11]
			E. coli	0.02	[12]
platencin	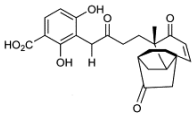	**FabH**	*S. aureus*	9.2–16.2	[10,11]
		FabF	*S. aureus*	0.1–4.6	[10,11]
(-)-epigallocatechin gallate	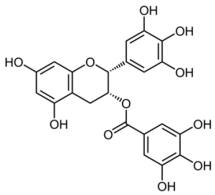	**FabG**	*E. coli*	5	[13]
			P. falciparum	0.3	[14,15]
		FabI	*E. coli*	15	[13]
			P. falciparum	0.2	[14]
		FabZ	*P. falciparum*	0.03–0.4	[14,15]
(-)-gallocatechin gallate	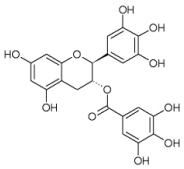	**FabG**	*E. coli*	10	[13]
			P. falciparum	1.1	[14]
		FabI	*E. coli*	5	[13]
			P. falciparum	0.5	[14]
		FabZ	*P. falciparum*	0.6	[14]
(-)-epicatechin gallate	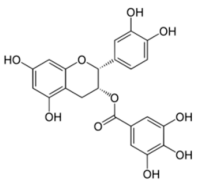	**FabG**	*E. coli*	15	[13]
			P. falciparum	1	[14]
		FabI	*E. coli*	10	[13]
			P. falciparum	0.2	[14]
		FabZ	*P. falciparum*	0.4	[14]
(-)-catechin gallate	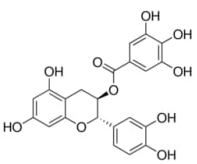	**FabG**	*E. coli*	10	[13]
			P. falciparum	1	[14]
		FabI	*E. coli*	5	[13]
			P. falciparum	0.3	[14]
		FabZ	*P. falciparum*	0.4	[14]

Table 1. *Cont.*

Inhibitor	Structure	Enzyme	Origin	IC_{50}, μM	References
butein	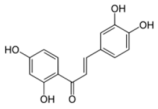	**FabG**	*E. coli*	10	[13]
		FabI	*E. coli*	30	[13]
isoliquiritigenin	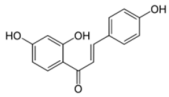	**FabG**	*E. coli*	20	[13]
		FabI	*E. coli*	40	[13]
2,2′,4′-trihydroxychalcone	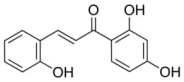	**FabG**	*E. coli*	25	[13]
		FabI	*E. coli*	40	[13]
fisetin	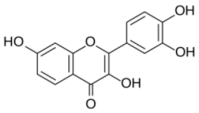	**FabG**	*E. coli*	30	[13]
			P. falciparum	4.1	[14]
		FabI	*E. coli*	50	[13]
			P. falciparum	1	[14]
		FabZ	*P. falciparum*	2	[14]
quercetin	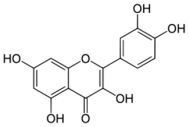	**FabG**	*E. coli*	20	[13]
			P. falciparum	5.4	[14]
		FabI	*E. coli*	20	[13]
			P. falciparum	1.5	[14]
		FabZ	*P. falciparum*	1.5	[14]
resveratrol	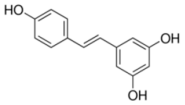	**FabG**	*E. coli*	65	[13]
		FabI	*E. coli*	30	[13]
piceatannol	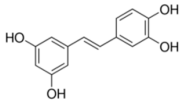	**FabG**	*E. coli*	35	[13]
		FabI	*E. coli*	15	[13]
fustin	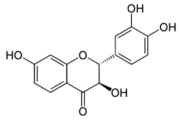	**FabG**	*E. coli*	25	[13]
		FabI	*E. coli*	40	[13]
taxifolin	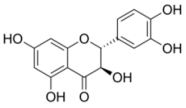	**FabG**	*E. coli*	20	[13]
		FabI	*E. coli*	30	[13]
kaempferol	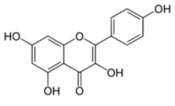	**FabG**	*P. falciparum*	4	[14]
		FabI	*P. falciparum*	20	[14]
luteolin	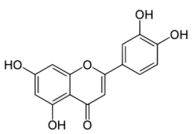	**FabG**	*P. falciparum*	4	[14]
		FabI	*P. falciparum*	2	[14]
		FabZ	*P. falciparum*	5	[14]
luteolin 7-O-β-D-glucopyranoside	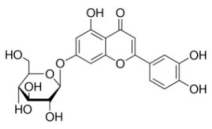	**FabI**	*P. falciparum*	22	[16]

Table 1. *Cont.*

Inhibitor	Structure	Enzyme	Origin	IC_{50}, μM	References
myricetin	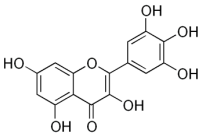	**FabG**	*P. falciparum*	14	[14]
		FabI	*P. falciparum*	0.4	[14]
		FabZ	*P. falciparum*	2	[14]
isorhamnetin	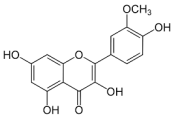	**FabG**	*P. falciparum*	8.3	[14]
		FabI	*P. falciparum*	5	[14]
7,3′,4′-trihydroxyisoflavone	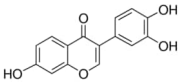	**FabG**	*E. coli*	35	[13]
		FabI	*E. coli*	25	[13]
morin	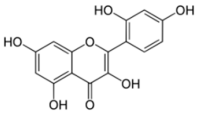	**FabG**	*P. falciparum*	2.3	[14]
		FabI	*P. falciparum*	5	[14]
		FabZ	*P. falciparum*	8	[14]
macrolactin S	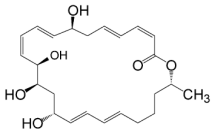	**FabG**	*S. aureus*	130	[17]
macrolactin B	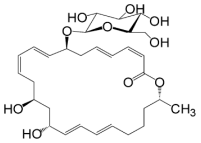	**FabG**	*S. aureus*	100	[17]
NAS-21	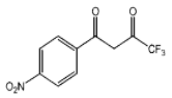	**FabZ**	*M. smegmatis*	360	[18]
NAS-91	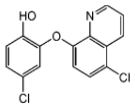	**FabZ**	*M. smegmatis*	498	[18]
emodin	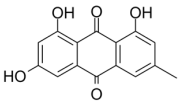	**FabZ**	*F. tularensis*	43.1 ± 9.2	[19]
			Y. pestis	29.7 ± 6.0	[19]
			H. pylori	9.70 ± 1.0	[20]
mangostin	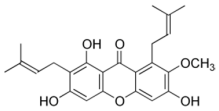	**FabZ**	*F. tularensis*	7.7 ± 2.0	[19]
			Y. pestis	6.1 ± 1.4	[19]
stictic acid	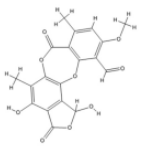	**FabZ**	*F. tularensis*	27.8 ± 6.1	[19]
			Y. pestis	13.0 ± 1.4	[19]
1,4-naphthoquinone	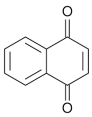	**FabD**	*M. catarrhalis*	23.18 ± 2.48	[21]
		FabZ	*M. catarrhalis*	26.67 ± 3.34	[21]

Table 1. *Cont.*

Inhibitor	Structure	Enzyme	Origin	IC_{50}, μM	References
juglone	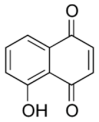	**FabD**	*H. pylori*	20 ± 1	[22]
		FabZ	*F. tularensis*	5.4 ± 1.4	[19]
			Y. pestis	5.3 ± 1.0	[19]
			H. pylori	30 ± 4	[22]
triclosan	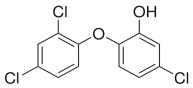	**FabI**	*E. coli*	0.98	[23]
			S. aureus	0.44–0.66	[23–25]
			P. falciparum	0.05–2	[15,26]
			C. trachomatis	0.32 ± 0.08	[27]
AFN-1252	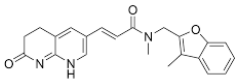	**FabI**	*C. trachomatis*	0.95 ± 0.21	[27]
xanthorrhizol	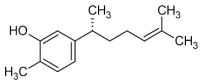	**FabI**	*E. coli*	17.1 ± 1.8	[28]
complestatin	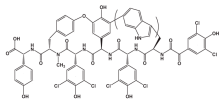	**FabI**	*S. aureus*	0.5	[25]
		FabK	*S. pneumoniae*	10	[25]
neuroprotectin A	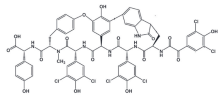	**FabI**	*S. aureus*	0.3	[25]
chloropeptin I	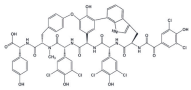	**FabI**	*S. aureus*	0.6	[25]
meleagrin	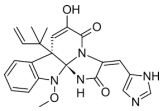	**FabI**	*S. aureus*	40.1	[23]
			E. coli	33.2	[23]
phellinstatin	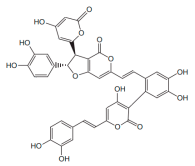	**FabI**	*S. aureus*	6	[29]
chalcomoracin	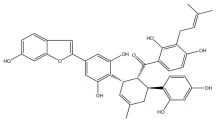	**FabI**	*S. aureus*	5.5	[30]
moracin C	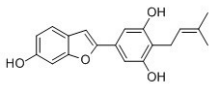	**FabI**	*S. aureus*	83.8	[30]

Table 1. *Cont.*

Inhibitor	Structure	Enzyme	Origin	IC_{50}, μM	References
aquastatin A	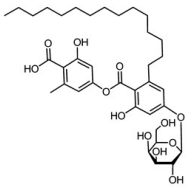	**FabI**	*S. aureus*	3.2	[31]
		FabK	*S. pneumoniae*	9.2	[31]
atromentin	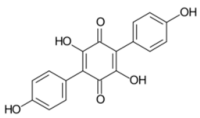	**FabK**	*S. pneumoniae*	0.24	[32]
leucomelone	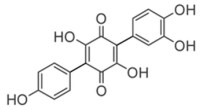	**FabK**	*S. pneumoniae*	1.57	[32]
(Z)-1-oxooctadec-11-enylphosphoramidic acid	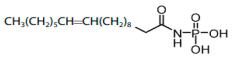	**PlsY**	*S. pneumoniae*	11	[33]
1,1-difluoro-2-oxotridecylphosphonic acid	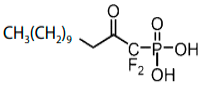	**PlsY**	*B. anthracis*	25	[33]
phenyl (8-phenyloctanoyl) sulfamate	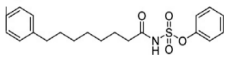	**PlsY**	*S. aureus*	25	[34]
dioctylamine	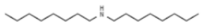	**CfaS**	*H. pylori*	63.81	[35]

IC_{50} is determined as concentration required for 50% inhibition of activity of appropriate enzyme.

The acetyl-CoA carboxylase is represented by a multiprotein complex, containing biotin carboxylase (**AccC**), the biotin carboxyl carrier protein (**AccB**), and biotin carboxyl transferase (**AccAD**), and performing the carboxylation of acetyl-CoA to generate malonyl-CoA (Figure 1) [36]. Via virtual screening and optimization of the small molecule library, antibacterials *aminooxazoles* and *benzimidazoles* were identified as potential **AccC** inhibitors (Table 1) [3,4]. Comparing the IC_{50} values, the optimization of the *benzimidazole* scaffold seems to be a more promising way to find more potent **AccC** inhibitors, but the appropriate toxicity tests should be carried out to estimate the safe therapeutic window. The biotin carboxylation step is also known to be inhibited by *pyrrolocin C* and *equisetin* [37]. The selectivity of *pyrrolocin C* and *equisetin* between bacterial and human cells does not exceed 10 [37], and the mechanisms of their toxic action should be elucidated to increase the therapeutic window for more potent **AccC** inhibitors.

The broad-spectrum antibacterial activity of *pyrrolidinedione* derivatives, particularly *moiramide B* and *andrimid*, is referred to as targeting **AccAD** (Table 1) [5,38–40]. An in silico evaluation of *andrimid* showed no systemic toxicity [41]. However, bacterial resistance to *andrimid* arising from a single amino acid mutation in **AccAD** was found [42]. A promising approach, including the development of dual-use conjugated inhibitors of acetyl-CoA carboxylase composed of covalently linked motifs of *aminooxazole* (interacting with **AccC**) and *moiramide B* (targeting **AccAD**), was proposed to lower the frequency of strain resistance [43]. Preliminary studies on the antibacterial mechanism of *yanglingmycin* exhibited the potent inhibition of **AccAD**, which led to fatty acid and lipid biosynthesis being blocked, and, as a result, cell membrane destruction [44]. Among herbicides, several *haloxyfop* derivatives were found to demonstrate antimycobacterial activity via the inhibition of **AccAD** [45].

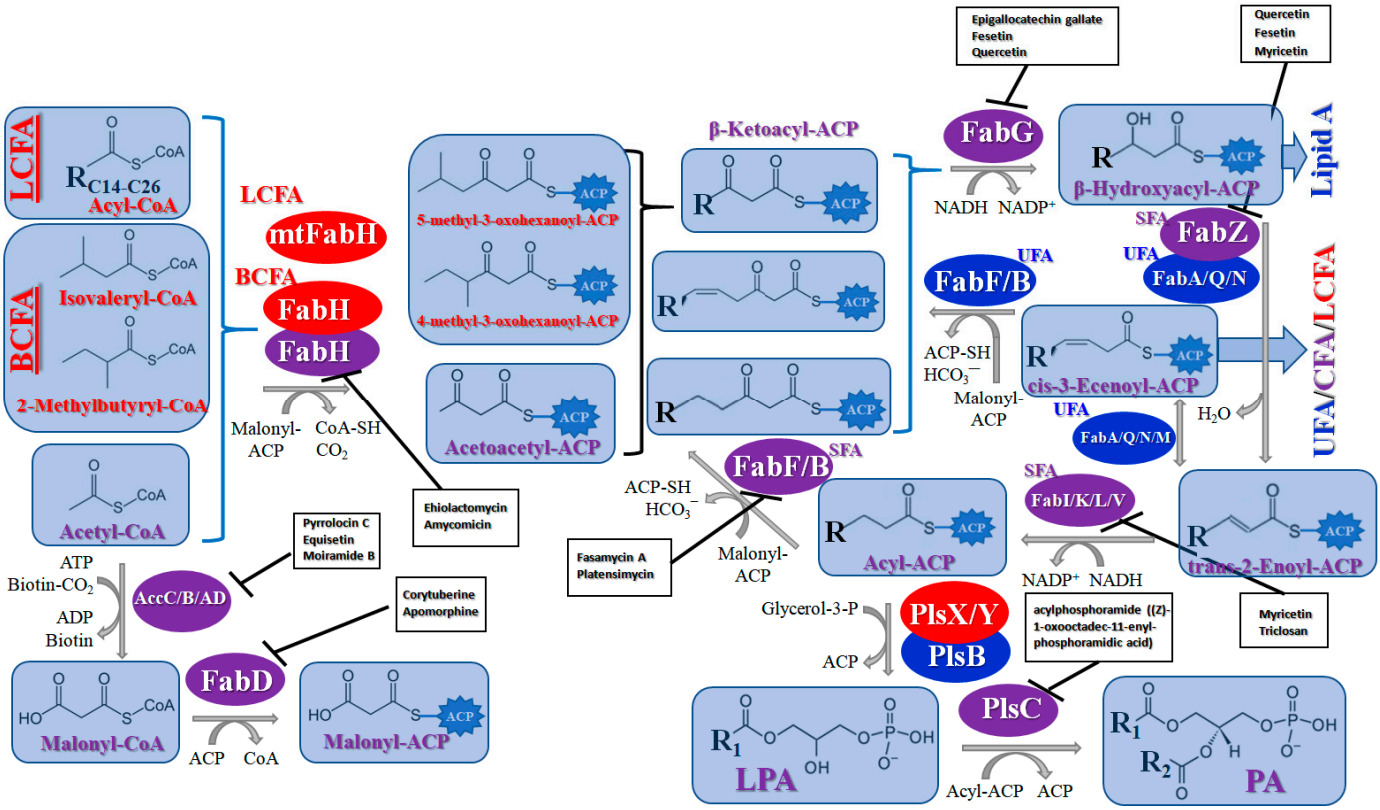

Figure 1. Schematic representation of the synthesis of fatty acids of bacterial membrane lipids. The red, blue, and purple ellipses indicate that the enzyme is produced by Gram-positive, Gram-negative, or both Gram-positive and Gram-negative bacteria, respectively. Some examples of enzyme inhibitors are shown in the black box. Abbreviations: **AccC**—biotin carboxylase; **AccB**—biotin carboxyl carrier protein; **AccAD**—biotin carboxyl transferase; **FabD**—malonyl-CoA:acyl carrier protein (ACP) transacylase; **FabH**, **FabF**, and **FabB**—β-ketoacyl-ACP synthase III (KAS III), II (KAS II), and I (KAS I), respectively; **mtFabH**—FabH homolog of *Mycobacterium tuberculosis*; **FabG**—NADPH-dependent β-ketoacyl-ACP reductase; **FabZ**—β-hydroxyacyl-ACP dehydratase; **FabA**/**FabQ**/**FabN**—bifunctional β-hydroxyacyl-ACP dehydratase/*trans*-2-,*cis*-3-decenoyl-ACP isomerase; **FabM**—*trans*-2-,*cis*-3-decenoyl-ACP isomerase; **FabI**/**FabK**/**FabL**/**FabV**—*trans*-2-enoyl-ACP reductase; **PlsX**—phosphate acyltransferase; **PlsY**—acyl-phosphate:glycerol-3-phosphate acyltransferase; **PlsB**—glycerol-3-phosphate acyltransferase; **PlsC**—1-acyl-sn-glycerol-3-phosphate acyltransferase; BCFA—branched-chain fatty acids; LCFA—long-chain fatty acids; LPA—lysophosphatidic acid; PA—phosphatidic acid; UFA—unsaturated fatty acids; SFA—saturated fatty acids; CFA—cyclopropane fatty acids; R, R′, R_1, and R_2—fatty acid hydrocarbon radicals.

A malonyl-CoA:acyl carrier protein (ACP) transacylase (**FabD**) transfers the malonate group from malonyl-CoA to ACP (Figure 1). It is known that **FabD** is the target for the antibacterial action of *aporphine* alkaloids [46].

The malonyl-ACP, produced by **FabD,** is used by several β-ketoacyl-ACP synthases (KASs) of FASII: KAS I (**FabB**), KAS II (**FabF**), and KAS III (**FabH**). **FabH** initiates the cycle of elongation by condensing malonyl-ACP and acyl-CoA (Figure 1). The origin of the latter strongly depends on the bacteria. The huge variety in the fatty acid profile produced by different bacteria is defined by the substrate specificity of **FabH**. **FabH** of *Escherichia coli* is most specific for acetyl-CoA and propionyl-CoA and incapable of using branched-chain substrates and longer straight-chain acyl-CoA [47,48]. The specificity of *Streptococcus pneumoniae* **FabH** is significantly higher towards short (C_2–C_4) straight-chain than for branched-chain acyl-CoAs [6]. Rather than synthesizing unsaturated fatty acids (UFA) to fluidify the membranes (as Gram-negative bacteria and streptococci do),

a number of Gram-positive bacteria (particularly *Bacillus subtilis* and *Staphylococcus aureus*) synthesize branched-chain fatty acids (BCFA) [2]. *B. subtilis* **FabH** displays higher efficiency with straight-chain and branched-chain acyl-CoA composed of C_4–C_8 compared to acetyl-CoA [48]. The substrate binding pocket of *S. aureus* **FabH** is substantially larger than that of *E. coli* FabH, and the activity of *S. aureus* **FabH** to elongate different acyl-CoAs decreases in the following order: isobutyryl → hexanoyl → butyryl → isovaleryl → acetyl-CoA [49]. The **FabH** homolog of *M. tuberculosis*, **mtFabH**, to synthesize long-chain fatty acids (LCFA) prefers long-chain acyl-CoA substrates composed of C_{10}–C_{16} rather than acetyl-CoA, short-chain, or branched-chain primers, due to the long internal acyl-binding channel [7,50]. Many **FabH** inhibitors have been discovered [51], and the dramatic variance in their activity against **FabH** from various stains clearly indicates the structural differences in the protein active sites. *Thiolactomycin* is known to inhibit BCFA and straight-chain fatty acid biosynthesis by targeting the **FabH** of *Streptomyces collinus* and *Streptomyces glaucescens* [52,53]. *E. coli* and *S. pneumoniae* FabH are weakly inhibited by *thiolactomycin*, while the indole compound *SB418011* significantly inhibits *E. coli*, *S. pneumoniae*, and *Haemophilus influenza* FabH (Table 1) [6]. A number of promising inhibitors of *E.coli* **FabH** have been found, including *thiazolidine*, *chrysin*, *thiazole*, *deoxybenzoin*, *salicylaldehyde*, *pyrazole*, *cinnamate*, *carbamate*, *benzaldehyde*, *o-benzylhydroxylamine*, *vanillic acylhydrazone*, *nitroimidazole*, *pyrazoline*, and *piperidine* derivatives, *furoxan/sulfonylhydrazone* hybrids, and others [54–75]. *S. aureus* **FabH** is weakly suppressed by *thiolactomycin* and is efficiently inhibited by different *1,2-dithiole-3-ones*, *1,3,5-oxadiazin-2-ones*, and *amycomicin* [76–78]. Selected *benzoylaminobenzoic acid* derivatives are also potent against **FabH** of *Enterococcus faecalis* and *Streptococcus pyogenes*, demonstrate only moderate activity against *S. aureus* **FabH**, and are ineffective against *H. influenzae* **FabH** [79–81]. *Alkylsulfonyl* compounds and *pyrrole-2-carboxylic acid* derivatives are specific inhibitors of **mtFabH** [82–84]. Analyzing Table 1, one can conclude that *SB418011* has the lowest IC_{50} against **FabH** among the presented chemicals. It should be also noted that it did not demonstrate inhibitory activity against human FAS at 200-times higher concentrations [6]. Despite promising differences in selectivity, the in vivo efficacy and toxicity of *SB418011* should be evaluated in further experiments.

Two other elongating KASs, **FabB** and **FabF**, operating later in the cycle, use acyl-ACP as the substrate for subsequent condensations, instead of the acetyl-CoA used by **FabH** [85] (Figure 1). The structural similarities between the active sites of **FabB**, **FabF**, and **FabH** [86–89] presume the development of antimicrobials that are able to hit several KASs at the same time, preventing the de novo synthesis of the fatty acids required for bacterial growth and survival. Two fungal products, *thiolactomycin* and *cerulenin*, are non-selective inhibitors of KASs, blocking **FabB**, **FabF**, and **FabH** with varying degrees of success [8,9,90,91]. It is found that *cerulenin* is characterized by its preferential selectivity towards **FabB** and **FabF** and is a very poor inhibitor of **FabH** (Table 1) [6–8,76]. The alteration in the inhibitory activity of *cerulenin* against various KASs is suggested to be a result of differences in the catalytic triads of the β-ketoacyl-ACP synthases and the size of the acyl-chain binding pockets [90]. Natural bacterial diterpenoid products *platensimycin* and *platencin* also target the KASs of FASII [92]. *Platensimycin* preferentially inhibits the chain elongation enzyme **FabF**, whereas *platencin* inhibits both chain initiation and elongation-condensing KASs, **FabH** and **FabF** (Table 1) [10–12,93–96]. According to the IC_{50} information presented in Table 1, *platensimycin* is the most potent inhibitor of **FabF**. Moreover, it has great potential to inhibit methicillin-resistant *Staphylococcus aureus* and vancomycin-resistant *Enterococci* [97]. The low mammalian cell toxicity and the lack of antifungal activity indicate that *platensimycin* acts selectively [12,98]. This makes it extremely promising to search for new *platensimycin*-based antimicrobials in order to improve its pure pharmacokinetic properties. Thus, several semisynthetic analogs of *platensimycin* with enhanced in vivo efficacy towards MRSA infection in a mouse peritonitis model and improved pharmacokinetic properties have been developed [99,100]. In silico docking studies clearly demonstrated that the specific structural motif presented in *fasamycins* is

predicted to be one more naturally occurring pharmacophore for the specific inhibition of **FabF** [101]. A series of *N-substituted benzoxazolinones* were also shown to be active towards elongating KASs, **FabB** and **FabF**, by docking into the *thiolactomycin* binding site [102].

An NADPH-dependent β-ketoacyl-ACP reductase (**FabG**) produces the reduction of β-ketoacyl-ACP to β-hydroxyacyl-ACP. β-hydroxyacyl-ACP dehydrases (**FabZ** or **FabA**) and dehydrates β-hydroxyacyl-ACP to yield *trans*-2-enoyl-ACP. Another NADPH-dependent reductase of the FASII, *trans*-2-enoyl-ACP reductase (**FabI**), reduces *trans*-2-enoyl-ACP to form acyl-ACP, which can reenter the elongation cycle as a substrate for elongating KASs, **FabB** or **FabF**, or can be used for lipid production via phospholipid acyltransferases (**PlsB**/**PlsC** or **PlsX**/**PlsY**/**PlsC** system) [36] (Figure 1).

A broad range of plant polyphenols, including epigallocatechin gallate, gallocatechin gallate, epicatechin gallate, catechin gallate, luteolin-7-O-glucoside, luteolin, quercetin, fisetin, morin, and myricetin, are potent inhibitors of all three crucial FASII enzymes, **FabG**, **FabZ**, and **FabI** (Table 1) [13,14,16]. Hexachlorophene and its anthelmintic bis-(2-hydroxyphenyl)methane/sulfide analogs are believed to exhibit antimalarial activity by inhibiting *Plasmodium falciparum* **FabG** [103]. Trans-cinnamic acid derivatives and macrolactins showed the inhibition of *E. coli* and *S. aureus* **FabG** (Table 1) [17,104]. Ethyl-6-bromo-2-((dimethylamino)methyl)-5-hydroxy-1-phenyl-1H-indole-3-carboxylate was demonstrated to be potent against Acinetobacter *baumannii* **FabG** [105]. A series of small-molecule *Pseudomonas aeruginosa* **FabG** inhibitors were identified [106]. According to Table 1, various catechin gallates demonstrate the most impressive activity (expressed as the lowest levels of IC_{50}) against three key FASII enzymes at once, compared to other inhibitors presented. The triple inhibiting action of these polyphenols, as well as their relatively low toxicity, has kept these naturally occurring compounds as the focus of researchers' attention in terms of finding more safe antibiotics. For example, a safe intake level of green tea polyphenol epigallocatechin gallate, derived from toxicological and human safety data, is about 300 mg per day for adults [107]. We find another approach that involves combining natural polyphenols with other antibiotics that have alternative mechanisms of action on pathogen metabolism to be the most relevant [108–110].

FabZ is a crucial enzyme to elongate both saturated fatty acids (SFA) and UFA, and this is why it is an attractive target for the discovery of new antibacterials. The inhibitors of *P. falciparum* **FabZ**, *NAS-21* (4,4,4-trifluoro-1-(4-nitrophenyl)-butane-1,3-dione), *NAS-91* (4-chloro-2-[(5-chloroquinolin-8-5 yl)oxyl]phenol), and their variants, were identified [111]. *NAS-21* and *NAS-91* analogs also demonstrated activity against mycobacterial **FabZ** (Table 1) [18]. The natural anthraquinone *emodin* (3-methyl-1,6,8-trihydroxyanthraquinone) and several synthetic inhibitors of *Helicobacter pylori* **FabZ**, based on two promising chemical scaffolds, namely (*3,5-dibromo-2,4-dihydroxy-benzylidene)-hydrazide* and *2-chloro-5-{5-[3-(2-methoxy-ethyl)-4-oxo-2-phenylimino-thiazolidin-5-ylidenemethyl]-furan-2-yl}-benzoic acid*, were discovered (Table 1) [20,112]. Two novel inhibitors of *Francisella tularensis* and *Yersinia pestis* **FabZ**, *mangostin* and *stictic acid*, have been found (Table 1) [19]. Moreover, *1,4-naphthoquinone* and *juglone* (5-hydroxyl-1,4-naphthoquinone) is a dual inhibitor of **FabZ** and **FabD** that might be potent against *M. catarrhalis* and *H. pylori* (Table 1) [21,22]. The therapeutic application of *juglone* is limited by its possible toxicity [113], but this pharmacophore might be used to find more safe and potent inhibitors of **FabZ** and **FabD**.

In Gram-negative bacteria, two enzymes, **FabA** and **FabB**, catalyze the production of UFA [114]. **FabA** has a dual function as a β-hydroxyacyl-ACP dehydratase, catalyzing the dehydration of β-hydroxyacyl-ACP to the *trans*-2-enoyl-ACP (as FabZ does), and as a *trans*-2-,*cis*-3-decenoyl-ACP isomerase, producing the transformation of the *trans*-2-decenoyl-ACP to a *cis*-3-decenoyl-ACP (Figure 1). The size of tunnel in the active site of **FabA**, which perfectly fits *trans*-2-decenoyl-ACP, determines the specificity of the isomerization reaction at the 10-carbon stage of the unbranched substrate [115]. **FabB** specifically elongates the *cis*-UFA produced by **FabA**. **FabA** and **FabI** rival *trans*-2-decenoyl-ACP, and this balance determines the UFA/SFA ratio and the fluidity of the bacterial membrane [116]. *S. pneumoniae* and *Streptococcus mutans* have only one β-hydroxyacyl-ACP dehydrase

(**FabZ**), while another enzyme, **FabM**, catalyzes the reaction of double-bond isomerization from *trans*-C_2-C_3 to *cis*-C_3-C_4 [117,118]. In *E. faecalis*, **FabN** performs the role of **FabA**, and **FabF** elongates the *cis*-UFA produced by **FabN** [119]. **FabQ** from *Aerococcus viridans* can act as a monofunctional dehydrase like **FabZ** or as a bifunctional dehydratase/isomerase like **FabA** (Figure 1) [120]. To produce UFA, some bacteria, particularly *B. subtilis* and *Pseudomonas aeruginosa*, contain fatty acid desaturases, introducing a double bond into saturated acyl chains attached to phospholipids or acyl-CoA [114,121]. *S. aureus* does not contain **FabA** (or its analogs) or any desaturases, but can utilize the exogeneous UFA via acyl-ACP synthetase [36].

Furthermore, *3-decynoyl-N-acetyl cysteamine* is a substrate-mimicking inhibitor of **FabA**, which covalently bonds to the active site of the enzyme [115]. *N42FTA* (3-(pyridin-2-yloxy)aniline and *N*-(4-chlorobenzyl)-3-(2-furyl)-1*H*-1,2,4-triazol-5-amine) may be a promising scaffold to design more potent inhibitors of *P. aeruginosa* **FabA** [122,123].

Many compounds targeting **FabI** (including those undergoing clinical trials) are known: the front-line antituberculosis drug *isoniazid*, the common antiseptic *triclosan* (which demonstrates strong antimalarial activity via *P. falciparum* **FabI** inhibition), *diazaborines*, *CG400462*, *CG400549*, *MUT056399*, *AFN-1252*, *AFN-1720*, *xanthorrhizol*, *benzoxaboroles*, and their derivatives (Table 1) [15,24,26–28,124–134]. **FabI** inhibition, in the cases of *triclosan*, *CG400462*, *CG400549*, *MUT056399*, *AFN-1252*, *xanthorrhizol*, and *benzoxaboroles*, was validated by the isolation of resistant clones (*Staphylococci* and *Chlamydia*) containing mutations in the **FabI** gene [28,127,128,131,134,135]. A series of *2,9-disubstituted 1,2,3,4-tetrahydropyrido [3,4-b]indoles*, *1,4-disubstituted imidazoles*, *1-benzyl-1H-benzimidazoles*, and *4-pyridone* derivatives, and *piperazine* and *imidazole coumarin* derivatives, as well as *N-carboxy pyrrolidine* analogs inhibiting *S. aureus* and/or *E. coli* **FabI**, were also reported [136–140]. Some natural macrocyclic compounds (*complestatin*, *neuroprotectin*, and *chloropeptin*), methyl-branched fatty acids (*14-methyl-9(Z)-pentadecenoic* and *15-methyl-9(Z)-hexadecenoic acids*), *meleagrin*, *phellinstatin*, *chalcomoracin*, and *moracin C* demonstrated a promising ability to target *S. aureus* **FabI** (Table 1) [23,25,29,30]. In addition to the *isoniazid*, the *trans*-2-enoyl-ACP reductase from *M. tuberculosis* (**InhA**), which is involved in the biosynthesis of long-chain fatty acids (LCFA) (mycolic acids), was shown to be a target for several *triclosan* and *benzodiazborine* derivatives; more specific inhibitors of **InhA** were also developed [141–150]. According to Table 1, *triclosan*- and *complestatin*-related compounds are characterized by similar low IC_{50} values against *S. aureus* **FabI**. Taking into account that *triclosan*'s application is limited by the possibility of bacterial resistance development via different mechanisms, including mutations in the genes of **FabI** or multidrug efflux pump [151–154] and significant cytotoxic effects [155], the search for natural macrocyclic compounds that are able to inhibit **FabI** seems to be a more promising approach to identify novel antibiotics.

It should be noted that four enoyl-ACP reductase isozymes have been reported in bacteria (Figure 1). *S. pneumoniae, E. faecalis*, and *Clostridia* have **FabK** instead of **FabI**, and **FabV** was discovered in *Vibrio cholerae.* Moreover, some pathogens have more than one enoyl-ACP reductase; for example, **FabI** and **FabK** in *pseudomonads* and *enterococci*, **FabI** and **FabL** in *B. subtilis*, and **FabI**, **FabK**, and **FabV** in *P. aeruginosa* [156–159]. *Triclosan*, inhibiting **FabI**, is a poor inhibitor of **FabL** and has no activity against **FabK** and **FabV** [157]. **FabMG**, isolated from the soil metagenome, was predicted to be a novel *triclosan*-resistant enoyl-ACP reductase, revealing that the main mechanism to develop *triclosan* resistance is a mutation of **FabI** [160]. *Indole naphthyridinones* and *aquastatin A* are inhibitors of both **FabI** and **FabK** [31,161], while *AG205*, *atromentin*, and *leucomelone* are thought to be specific to **FabK** (Table 1) [32,162]. *Carfilzomib* showed high binding affinity with *Klebsiella pneumoniae* **FabI** and **FabV** [163]. Despite the fact that *atromentin* has a low IC_{50} against *S. pneumoniae* **FabK** (Table 1), compounds that are able to inhibit various enoyl-ACP reductase isozymes (in particular, *complestatin*, *aquastatin A*, and *carfilzomib*) are more preferable for the development of broad-spectrum antibacterials.

The length of the hydrocarbon chains of the membrane lipids of bacteria is determined by competition between elongating KASs (**FabF/FabB**) and acyltransferases for acyl-ACP pro-

duced by *trans*-2-enoyl-ACP reductases (**FabI/FabK/FabL/FabV**). The upper limit is defined by the substrate specificity of the elongating KASs, while the lower limit is a result of the specificity of acyltransferases [164–166]. Glycerol-3-phosphate acyltransferases transfer two acyl chains from two acyl-ACPs to the 1 and 2 positions of glycerol-3-phosphate to produce phosphatidic acid (PA), a universal precursor of bacterial phospholipids (Figure 1). Two various acyltransferase systems, **PlsX/PlsY/PlsC** and **PlsB/PlsC**, have been discovered [167,168].

The more widespread bacterial pathway for the formation of PA involves the sequential transfer of acyl from acyl-ACP to acyl-phosphate (acyl-PO_4) via phosphate acyltransferase (**PlsX**) and then to the 1 position of glycerol-3-phosphate to produce lysophosphatidic acid (LPA) through acyl-phosphate:glycerol-3-phosphate acyltransferase (**PlsY**) [164]. Acyl-PO_4 is a single substrate for **PlsY**; it cannot utilize acyl-ACP or acyl-CoA [168]. A series of stabilized acyl-phosphate mimetics, including *acyl-phosphonates*, reverse *amide-phosphonates*, and *acyl-sulfamates*, demonstrated promising activity against *S. pneumoniae*, *Bacillus anthracis*, and *S. aureus* through the inhibition of **PlsY** (Table 1) [33,34]. The lead compound, having a low IC_{50} against *S. pneumoniae* **PlsY**, *(Z)-1-oxooctadec-11-enylphosphoramidic acid*, demonstrated potential toxicity [33]. These data necessitate a further search for ways to expand the therapeutic window of acyl-phosphate mimetics.

A glycerol-3-phosphate acyltransferase (**PlsB**) catalyzes the ligation of the acyl chain to the 1 position of glycerol-3-phosphate to produce LPA. A 1-acyl-sn-glycerol-3-phosphate acyltransferase (**PlsC**) ligates the second acyl chain (in the 2 position) to the LPA produced by **PlsX/PlsY** or **PlsB** to form PA. The advantage of the existence in bacteria of two distinct pathways, the **PlsB/PlsC** and **PlsX/PlsY/PlsC** acyltransferase systems, is the possibility of using exogenous fatty acids, because **PlsB/PlsC** might utilize not only the acyl-ACP produced by *trans*-2-enoyl-ACP reductases (**FabI/FabK/FabL/FabV**) but also the acyl-CoA thioesters derived from exogenous fatty acid metabolism—for example, those produced by **FabD** [168,169]. A fatty acid-rich environment in the host might facilitate the pathogen strain's resistance to FASII inhibitors by enhancing the assimilation of exogenous fatty acids [170,171]. *S. aureus* can become insensitive to the **FabI** inhibitor *triclosan* via mutations in **FabD**, lowering **FabD** activity and inducing the integration of exogenous fatty acids [171,172]. The UFA-to-SFA ratio, membrane fluidity, and cell growth of *Rhodobacter sphaeroides* were reinstated upon both the inhibition of **FabI** with *diazaborine* and the introduction of exogenous UFA [173].

The cyclopropanation of fatty acids is intended to rigidify the bacterial membranes under stress conditions [174–178]. Cyclopropane fatty acids (CFA) are synthesized by cyclopropane fatty acid acyl-phospholipid synthase (**CfaS**) via the addition of a methylene group to the *cis* double bonds of the UFA chains of membrane phospholipids (Figure 1) [179]. *Dioctylamine* inhibits the **CfaS** of *H. pylori* (Table 1), preventing bacterial insensitivity to acid stress, antibiotics, and macrophage killing [35]. *M. tuberculosis* produces a number of cyclopropanated lipids, including mycolic acids, which are essential components to maintain cell wall integrity (Figure 1). This may indicate that agents capable of inhibiting the lipid cyclopropanation enzymes may be an approach to combatting tuberculosis pathogens [180,181].

2.1.2. Biosynthesis of Head Groups of Bacterial Lipids

In addition to the enzymes participating in the synthesis of the fatty acids of bacterial membrane lipids, there are unique enzymes that are involved in the synthesis of the heads of lipid molecules. Figure 2 summarizes the information about the synthesis of the lipid heads.

Cytidine disphosphate-diacylglycerol synthase (**CdsA**) is the critical enzyme catalyzing the production of the key intermediate in phospholipid diversity, CDP-diacylglycerol (CDP-DG), from cytidine triphosphate (CTP) and PA (Figure 2). CDP-DG is a precursor of the major phospholipids, including phosphatidylglycerol (PG), cardiolipin (CL), phosphatidylethanolamine (PE) (produced through the decarboxylation of phosphatidylserine (PS)), and even phosphatidylinositol (PI) and phosphatidylcholine (PC), which is absent in

most prokaryotic cells. The fundamental nature of the CDP-DG-dependent pathway, characteristic of both prokaryotic and eukaryotic phospholipid biosynthesis [182,183], makes the majority of CDP-DG-converting enzymes poor targets for antibiotic therapy.

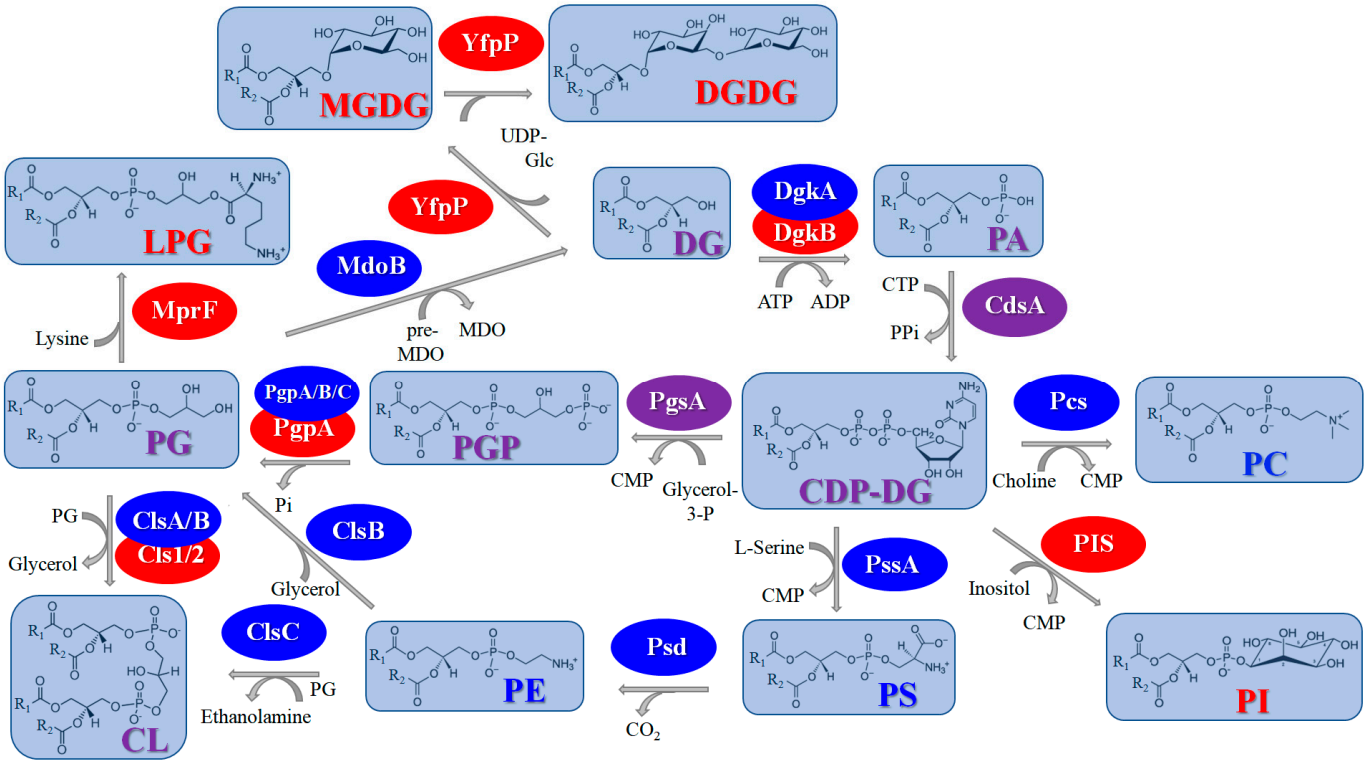

Figure 2. Schematic representation of the synthesis of "heads" of bacterial membrane lipids. The red, blue, and purple ellipses indicate that the enzyme is produced by Gram-positive, Gram-negative, or both Gram-positive and Gram-negative bacteria, respectively. Some examples of enzyme inhibitors are shown in a black box. Abbreviations: **CdsA**—cytidine diphosphate-diacylglycerol synthase; **PgsA**—phosphatidylglycerophosphate synthase; **PgpA**, **PgpB**, and **PgpC**—phosphatidylglycerolphosphate phosphatases; **ClsA**, **ClsB**, **ClsC**, **Cls1**, and **Cls2**—cardiolipin synthases; **PssA**—phosphatidylserine synthase; **Psd**—phosphatidylserine decarboxylase; **Pcs**—phosphatidylcholine synthase; **PIS**—phosphatidylinositol synthase; **MprF**—lysil phosphatidylglycerol synthase and flippase (multiple peptide resistance factor); **MdoB**—phosphoglycerol transferase; **DgkA** and **DgkB**—diacylglycerol kinases; **YpfP**—diacylglycerol β-glucosyltransferase; PA—phosphatidic acid; CDP-DG—CDP-diacylglycerol; PS—phosphatidylserine; PE—phosphatidylethanolamine; PC—phosphatidylcholine; PI—phosphatidylinositol; PGP—phosphatidylglycerol phosphate; PG—phosphatidylglycerol; CL—cardiolipin; LPG—lysil phosphatidylglycerol; DG—diacylglycerol; MGDG—monoglycosyl-DG; DGDG—diglycosyl-DG; R_1 and R_2—fatty acid hydrocarbon radicals.

Phosphatidylglycerol phosphate (PGP) is synthesized by phosphatidylglycerophosphate synthase (**PgsA**) from CDP-DG via the displacement of cytidine monophosphate (CMP) by glycerol-3-phosphate (glycerol-3-P) (Figure 2). Further, phosphatidylglycerolphosphate phosphatase (**PgpA**) dephosphorylates PGP to yield PG (Figure 2). Two additional genes of phosphatidylglycerolphosphate phosphatases, **PgpB** and **PgpC**, were discovered in *E. coli* [184]. Subsequently, a cardiolipin synthase (**ClsA**) utilizes two PG molecules to produce CL and glycerol (Figure 2). Two extra CL synthases have been discovered in *E. coli*, **ClsB** and **ClsC** [185]. The first one can use one molecule of PG and the molecule of another phospholipid as the second substrate [186]. Moreover, **ClsB** of *E. coli* can convert PE and glycerol into PG in a **PgsA**-independent manner [187]. To form CL, **ClsC** uses PG and PE instead of the two PG molecules [185]. The products of the **Cls1** and **Cls2** genes of *S. aureus*

are CL synthases with various types of stress-activated production [188]. Three genes of CL synthases have been identified in *B. subtilis* [189].

The phosphatidylserine synthase (**PssA**) synthesizes PS from CDP-DG via the displacement of CMP by serine (Figure 2). PS is only a minor biosynthetic intermediate in most bacteria and is decarboxylated by phosphatidylserine decarboxylase (**Psd**) to produce PE.

PC is also absent in most prokaryotic cells, although some Gram-negative bacteria contain phosphatidylcholine synthases (**Pcs**) to condense choline into the phosphatidyl moiety of CDP-DG, similar to PssA with serine (Figure 2) [190,191].

One more component that is rarely present in bacterial membranes is PI. For example, *Mycobacteria* are able to form PI using phosphatidylinositol synthase (**PIS**) via the exchange of the CMP moiety of CDP-PG for inositol (Figure 2) [192]. Due to the lack of sequence homology between bacterial and mammalian **PIS**s, their different kinetic characteristics, and the essential role of PI in mycobacteria, the **PIS** of mycobacteria seems to be a good potential drug target for antimycobacterial therapy. Structural analogs of inositol were shown to be more potent inhibitors of mycobacterial **PIS** compared to mammalian **PIS** [193]. Alternatively, there is a difference in the bacterial and mammalian biosynthetic pathways used to form PI: in *Mycobacteria*, PI is produced from CDP-DG and inositol 1-phosphate through an intermediate, phosphatidylinositol phosphate (PIP), which is dephosphorylated subsequently to PI, and inositol 1-phosphate analogs serving as inhibitors of PIP synthase can be used as antimycobacterials [194].

In some Gram-positive bacteria, the anionic glycerophospholipids, particularly PG and CL, can be decorated with aminoacyl residues, most often with lysil, to form cationic PG and CL derivatives by lysil phosphatidylglycerol (LPG) synthase and flippase, multiple peptide resistance factors (**MprF**) (Figure 2). This pathway is crucial for the adaptation of bacteria to cationic antimicrobial peptides [195–197]; for this reason, **MprF**-targeting antibodies or inhibitors of the factors involved in **MprF** regulation might sensitize resistant strains to antimicrobial agents [198,199].

In Gram-negative bacteria, a phosphoglycerol transferase (**MdoB**) transfers sn-1-phosphoglycerol from PG to membrane-derived oligosaccharides (MDO) to obtain diacylglycerol (DG). Further, it is phosphorylated by DG kinases (**DgkA** and **DgkB** in Gram-negative and Gram-positive bacteria, respectively) to generate PA, which can be recycled in the phospholipid biosynthetic pathway (Figure 2). **DgkA** presents a large family of prokaryotic DG kinases that are unrelated to the eukaryotic DG kinases and **DgkB** [200]. Some products of the *dgkA* gene are undecaprenol kinases [201].

In Gram-positive bacteria, DG is used to form glycolipids. A diacylglycerol β-glucosyltransferase (**YpfP**) uses uridine diphosphate-glucose (UDP-Glc) to attach one monosaccharide unit to DG to form monoglycosyl-DG (MGDG) and to add one more Glc residue to MGDG to yield diglycosyl-DG (DGDG) (Figure 2). Although **YpfP** is a viable target for the development of novel antibacterial drugs [202], there are no approved inhibitors for this enzyme. Anionic glycopolymers, called lipoteichoic acids, composed of 1,3-polyglycerol-phosphate attached to DGDG (anchoring lipoteichoic acids in the membrane), are exposed on the cell walls of Gram-positive bacteria.

2.1.3. Biosynthesis of Lipid A

The outer leaflets of the outer membranes of Gram-negative bacteria are formed by specific lipopolysaccharides (LPS). They consist of O-antigen and core sugar domains and a lipid anchor, known as lipid A. This phosphorylated disaccharide lipid is highly conserved and absolutely required for bacterial growth and survival [203,204]. For this reason, many enzymes involved in lipid A biosynthesis have been identified as targets for antibiotic development [205] (Figure 3, Table 2).

Table 2. Major inhibitors of lipid A biosynthetic pathway.

Inhibitor	Structure	Enzyme	Origin	IC_{50}, μM	References
peptide 920	NH_2-SSGWMLDPIAGKWSR-COOH	**LpxA**	*E. coli*	0.06 ± 0.01	[206]
RJPXD33	TNLYMLPKWDIP-NH_2	**LpxA**	*E. coli*	19.0 ± 1.2	[207]
		LpxD	*E. coli*	3.5 ± 0.1	[207]
(R)-(3-(2-chloro-6-methoxybenzyl)morpholino)(3-(4-methylpyridin-2-yl)-1H-pyrazol-5-yl)methanone	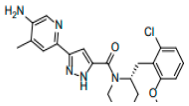	**LpxA**	*E. coli*	0.6	[208]
BB-78485	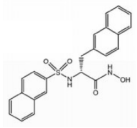	**LpxC**	*E. coli*	0.16 ± 0.07	[209]
L-161,240	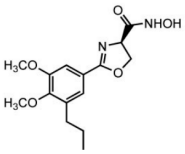	**LpxC**	*E. coli*	0.023 ± 0.003	[210]
			P. aeruginosa	0.22 ± 0.003	[210]
L-573,655	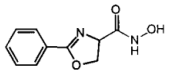	**LpxC**	*E. coli*	8.5	[211]
CHIR-090	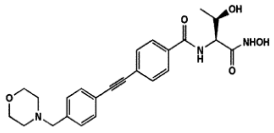	**LpxC**	*A. aeolicus*	~0.003	[212]
			E. coli	0.009	[213]
			R. leguminosarum	0.69	[213]
LpxC-4	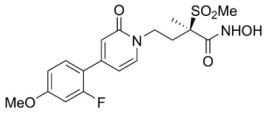	**LpxC**	*P. aeruginosa*	0.001	[214]
			K. pneumoniae	0.00007	[214]
			A. baumannii	0.183	[214]
TU-514	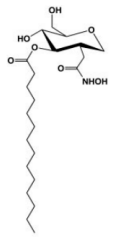	**LpxC**	*A. aeolicus*	7.0 ± 0.5	[215]
			E. coli	7.2 ± 1.9	[215]
4-(2-Chlorophenyl)-3-hydroxy-7,7-dimethyl-2-phenyl-6,7,8,9-tetrahydro-2H-pyrazolo[3,4-b]quinolin-5(4H)-one	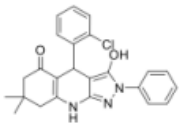	**LpxD**	*E. coli*	3.2	[216]
1-(5-((4-(3-(trifluoromethyl)phenyl)piperazin-1-yl)sulfonyl)indolin-1-yl)ethan-1-one	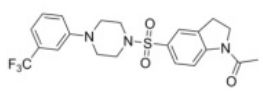	**LpxH**	*E. coli*	1.2 ± 0.2	[217]

Table 2. *Cont.*

Inhibitor	Structure	Enzyme	Origin	IC_{50}, μM	References
AZ1	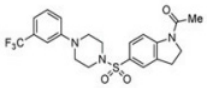	**LpxH**	*K. pneumoniae*	0.36	[218]
			E. coli	0.14	[218,219]
JH-LPH-28	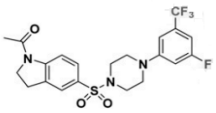	**LpxH**	*K. pneumoniae*	0.11	[218]
			E. coli	0.083	[218]
JH-LPH-33	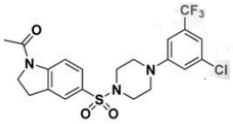	**LpxH**	*K. pneumoniae*	0.026	[218]
			E. coli	0.046	[218]

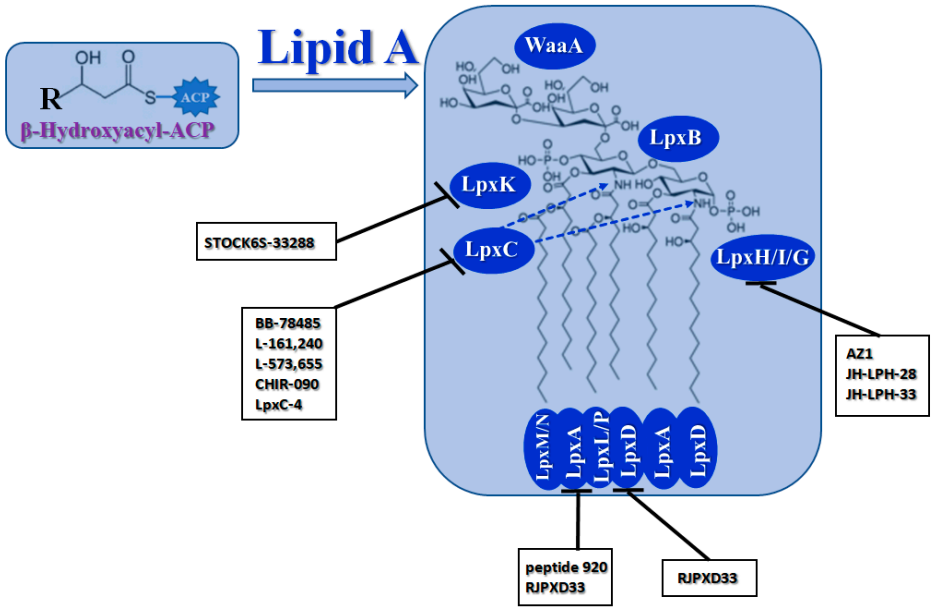

Figure 3. Schematic representation of the biosynthesis of lipid A. The blue ellipses indicate that all enzymes are only produced by Gram-negative bacteria. Some examples of enzyme inhibitors are shown in a black box. Abbreviations: **LpxA**—UDP-N-acetylglucosamine acyltransferase; **LpxC**—UDP-3-*O*-(*R*-3-hydroxyacyl)-*N*-acetylglucosamine deacetylase; **LpxD**—UDP-3-*O*-(*R*-3-hydroxyacyl)glucosamine N-acyltransferase; **LpxH, LpxI**, and **LpxG**—UDP-diacylglucosamine pyrophosphohydrolases; **LpxB**—lipid-A-disaccharide synthase; **LpxK**—tetraacyldisaccharide-1-phosphate 4′-kinase; **WaaA**—3-deoxy-D-*manno*-oct-2-ulosonic acid (Kdo) transferase; **LpxL**, **LpxM**, and **LpxP**—lysophospholipid acyltransferases.

A UDP-N-acetylglucosamine acyltransferase (**LpxA**) induces the first step of lipid A biosynthesis (Raetz pathway). It transfers a β-hydroxyacyl chain from β-hydroxyacyl-ACP generated by **FabG** to the 3 position of UDP-N-acetyl-glucosamine (UDP-GlcNAc) (Figure 3). It should be noted that LPS-producing enzymes are highly selective towards ACP thioesters; they cannot be substituted by normal fatty acids [220]. **LpxA** enzymes are highly specific regarding the acyl chain length. For example, *E. coli* **LpxA** transfers only β-hydroxymyristoyl chains [221]. Peptide (*Peptide 920*, *RJPXD33*) and small-molecule inhibitors (particularly *(R)-(3-(2-chloro-6-methoxybenzyl)morpholino)(3-(4-methylpyridin-2-yl)-1H-pyrazol-5-yl)methanone* and *erythroskyrin*) of **LpxA** were reported to compete with the substrate or interact with the complex product (Table 2) [206–208,222–227]. Analyzing

Table 2, one can conclude that *peptide 920* is of interest due to its relatively low IC_{50} value, while *RJPXD33* demonstrates dual targeting of **LpxA** and **LpxD**, offering the possibility to develop novel dual-binding antimicrobials. However, systematic studies of the safety of the peptide's administration must be performed before it can be determined how promising these methods are.

The acyl transfer reaction by **LpxA** is thermodynamically reversible and unfavorable, and the subsequent second reaction of the Raetz pathway, catalyzed by UDP-3-*O*-(*R*-3-hydroxyacyl)-*N*-acetylglucosamine deacetylase (**LpxC**), should occur (Figure 3). **LpxC** splits the acetyl radical from the UDP-3-(β-hydroxyacyl)-*N*-acetylglucosamine to produce UDP-3-(β-hydroxyacyl)-D-glucosamine (acyl-UDP-GlcN). Small-molecule inhibitors of the **LpxC** have been discovered, including hydroxamate-based compounds, exemplified by *TU-514*, *BB-78484*, *BB-78485*, *L-159,692*, *L-161,240*, *L-573,655*, *CHIR-090*, *LPC-009*, *LPC-011*, and *LpxC-4* (Table 2) [209–215,228–234]. Some of them are highly potent and have proven to be active against various multidrug-resistant Gram-negative bacteria. Analyzing Table 1, it can be assumed that the greatest interest regarding the design of new antibacterials targeting LpxC is in the further optimization of the most effective compounds, *L-161,240*, *CHIR-090*, and *LpxC-4*, in order to avoid emerging resistance [214,234–237].

A UDP-3-*O*-(*R*-3-hydroxyacyl)glucosamine N-acyltransferase (**LpxD**) performs the third reaction of the lipid A biosynthetic pathway; it transfers a second acyl group from β-hydroxyacyl-ACP to acyl-UDP-GlcN to produce UDP-2,3-bis(β-hydroxyacyl)-D-glucosamine (Figure 3). Some **LpxA** inhibitors, particularly *RJPXD33*, also bind to and inhibit **LpxD** [207,222,224]. It is also believed that **LpxD** is a drug target of natural compounds like *curcumin*, *gallotannin*, *isoorientin*, *neral*, *isovitexin*, *vitexin*, *allicin*, *ajoene*, and *cinnamaldehyde* [237]. Several synthetic compounds related to *hydro-pyrazolo-quinolinones* were identified as **LpxD** inhibitors (Table 2) [216].

A UDP-diacylglucosamine pyrophosphohydrolase (**LpxH**) hydrolyses UDP-2,3-bis(β-hydroxyacyl)-D-glucosamine to split UMP and to generate 2,3-diacylglucosamine-1-phosphate (lipid X) (Figure 3). **LpxI** and **LpxG** are functional orthologs of LpxH in α-proteobacteria and in *Chlamydiae*, respectively [238–240]. **LpxH** is inhibited by *sulfonyl piperazine* antibiotics (such as *AZ1*, *JH-LPH-28*, *JH-LPH-33*) (Table 2) [217–219,241–243]. Bacterial efflux pump functioning was found to be a significant deterrent for LpxH-targeting antimicrobials, highlighting the significance of their combination with antibiotics, permeabilizing the outer membrane to fight multidrug-resistant Gram-negative pathogens [218].

A lipid-A-disaccharide synthase (**LpxB**) combines the substrate and the product of the **LpxH**-catalyzed reaction to form the lipid A disaccharide (Figure 3). Compounds that target LpxB have not been discovered to date; only antisense pPNA technology is used to block the *lpxB* gene [244].

A tetraacyldisaccharide-1-phosphate 4′-kinase (**LpxK**) translocates the gamma-phosphate of ATP to the 4′ position of the lipid A disaccharide to produce lipid IV_A (Figure 3). The *5-(4-carbamoylbenzenesulfonyl)-N-hydroxy-1H-imidazole-2-carboxamide* analogs (*STOCK6S-33288*, *35740*, *37164*, *39892*, and *43621*) are believed to be a promising template to develop novel potent **LpxK** inhibitors [245].

A 3-deoxy-D-*manno*-oct-2-ulosonic acid (Kdo) transferase (**WaaA**/**KdtA**) adds two Kdo residues to lipid IV_A to form Kdo_2-lipid IV_A (Figure 3). Lysophospholipid acyltransferases, **LpxL** and **LpxM**, incorporate two additional acyl chains at positions 2′ and 3′ of Kdo_2-lipid IV_A to yield a hexa-acylated Kdo_2-lipid A (Figure 3). At lower temperatures, **LpxP** might partially perform the function of **LpxL**. The structure of the active sites of **LpxA** and **LpxD** permits the incorporation of myristoyl residues, while acyltransferases **LpxL**, **LpxP**, and **LpxM** transfer lauroyl, palmitoleoyl, and myristoyl chains, respectively [246,247]. **LpxN** is an ortholog of **LpxM** in *V. cholerae* [248]. No information about the specific compounds inhibiting the enzymes in the last steps of LPS biosynthesis are available in the literature.

2.2. Agents with Direct Action on Bacterial Lipid Membranes

Figure 4 summarizes the major mechanisms of the direct action of antibacterial agents on target lipid membranes. The mechanisms include pore formation and a detergent-like manner of action [249]. In the first case, the bacterium dies due to a violation in the water–salt balance via the formation of unauthorized transport pathways for water, ions, and small organic molecules. In the second case, the cause of death is the destruction of the membrane after reaching a critical detergent concentration, and a dramatic enhancement in the membrane fluidity and micellization of membrane lipids.

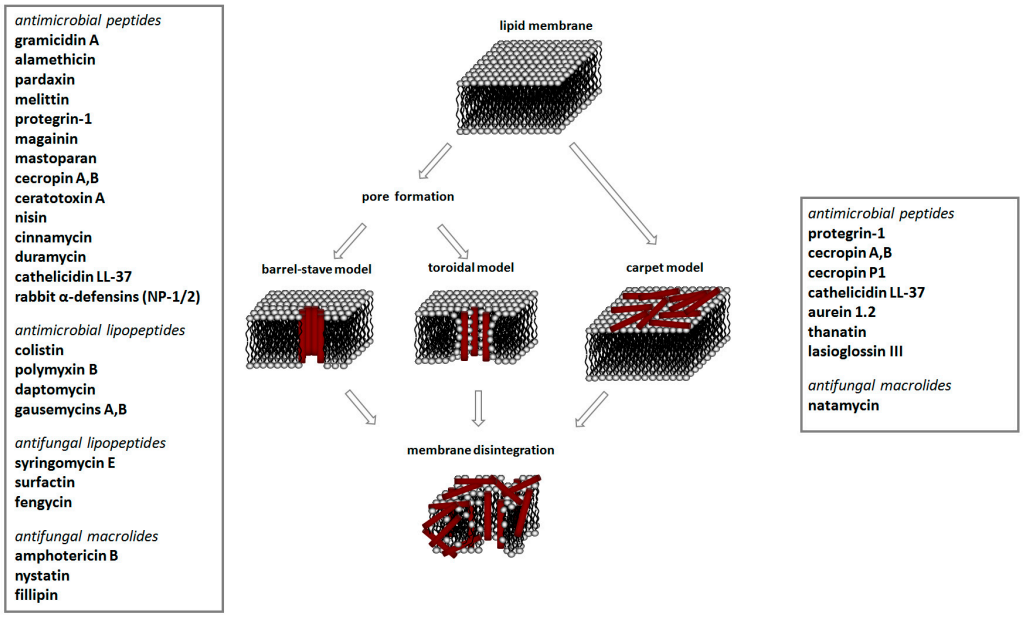

Figure 4. Schematic representation of major mechanisms of antimicrobial action via pore formation (described by two distinct models: barrel-stave channel and toroidal pore-containing lipids) and membrane disruption. Some examples of antibacterials and antifungals directly targeting lipid membranes by two different mechanisms are shown in black boxes.

Antimicrobial peptides are synthetized as components of the immune system in higher eukaryotes to defend them against a wide variety of invasive pathogens [250,251]. Antimicrobial lipopeptides are produced in bacteria or fungi as metabolites and/or to gain a competitive advantage over other species. A number of natural antimicrobial agents exert their defending activities primarily via pathogens' membrane disruption due to pore formation or the disordering of membrane lipids, and they are characterized by a lower probability of inducing microbial resistance. Thus, owing to the high efficiency of these compounds, their broad-spectrum bactericidal effects, and the low rate of pathogens' resistance to them, the use of antimicrobial peptides and lipopeptides in clinical practice, as well as in the search for new "natural" antibiotics, seems to be a productive anti-infective therapeutic strategy [252,253]. As a rule, antimicrobial peptides and lipopeptides share common structural features, such as molecular amphiphilicity and a net-positive electrical charge, which govern the binding and permeabilization of the negatively charged bacterial membranes through the mechanisms indicated above.

Table 3 presents examples of natural antimicrobial peptides and lipopeptides, their possible lipid targets, and the threshold concentrations needed to form pores and disintegrate lipid bilayers, mimicking the membranes of sensitive bacteria. Most of the antimicrobial peptides—gramicidin A from *Bacillus brevis*; alamethicin produced by the fungus *Trichoderma viride*; pardaxin isolated from secretions of the Red Sea Moses sole; melittin and mastoparan isolated from bee and wasp venom, respectively; protegrin-1 found in porcine leukocytes; magainin found in frog skin; ceratotoxins and cecropins discovered

in the accessory gland secretion fluid of the insect *Ceratitis capitata* and the hemolymph of *Hyalophora cecropia*, respectively; nisin from *Streptococcus lactis*; cinnamycin and its close analog duramycin from *Streptomyces* sp.; mammalian defensins; human cathelicidin LL-37 [254–274]; lipopeptides; colistins (polymyxins) from *Bacillus polymyxa*; daptomycin from *Streptomyces roseosporus*; and gausemycin from *Streptomyces* sp. [108,275–279]—manifest their action via the pore formation mechanism (Table 3). The pores formed by antimicrobial agents are characterized by their different architectures [280]. For example, alamethicin, pardaxin, and seratotoxin A pores are believed to be "barrels" composed of peptide aggregates [271,272,281,282], while mellitin, magainin, and polymyxin B form (lipo)peptide–lipid toroidal pores [108,270,283–285] (Figure 4). Some antimicrobial agents are not shown to form transmembrane pores; they act as detergents by forming a peptide "carpet" on the membrane surface (Figure 4). Such properties are exhibited by cecropin P1, lasioglossin III, and aurein 1.2 (Table 3) [264,286–288]. The peptide thanatin disrupts the bacterial outer membrane [289]. In the case of cecropins and protegrins, dual activity was found, including pore formation and detergent-like model action [259,264,290]. In any case, it is likely that when a critical antibiotic concentration is reached, regardless of whether the agent can form pores and in what way, an irreversible change in the rheological properties of the lipid bilayer occurs and it will be destroyed [291,292] (Figure 4).

Table 3. The effects of antibacterial agents on the model lipid membrane's permeability.

Agent	Structure	C_{min}, μM	C_{tr}, μM	Lipid Composition	References
Pore formation					
gramicidin A	HCO – Val – Gly – Ala – *D*-Leu – Ala – *D*-Val – Val – *D*-Val Trp – *D*-Leu – Trp – *D*-Leu – Trp – *D*-Leu – Trp – Gly – ol	0.001	– *	DSPC	[254]
alamethicin	N-acetyl-Ala(αMe) – Pro – Ala(αMe) – Ala – Ala(αMe) – Ala – Gln – Ala(αMe) – Val – Ala(αMe) Gly – Leu – Ala(αMe) – Pro – Val – Ala(αMe) – Ala(αMe) – Glu – Gln – Phe–ol	0.1	– *	DOPS:DOPE 1:1 (m/m)	[293]
pardaxin	H–Gly – Phe – Phe – Ala – Leu – Ile – Pro – Lys – Ile – Ile Ser – Ser – Pro – Leu – Phe – Lys – Thr – Leu – Leu – Ser Ala – Val – Gly – Ser – Ala – Leu – Ser – Ser – Ser – Gly Gly – Gln – Glu–OH	0.006	– *	soybean lecithin	[258]
melittin	H–Gly – Ile – Gly – Ala – Val – Leu – Lys – Val – Leu – Thr Thr – Gly – Leu – Pro – Ala – Leu – Ile – Ser – Trp – Ile Lys – Arg – Lys – Arg – Gln – Gln–NH_2	0.23	– *	POPC:cholesterol 3:1 (m/m)	[294]
magainin I	H–Gly – Ile – Gly – Lys – Phe – Leu – His – Ser – Ala – Gly Lys – Phe – Gly – Lys – Ala – Phe – Val – Gly – Glu – Ile Met – Lys – Ser–OH	10	– *	DOPC; DOPE:DOPG 3:1 (m/m)	[260]
magainin II	H–Gly – Ile – Gly – Lys – Phe – Leu – His – Ser – Ala – Lys Lys – Phe – Gly – Lys – Ala – Phe – Val – Gly – Glu – Ile Met – Asn – Ser–OH	0.08	– *	POPC:DOPG 6:1 (m/m); DOPS:ergosterol 3:1 (m/m); POPC:ergosterol 3:1 (m/m)	[261]

Table 3. *Cont.*

Agent	Structure	C_{min}, μM	C_{tr}, μM	Lipid Composition	References
mastoparan	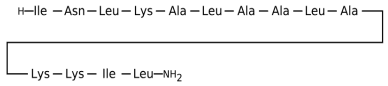	0.68	– *	DPhPC	[262]
ceratotoxin A	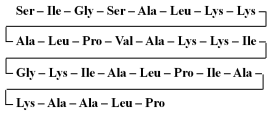	0.02	– *	POPC:DOPE 7:3 (*w*/*w*); POPC:DOPE:POPS 7:3:1 (*w*/*w*)	[271,272]
protegrin-1	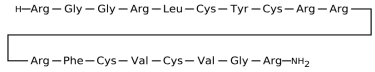	0.25–10	– *	DOPC:DOPE 1:1 (m/m)	[259]
nisin	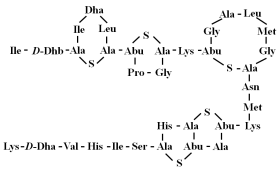	0.1		lipid II	[295]
		~40	>500	TOCL	[265]
cinnamycin	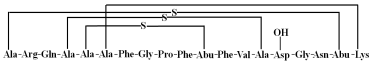	~1.5	>10	DOPE; TOCL	[265]
duramycin	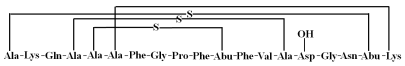	4.5–10	– *	GMO	[266]
		~2	>12	DOPE; TOCL	[265]
rabbit α-defensins (NP-1/2)	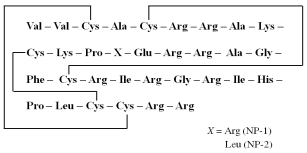	~1	>16	PE/PC/PS 2:2:1 (*w*/*w*); PE/CL	[296,297]
daptomycin	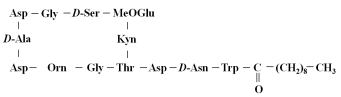	6.2	– *	DPhPG	[298]
polymyxin B	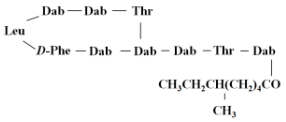	2.5	>100	DOPG	[108]
		1	>20	Kdo_2-Lipid A	
gaysemycin	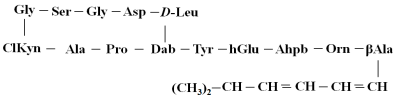	~26	– *	DOPG	[279]
Pore formation and detergent action					
cecropin A	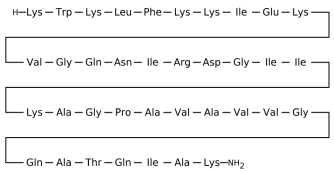	1	>5	DOPS:DOPE 1:1 (m/m)	[264]

Table 3. *Cont.*

Agent	Structure	C_{min}, μM	C_{tr}, μM	Lipid Composition	References
cecropin B	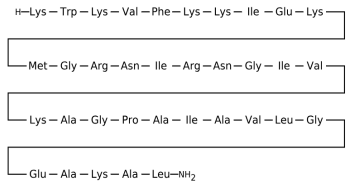	1	>5	DOPS:DOPE 1:1 (m/m)	[264]
Detergent action					
cecropin P1		– *	>50	DOPS:DOPE 1:1 (m/m)	[264]
aurein 1.2	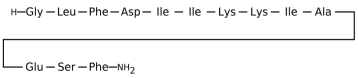	– *	>10	DMPG	[287]

C_{min}—the antibiotic threshold concentration required to observe single pores; C_{tr}—the antibiotic threshold concentration required to disintegrate the lipid bilayers; *—data are absent. Abbreviations: DSPC—1,2-distearoyl-*sn*-glycero-3-phosphocholine; DPPC—1,2-dipalmitoyl-*sn*-glycero-3-phosphocholine; POPC—1-palmitoyl-2-oleoyl-*sn*-glycero-3-phosphocholine; DOPC—1,2-dioleoyl-*sn*-glycero-3-phosphocholine; DOPE—1,2-dioleoyl-*sn*-glycero-3-phosphoethanolamine; DOPG—1,2-dioleoyl-*sn*-glycero-3-phospho-(1′-rac-glycerol); DOPS—1,2-dioleyl-*sn*-glycero-3-phosphoserine; DPhPC—1,2-diphytanoyl-*sn*-glycero-3-phosphocholine; DPhPG—1,2-diphytanoyl-*sn*-glycero-3-phospho-(1′-rac-glycerol); DMPG—1,2-dimyristoyl-*sn*-glycero-3-phospho-(1′-rac-glycerol); TOCL—1′,3′-bis-[1,2-dioleoyl-*sn*-glycero-3-phospho]-1′,3′-glycerol; GMO—glyceryl monooleate; Kdo_2-Lipid A—di [3-deoxy-D-manno-octulosonyl]-lipid A. Abbreviations for nonproteinogenic amino acids: α-Me-Ala—α-methyl-alanyl; Phe-ol—phenylalaninol; Dab—2,4-diaminobutyric acid; Dhb—2,3-dehydroaminobutyric acid; Dhb—2,3-didehydrobutyrine, Abu—α-aminobutyric acid; MeOGlu—3-methyl-glutamic acid; Kyn—kynurenine; Orn—ornithine. Only D-enantiomers of amino acids are indicated.

Despite the lower bacterial resistance to the naturally occurring antibiotics acting on the microbial membranes compared to classical antibiotics, including those inhibiting lipid biosynthesis, antimicrobial peptides and lipopeptides are not a panacea for the emergence of resistance in pathogenic bacteria. One of the evolutionary mechanisms by which to develop pathogenic resistance to cationic antibacterial agents is a reduction in the total negative charge of the cell surface of a microorganism to reduce the initial electrostatic binding. Thus, the resistance of *S. aureus* to defensins and protegrins is determined by the activity of **MprF**, an enzyme that modifies phosphatidylglycerol with L-lysine (1.1.2), which, in turn, leads to a decrease in the surface membrane charge and the repulsion of cationic peptides [299]. *Pseudomonas fluorescens* was proposed to diminish the net anionic charge of the cytoplasmic membrane by reducing the content of anionic phospholipids and increasing the concentration of positively charged ornithine–amide lipids that lead to the resistance to the cationic polymyxin B [300]. According to the literature data, a change in the structure of the LPS of Gram-negative bacteria *E. coli*, *Salmonella enterica*, *Salmonella typhimurium*, *K. pneumoniae*, and *P. aeruginosa* induced by the attachment of *L*-arabinose or phosphatidylethanolamine to the phosphate residues of lipid A leads to the emergence of resistance among these microorganisms to polymyxins due to changes in the membrane surface charge [301–305]. In turn, daptomycin is recommended for application as a therapy against β-lactam-resistant *Streptococcus mitis*. The target of daptomycin is thought to be phosphoglycerol [306]. However, *S. mitis* can rapidly develop resistance to daptomycin via loss-of-function mutations in the gene of **CdsA**, which catalyzes the formation of a common phospholipid precursor, CDP-DG (1.1.2); moreover, daptomicin-resistant strains exhibit the absence of anionic phospholipid membrane microdomains composed of CL and PG [307]. Daptomicin resistance in *E. faecalis* was found to be associated with changes in the

genes of cardiolipin synthase, **Cls**, and cyclopropane fatty acid synthase, **CfaS** (1.1.2) [308]. The latter indicates that reducing the level of negatively charged lipids is not the only strategy for resistance development by changing the membrane properties; the fatty acid profile is also of fundamental importance. For example, the development of resistance of *S. aureus* to gausemycin A is accompanied by growth in the ratio between the levels of *anteiso*- and *iso*-BCFA [309]. The membrane fluidity is significantly enhanced when *anteiso* acyl chains replace *iso* acyl chains. In contrast, the resistance of *S. aureus* to daptomycin and *Listeria monocytogenes* to nisin develops with an increase in the percentage of SFA compared to BCFA, which should lead to a decrease in membrane fluidity [310,311]. Thus, alterations in the fatty acid profile and rheological properties of the membrane may be another important factor determining the sensitivity of pathogens to antibiotics. Moreover, whether the fluidity of the membrane should be increased or decreased depends on the architecture of the pores formed by a specific antimicrobial agent.

3. Antifungal Agents with Lipid-Related Mechanisms of Action

3.1. Inhibition of Biosynthesis of Fungal Cell Membrane Components

Fundamentally, fungal walls are all engineered in a similar way and contain the cell membrane and cell wall [312]. The absence of a cell wall in mammalian cells provides an opportunity for the development of antifungal agents that target the enzymes involved in the biosynthesis of cell wall components in fungi, chitin synthase (Chs) and β-1,3-glucan synthase (Fks) [313–315]. The resistance of *Aspergillus fumigatus* and *Candida glabrata* to semisynthetic ehinocandin and caspofungin might arise from not only mutations in the Fks gene but also from alterations in the lipid microenvironment of the enzyme due to an increase in dihydrosphingosine and phytosphingosine content [316,317]. Thus, it should be taken into account that although the cell wall is an essential structure, maintaining the integrity and viability of fungal cells, the fungal lipid membrane serves as both a second barrier and a platform for the functioning of the enzymes that are responsible for the cell wall's biosynthesis (Chs and Fks) [318,319]. The fungal cell membrane is composed of various glycerophospholipids, sphingolipids, and ergosterol. The latter component is particularly interesting in terms of antifungal targeting, since mammalian cell membranes include another sterol, cholesterol.

3.1.1. Biosynthesis of Fatty Acids of Fungal Membrane Lipids

Recently, a discrepancy between the human and fungal FASI has been discovered [320]. The human FAS encoded by the FASN gene is a type Ib FAS. It consists of one polypeptide chain, including seven domains that assemble into homodimers [321]. Yeast FAS belongs to type Ia FAS and includes a heterododecameric complex composed of six subunits α and six subunits β, which are encoded by the genes Fas1 and Fas2 [322]. It was shown that the deletion of the FAS genes in *Cryptococcus neoformans* significantly reduced the growth and virulence of the fungi [323–325]. Thus, the differences in fungal and human FAS [320] can, in *Candida albicans*, potentially be used to target broad-spectrum antifungals towards the products of the Fas1 and Fas2 genes. However, the fungal mutants for the corresponding FAS genes could survive due to the utilization of exogenous fatty acids [326], which might significantly reduce the possibilities of anti-FAS therapy. There have been few fruitful efforts to repurpose antibacterial FAS inhibitors. FAS inhibition in *C. neoformans* with the FASII inhibitor *cerulenin* (1.1) drastically reduced the inhibitory concentration of the inhibitor of ergosterol synthesis, fluconazole (2.4) [323]. *Cerulenin* (but not platensimycin and thiolactomycin) was shown to inhibit *Saccharomyces cerevisiae* FAS [327]. The attempts to inhibit a product of the *OLE1* gene, fatty acid Δ9 desaturase, were more successful in terms of targeting fatty acid biosynthesis in *C. albicans* [328,329].

3.1.2. Biosynthesis of Phospholipid Head Groups

Similar to bacteria (Figure 2), the biosynthesis of the fungal phospholipids begins with the common precursor CDP-DG, which is produced from PA by **CdsA** [330,331]. Further, PI, PGP,

and PS are generated from CDP-DG by **PIS**, **PgsA**, and **PssA**, respectively [330,332]. PGP is dephosphorylated by **PgpA** to form PG, and PG is condensed to CL by **ClsA** [330,332]. It is important that the major phospholipid present in most eukaryotic membranes is PC, and PS is a key substrate for PC synthesis in yeast and fungi [333]. The **Psd** enzyme converts PS to PE. The main pathway for PC synthesis in yeast involves the three-step methylation of PE (Figure 5). The first stage includes the methylation of PE by phosphatidylethanolamine N-methyltransferase (**Pems**) to form the phosphatidyl-N-monomethylethanolamine (PMME) and the methylation of PMME to form phosphatidyl-*N*,*N*-dimethylethanolamine (PDME) [330]. PDME is converted to PC by **PgpA**. It was shown that the disruption of PS and PE biosynthesis within the CDP-DG pathway causes the avirulence of *C. albicans* [334]. Moreover, the action of some fungicides is associated with **Pems** inhibition [335]. As, in the cells of higher eukaryotes, PC is mainly synthesized from exogenous ethanolamine and choline via the Kennedy pathway [336,337] (Figure 5), one might suggest that the enzymes that perform the methylation reactions in PC biosynthesis by the CDP-DG pathway can be potential targets for antifungals. However, the alternative Kennedy pathway can be used by lower eukaryotes to produce PC and determines the possibility of developing resistance to the action of such antibiotics.

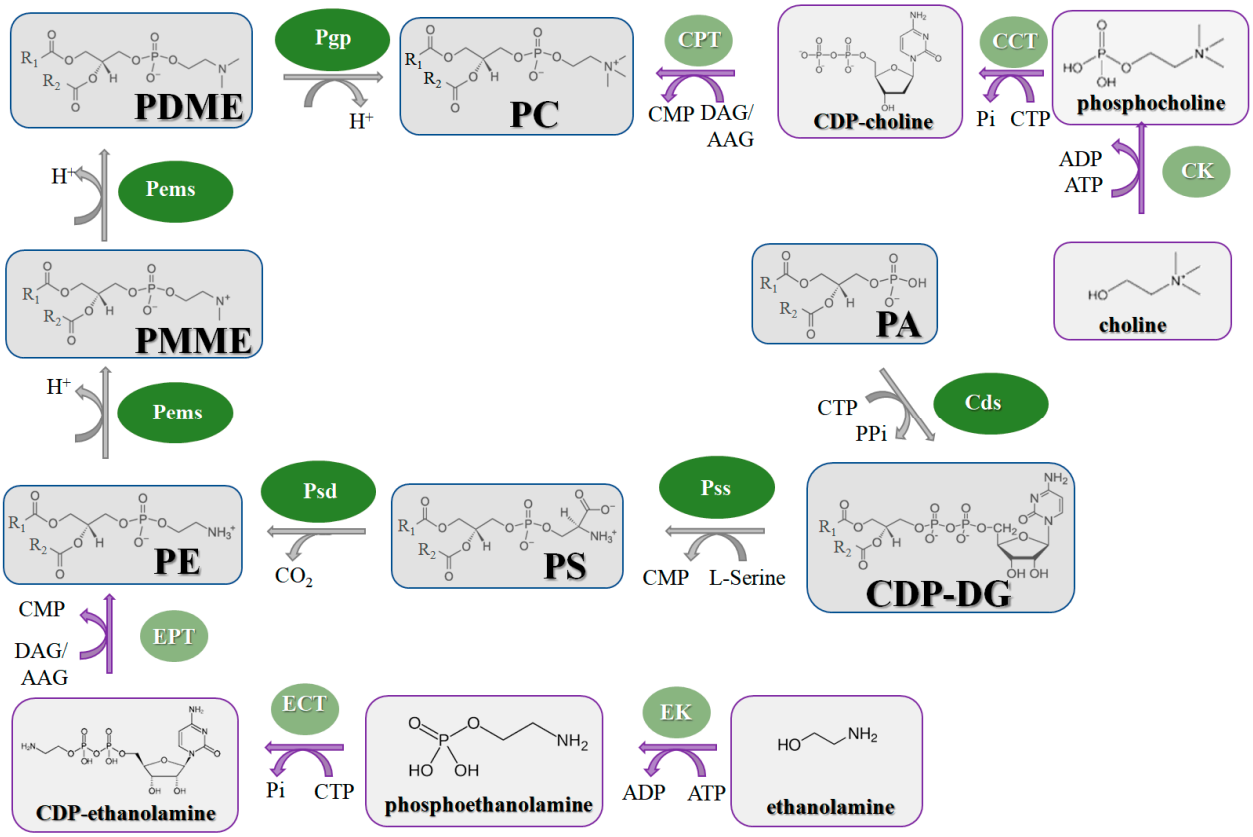

Figure 5. The PC biosynthesis in *S. cerevisiae*. The de novo and Kennedy pathways are represented by the grey and violet lines, respectively. The enzymes of the indicated pathways are highlighted with green and light-green ellipses, respectively. Abbreviations: **Pems**—phosphatidylethanolamine N-methyltransferase; **EK**—ethanolamine kinase; **CK**—choline kinase; **ECT**—phosphoethanolamine cytidylyltransferase; **CCT**—phosphocholine cytidylyltransferase; **EPT**—ethanolaminephosphotransferase; **CPT**—cholinephosphotransferase; PMME—phosphatidyl-N-monomethylethanolamine; PDME—phosphatidyl-*N*,*N*-dimethylethanolamine.

3.1.3. Biosynthesis of Sphingolipids

Figure 6 demonstrates the pathway for the synthesis of sphingolipids in *S. cerevisiae* [338–340]. Serine palmitoyltransferase (**SPT**) performs the condensation of *L*-serine and palmitoyl-CoA to lead to 3-ketodihydrosphingosine [341]. Meanwhile, 3-ketodihydro-

sphingosine reductase (**KDSR**) converts 3-ketodihydrosphingosine to dihydrosphingosine. Phytoceramide can be synthesized from dihydrosphingosine by ceramide synthase (**CerS**) and sphingosine C_4-hydroxylase (**SCH**) through two alternative intermediates, ceramide and phytosphingosine (Figure 6). The next reaction involves inositol-phosphoceramide synthase (**IPCS**), which converts phytoceramide to inositolphosphatyl-ceramide (IPC). IPC can be further mannosylated by mannosylinositol phosphorylceramide synthase (**MIPCS**) and condensed with additional inositolphosphate using inositolphosphotransferase (**IPS**) to yield the more complex sphingolipids MIPC and $M(IP)_2C$, respectively [341–343].

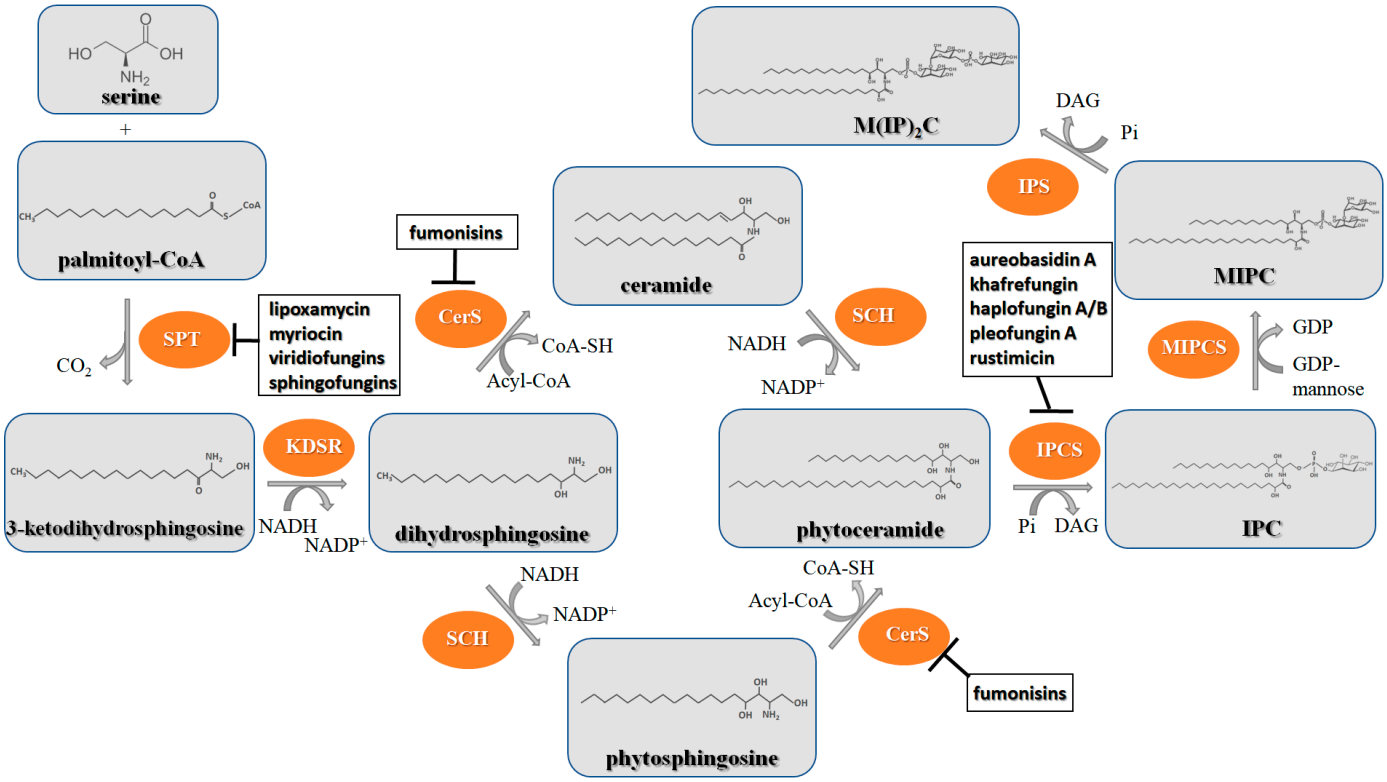

Figure 6. Schematic representation of the sphingolipid biosynthetic pathways in *S. cerevisiae*. The enzymes are highlighted with orange ellipses. Some examples of enzyme inhibitors are shown in black boxes. Abbreviations: **SPT**—serine palmitoyltransferase; **KDSR**—3-ketodihydrosphingosine reductase; **CerS**—ceramide synthase; **SCH**—sphingosine C_4-hydroxylase; **IPCS**—inositol-phosphoceramide synthase; **MIPCS**—mannosylinositol phosphorylceramide synthase; **IPS**—inositolphosphotransferase; IPC—inositol-phosphoceramide; MIPC—mannose-inositol-phosphoceramide; $M(IP)_2C$—mannose-(inositol-P)$_2$-ceramide.

Comparing the enzymes in the fungal and mammalian cells required for sphingolipid biosynthesis, it can be concluded that they are homologous and, consequently, are not suitable as targets for the development of low-toxicity antifungal drugs. Nevertheless, potent inhibitors of fungal sphingolipid biosynthesis are described in the literature, although a proper assessment of their possible toxicity has not been completed yet. Mainly, the compounds target **SPT** and **IPCS**. Table 4 summarizes the available information about the agents targeting the synthesis of sphingolipids in different fungi, their chemical structures, and the IC_{50} values against appropriate fungal enzymes. In particular, a variety of different **SPT** inhibitors have been isolated, including lipoxamycin [344,345], myriocin [346], sphingofungins [347–349], and viridiofungins [350]. It is interesting that sphingofungins are characterized by similar activity against *C. albicans* and *S. cerevisiae* **SPT**, while *viridiofungins* show 70-200-fold higher selectivity towards *C. albicans* **SPT** (Table 4). Unfortunately, **SPT** inhibitors demonstrated high toxicity towards mammalian cells due to the inhibition

of human SPT1 [351]. Interestingly, the *S. cerevisiae* **SPT** is composed of three different subunits, known as Lcb1, Lcb2, and Tsc3, and a homologue of Tsc3 has not been found in mammals [352]. Thus, the question of whether Tsc3 inhibition would be sufficient to effectively suppress the fungal **SPT** activity in pathogenic fungi awaits elucidation. *Fumonisins* are effective inhibitors of **CerS**, but also demonstrate toxicity to mammalian cells [353]. *Australifungin* is a very potent inhibitor of fungal **CerS** from several species; however, the α-diketone and β-ketoaldehyde functional groups present in this compound have high chemical reactivity, which seriously limits *australifungin*'s use [348]. The inositol-phosphoceramide synthase (**IPCS**) identified in *S. cerevisiae* and other different fungi [354] is a potential target for antifungals. **IPCS** inhibitors include *aureobasidin A* [355], *khafrefungin* [356], *haplofungins* [357], and *pleofungin* [358]. *Galbonolide A* and *B* inhibit the **IPCS** of *B. cinerea* and *C. neoformans* [359–361]. An analysis of Table 4 shows that *khafrefungin*, *pleofungin A*, and *galbonolide A*, also known as *rustmicin*, are the most potent inhibitors of *C. albicans*, *A. fumigatus*, and *C. neoformans* **IPCS**, respectively. *Khafrefungin* seems to be a more promising candidate due to its relevant selectivity between fungal and mammalian **IPCS** [356,362], while *rustmicin*'s application is limited by its low metabolic stability and drug efflux in fungi [359]. Thus, a further search may accelerate the discovery of selective low-toxicity natural inhibitors for fungi.

Table 4. Major inhibitors of fungal sphingolipid biosynthesis.

Inhibitor	Structure	Enzyme		IC_{50}, μM	References
sphingofungin B	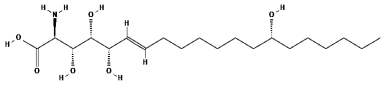	**SPT**	*C. albicans*	0.049	[350]
			S. cerevisiae	0.051	
viridiofungin A	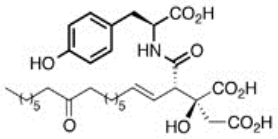	**SPT**	*C. albicans*	0.022	[350]
			S. cerevisiae	4.7	
viridiofungin B	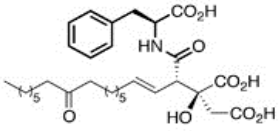	**SPT**	*C. albicans*	0.017	[350]
			S. cerevisiae	1.84	
viridiofungin C	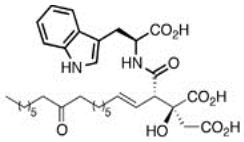	**SPT**	*C. albicans*	0.025	[350]
			S. cerevisiae	1.68	
aureobasidin A	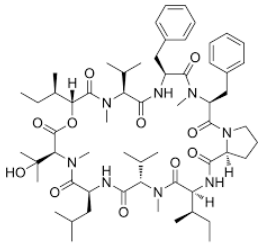	**IPCS**	*C. albicans*	0.002	[363]
			C. glabrata	0.002	
			Candida tropicalis	0.003	
			Candida parapsilosis	0.003	
			Candida krusei	0.003	
			A. fumigatus	0.005	
			Aspergillus flavus	0.002	
			Aspergillus terreus	0.004	
			Aspergillus niger	0.004	
			S. cerevisiae	0.0009	[358]

Table 4. *Cont.*

Inhibitor	Structure	Enzyme		IC_{50}, μM	References
khafrefungin	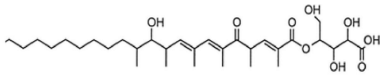	**IPCS**	*C. albicans*	0.0006	[356]
			C. neoformans	0.031	
			S. cerevisiae	0.007	
haplofungin A	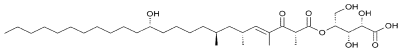	**IPCS**	*S. cerevisiae*	0.0025	[357]
			A. fumigatus	0.41	
haplofungin B	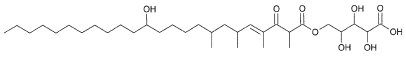	**IPCS**	*S. cerevisiae*	0.042	[357]
			A. fumigatus	1.33	
pleofungin A	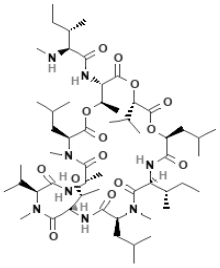	**IPCS**	*S. cerevisiae*	0.007	[358]
			A. fumigatus	0.0009	
galbonolide A (rustmicin)	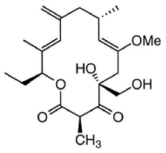	**IPCS**	*C. albicans*	0.0038	[359]
			C. neoformans	0.00007	
			S. cerevisiae	0.0198	

3.1.4. Ergosterol Synthesis

Contrary to the cholesterol-containing membranes of mammalian cells, fungal cell membranes are enriched with ergosterol [364]. Figure 7 demonstrates the ergosterol biosynthesis pathway in *S. cerevisiae* [365].

The ergosterol biosynthesis in *S. cerevisiae* includes three different modules, mevalonate, farnesyl-PP, and ergosterol biosynthesis [366]. Table 5 provides the available information about the potential inhibitors of enzymes participating in the ergosterol biosynthetic pathway.

Acetyl-CoA C-acetyltransferase (**ERG10**) catalyzes the additional acetylation of acetyl-CoA molecules to produce acetoacetyl-CoA, which is further transformed by hydroxymethylglutaryl-CoA synthase (**ERG13**) to 3-hydroxy-3-methylglutaryl-CoA. Mevalonate is synthesized by NADPH-dependent hydroxymethylglutaryl-CoA reductase (**HMG1/2**) [366,367]. As the synthesis of mevalonate is the critical step in the ergosterol biosynthetic pathway, it is believed that **HMG1/2** might be a good target for antifungals. It is well known that statins competitively bind to human 3-hydroxy-3-methylglutaryl coenzyme-A reductase, preventing the conversion of 3-hydroxy-3-methylglutaryl-CoA into mevalonate [368,369], and the prospects for the repurposing of statins to treat fungal infections should be estimated. Supporting this theory, *simvastatin*, *lovastatin*, *atorvastatin*, *pravastatin*, *fluvastatin*, and related compounds were reported to decrease the intracellular ergosterol level via the inhibition of **HMG1/2** in *C. glabrata*, *C. albicans*, *Ustilago maydis*, *Trichothecium roseum*, *S. cerevisiae*, *C. neoformans*, *Zygomycetes*, and *Aspergillus* spp. [370–381]. Moreover, statin therapy is associated with a reduction in oral *Candida* carriage in hyperlipidemic patients [382]. Statins also reduced mortality due to the diminishing risk of fungal-related complications in patients with diabetes, hematologic malignancies, and COVID-19 [368,383–385].

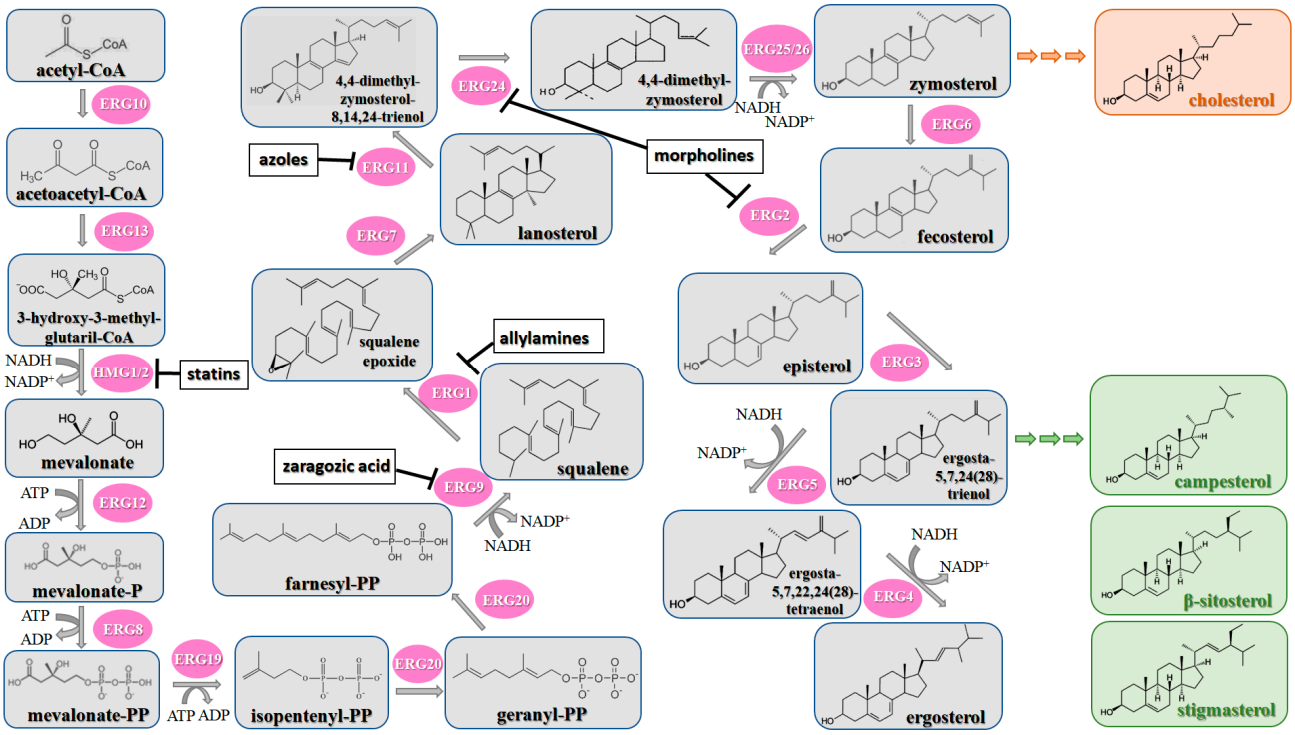

Figure 7. Schematic representation of the ergosterol biosynthetic pathway in *S. cerevisiae*. The enzymes are highlighted with pink ellipses. The branch for the cholesterol biosynthesis in mammalian cells is marked with an orange color. The branch for the biosynthesis of phytosterols (campesterol, β-sitosterol, and stigmasterol) is marked with a green color. Some examples of enzyme inhibitors are shown in the black box. Abbreviations: **ERG10**—acetyl-CoA C-acetyltransferase; **ERG13**—hydroxymethylglutaryl-CoA synthase; **HMG1/2**—hydroxymethylglutaryl-CoA reductase; **ERG12**—mevalonate kinase; **ERG8**—phosphomevalonate kinase; **ERG19**—diphosphomevalonate decarboxylase; **ERG20**—farnesyl diphosphate synthase; **ERG9**—squalene synthase; **ERG1**—squalene epoxidase; **ERG7**—2,3-oxidosqualene cyclase; **ERG11**—lanosterol 14α-demethylase; **ERG24**—sterol C14-reductase; **ERG25/26**—sterol C4-methyloxidase; **ERG6**—sterol C24-methyltransferase; **ERG2**—sterol C8,7-isomerase; **ERG3**—sterol C5(6)-desaturase; **ERG5**—sterol C22-desaturase; **ERG4**—sterol C24-reductase.

Further, mevalonate is successively phosphorylated to mevalonate-PP by two different kinases, mevalonate kinase (**ERG12**) and phosphomevalonate kinase (**ERG8**). Diphosphomevalonate decarboxylase (**ERG19**) performs the transformation of mevalonate-PP to isopentenyl-PP [386]. Farnesyl-PP is a product of two successive reactions catalyzed by farnesyl diphosphate synthase (**ERG20**) [387].

Using NADPH, squalene synthase (**ERG9**) produces squalene from farnesyl-PP. Natural fungal metabolites, such as *zaragozic acids*, are potent inhibitors of **ERG9** [388]; however, due to their high toxicity, the compounds failed to reach the clinical trial phase [389].

Squalene epoxidase (**ERG1**) and 2,3-oxidosqualene cyclase (**ERG7**) catalyze the synthesis of squalene epoxide and lanosterol, respectively. It was found that allylamines, *naftifine*, and *terbinafine* are reversible inhibitors of the *Candida* **ERG1** (Table 5) [390,391]. In addition to allylamines, the thiocarbamates *tolciclate* and *tolnaftate* were also shown to be potent inhibitors of **ERG1** (Table 5) [392]. Table 5 clearly demonstrates that all presented allylamines and thiocarbamates are more effective against *T. rubrum* **ERG1** than against *C. albicans* squalene epoxidase. However, the resistance of *Trichophyton* spp. to *terbinafine*, licensed for the treatment of dermatophytic infections, increases dramatically [393–395], creating a serious limitation to its further clinical application. Moreover, there is evidence in favor of *terbinafine*-induced hepatotoxicity [396]. The emerging resistance of dermatophytes

to *terbinafine* and the moderate activity of both allylamines and thiocarbamates against *C. albicans* show the need for a further search for highly effective **ERG1** inhibitors.

Lanosterol is converted to zymosterol via two intermediates, 4,4-dimethyl-zymosterol-8,14,24-trienol and 4,4-dimethyl-zymosterol, by lanosterol 14α-demethylase (**ERG11**) and sterol C14-reductase (**ERG24**). *Azoles* were identified as effective inhibitors of **ERG11** (Table 5) via selective coordination with heme iron [397,398] and demonstrated striking antifungal activity against a variety of human fungal pathogens [399,400]. Importantly, *azoles* inhibit human lanosterol 14α-demethylase at substantially higher concentrations than the fungal enzyme [397]. A series of *steroidal 1,4-dihydropyridines* also showed promising activity against various *Candida* spp. via the inhibition of **ERG11** [401]. Despite the pronounced activity of azoles against *Candida* spp. **ERG11** (Table 5), the enlarged resistance to azoles by *Candida* species is a serious threat in their clinical use [402,403]. Therefore, the novel azole-based derivatives could attract attention as **ERG11** inhibitors.

In the fungal cell, sterol C24-methyltransferase (**ERG6**) transforms zymosterol to fecosterol. It is converted to episterol by sterol C8,7-isomerase (**ERG2**). Sterol C5(6)-desaturase (**ERG3**) converts episterol to ergosta-5,7,24(28)-trienol [404–406]. NADPH-dependent sterol C22-desaturase (**ERG5**) catalyzes the formation of the next intermediate, ergosta-5,7,22,24(28)-tetraenol. At the final step, NADPH-dependent sterol C24-reductase (**ERG4**) converts ergosta-5,7,22,24(28)-tetraenol to ergosterol molecules [365]. It was demonstrated that *amorolfine*, *fenpropidin*, *fenpropimorph*, and the related *morpholines* and *piperidines* act as dual inhibitors of **ERG24** and **ERG2** [407,408]. Thus, these compounds seem to be ideal antifungals, as acquiring resistance against them will be difficult for pathogens because of the requirement to mutate two enzyme genes at once. Among the aminopiperidine derivatives, as presented in Table 5, *compound 1b* has a lower IC_{50} value, and the substantial prolongation of survival in infected mice with its oral administration [409] indicates the potential clinical benefits. However, presently, only amorolfine is used clinically to treat nail infections.

It should be noted that zymosterol is a precursor in cholesterol biosynthesis in mammalian cells [410] (this branch of the biosynthetic pathway is marked with an orange color in Figure 7). Ergosta-5,7,24(28)-trienol is a precursor of phytosterols, campesterol, β-sitosterol, and stigmasterol [411] (this branch of the biosynthetic pathway is indicated with a green color in Figure 7).

Table 5. Major inhibitors of fungal sterol biosynthesis.

Inhibitor	Structure	Enzyme		IC_{50}, μM	References
terbinafine	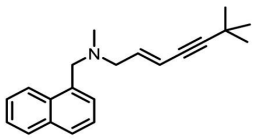	**ERG1**	*C. albicans*	0.03	[390,392]
			C. parapsilosis	0.02–0.04	[390]
			C. glabrata	0.137	[390]
			Trichophyton rubrum	0.002–0.016	[390,392]
			A. fumigatus	0.24	[390]
naftifine	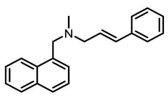	**ERG1**	*C. albicans*	1.1	[390]
			C. parapsilosis	0.34	[390]
			T. rubrum	0.115 ± 0.030	[392]
SDZ 87-469	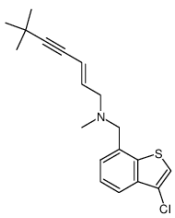	**ERG1**	*T. rubrum*	0.020 ± 0.005	[392]
			C. albicans	0.011	[392]

Table 5. *Cont.*

Inhibitor	Structure	Enzyme		IC_{50}, μM	References
tolciclate	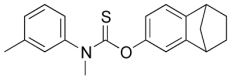	**ERG1**	*T. rubrum*	0.028 ± 0.003	[392]
			C. albicans	0.12	[392]
tolnaftate	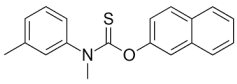	**ERG1**	*T. rubrum*	0.052± 0.009	[392]
			C. albicans	1.04	[392]
bifonazole	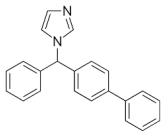	**ERG11**	*C. albicans*	0.3	[397]
clotrimazole	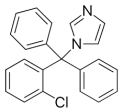	**ERG11**	*C. albicans*	0.091	[397]
miconazole	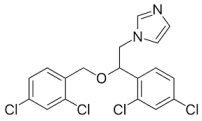	**ERG11**	*C. albicans*	0.072	[397]
fluconazole	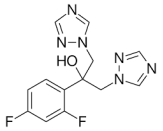	**ERG11**	*C. albicans*	0.051–0.6	[397,412]
			C. neoformans	0.17	[413]
			Malassezia globosa	0.206 ± 0.008	[414]
itraconazole	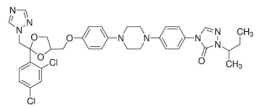	**ERG11**	*C. albicans*	0.039–0.4	[397,412]
			C. neoformans	0.17	[413]
			M. globosa	0.188 ± 0.008	[414]
voriconazole	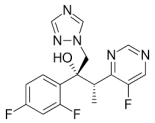	**ERG11**	*C. neoformans*	0.17	[413]
VT-1129	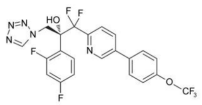	**ERG11**	*C. neoformans*	0.16	[413]
ketoconazole	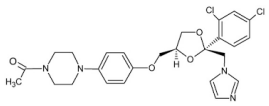	**ERG11**	*C. albicans*	0.064–0.5	[397,412]
			M. globosa	0.176 ± 0.016	[414]
ketaminazole	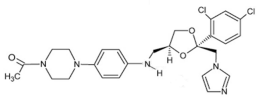	**ERG11**	*M. globosa*	0.321 ± 0.042	[414]

Table 5. *Cont.*

Inhibitor	Structure	Enzyme		IC_{50}, μM	References
compound 1a	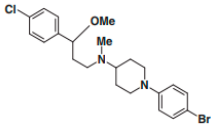	**ERG24**	*C. albicans*	0.063	[415]
compound 1b	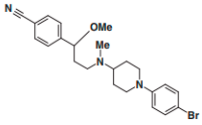	**ERG24**	*C. albicans*	0.016	[415]

3.2. Agents with Direct Action on Fungal Lipid Membrane

The principles of action of naturally occurring antibiotics on fungal membranes are similar to those of antibacterial peptides and lipopeptides (Figure 4).

Table 6 summarizes the data concerning the effect of antifungal lipopeptides and polyene macrolides on the permeability of lipid bilayers that mimic the cell membranes of target fungi. One of the most attractive groups is the cyclic lipopeptides, which are secondary metabolites of certain bacteria and are used to combat plant fungal pathogens. It is well known that the syringomycins and syringopeptines from *Pseudomonas syringae*, and surfactins, fengycins, iturins, bacillomycins, and mycosubtilin from *B. subtilis*, form the transmembrane pores in model lipid membranes [416–427].

Table 6. The effects of antifungal agents on the model lipid membrane's permeability.

Agent	Structure	C_{min}, μM	C_{tr}, μM	Target Lipid	References
Pore formation					
syringomycin E	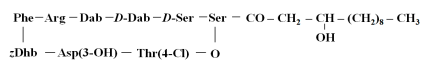	1–5	– *	DPhPC; DOPS:DOPE 1:1 (m/m)	[422]
syringopeptin 22A	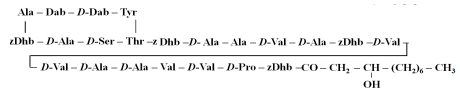	0.003	– *	DPhPC; DOPS:DOPE 1:1 (m/m)	[416]
syringopeptin 25A	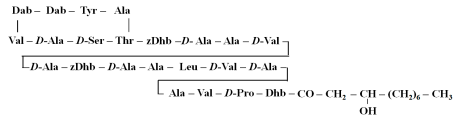	0.004	– *	PC:PE:PS 2:2:1 (m/m/m)	[428]
fengycins	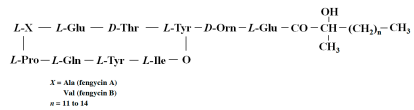	0.1–0.5	>10	POPC:POPE:POPG: ergosterol 2:2:5:1 (m/m)	[425]
surfactin	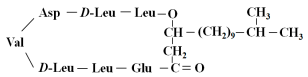	0.2–0.4	– *	DPhPC	[424]
		1.4	– *	glyceryl monooleate	[426]
iturin A	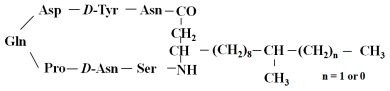	0.001	– *	egg-PC; egg-PC:DMPE 8:2 (*v*/*v*)	[429]
		– *	– *	glyceromonoolein	[421]

Table 6. *Cont.*

Agent	Structure	C_{min}, μM	C_{tr}, μM	Target Lipid	References
mycosubtilin	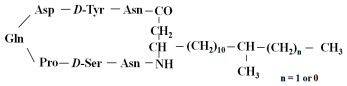	– *	–*	DPhPC	[430]
bacillomycins	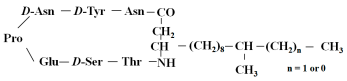	– *	– *	glyceromonoolein	[421]
amphotericin B	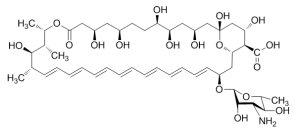	0.02–0.03	– *	phospholipid:cholesterol 20:1 (m/m)	[431]
		0.01	>20	DPhPC:ergosterol 2:1 (m/m)	[432]
nystatin	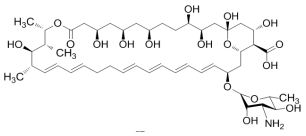	0.1	– *	phospholipid: cholesterol 20:1 (m/m)	[431]
		0.01	>100	DPhPC:ergosterol 2:1 (m/m)	[433]
filipin	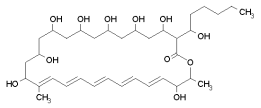	0.02	– *	phospholipid:cholesterol 2:1 (*v*/*v*)	[434]
		0.01	>100	DPhPC:ergosterol 2:1 (m/m)	[435]
piscidin	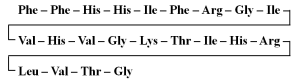	0.005	– *	azolectin	[436]
Detergent action					
natamycin	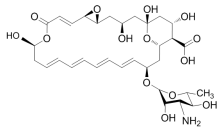	– *	110	DPhPC:ergosterol 2:1 (m/m)	[437]

C_{min}—the antibiotic threshold concentration required to observe single pores; C_{tr}—the antibiotic threshold concentration required to disintegrate the lipid bilayers; *—data are absent. Abbreviations: DPhPC—1,2-diphytanoyl-*sn*-glycero-3-phosphocholine; DOPS—1,2-dioleoyl-*sn*-glycero-3- phosphoserine; DOPE—1,2-dioleoyl-*sn*-glycero-3-phosphoethanolamine; POPC—1-palmitoyl-2-oleoyl-*sn*-glycero-3-phosphocholine; POPE—1-palmitoyl-2-oleoyl-*sn*-glycero-3-phosphoethanolamine; POPG—1-palmitoyl-2-oleoyl-*sn*-glycero-3-phospho-(1′-rac-glycerol); DOPG—1,2-dioleoyl-*sn*-glycero-3-phospho-(1′-rac-glycerol); DMPE—1,2-dimyristoyl-*sn*-glycero-3-phosphoethanolamine. Abbreviations for nonproteinogenic amino acids: α-Me-Ala—α-methyl-alanyl; Phe-ol—phenylalaninol; Dab—2,4-diaminobutyric acid; Dhb—2,3-dehydroaminobutyric acid; Dhb—2,3-didehydrobutyrine; Abu—α-aminobutyric acid; MeOGlu—3-methyl-glutamic acid; Kyn—kynurenine; Orn—ornithine. Only D-enantiomers of amino acids are indicated.

Another clinically important group is antifungal macrolides and polyene antibiotics. Amphotericin B, nystatin, and fillipin demonstrate antimicrobial activity via the formation of transmembrane pores in the target-sterol-containing membranes [432–434,438–443]. The three-dimensional structure of the amphotericin B channel was proposed as an asymmetric heptameric complex of polyene and sterol molecules penetrating the membrane [444]. In addition to natamycin's inhibitory effect on transport proteins, it was suggested to specifically interact with the sterol- and sphingomyelin-enriched ordered phase and disrupt lipid packing [437,445]. Amphidinol 3, an antifungal polyene isolated from a marine dinoflagellate, is also able to induce pore-like defects in model membranes [446].

Antimicrobial peptides also demonstrate antifungal efficiency. Piscidins identified in the mast cells of fish exert their fungicidal effects on *C. albicans* by disrupting the fungal membranes through pore formation [436,447]. An antimicrobial peptide from the tree frog *Hyla punctata*, hylaseptin P1-NH_2, demonstrates strong antifungal potential by promoting membrane disruption [448].

Saccharomyces cerevisiae strains, resistant to syringomycin E, are characterized by a decrease in the length of fatty acid chains and sphingolipid content. Mutants were defective in two key enzymes of the terminal sphingolipid biosynthetic pathway, **IPCS** and **IPS** (2.1.3) [449]. The sensitivity of *S. cerevisiae* towards syringomycin E was also shown to depend on the C_4-hydroxylation of sphingoid bases to form phytoceramide, catalyzed by **SCH** [450]. The relevance of $M(IP)_2C$ [451] and sphingolipid C_4-hydroxylation [452] for the lateral segregation of lipids in *S. cerevisiae* membranes might suggest that syringomycin E may interact with sphingolipid-enriched microdomains, and its pore-forming ability is sensitive to their composition [453,454].

As expected for the sterol-dependent mechanism of pore formation by polyene antibiotics, the decline in the ergosterol content in the plasma membranes of target fungi results in the development of resistance [455]. In fact, it was found that the minimal inhibitory concentration of amphotericin B against *C. albicans* was increased by the deletion of **ERG2**, **ERG6**, **ERG3**, and **ERG11**, the enzymes participating in the ergosterol biosynthetic pathway (2.1.4). It should be noted that the emergence of resistance to amphotericin B through a decrease in ergosterol content makes resistant strains extremely sensitive to osmotic and other types of stress. The reduced level of ergosterol in clinical strains of *Candida lusitaniae*, which is resistant to amphotericin B, might arise from mutations in the **ERG3** gene [456].

4. Antivirals Targeting Lipid Envelope

Since we have narrowed our focus to reviewing only compounds that directly target pathogen membranes, antivirals that have been shown to affect the membranes of virions, which lead to the destruction of the lipid envelope or suppression of virus fusion with the host cell, are discussed below.

Many socially significant viruses are enveloped, i.e., the virions are surrounded by a supercapsid composed of a lipid bilayer. Despite the fact that the origin of the lipid envelope is the host cell membrane, in some cases, a quantitative difference has been found in the content of various lipids in the viral envelope and the host cell membrane from which the virions have been budded [457–461]. This may also be due to virus-induced changes in the host cell's lipid metabolism [462,463]. Thus, the lipid membranes of enveloped viruses might be considered a target for innovative antiviral drugs. The compounds are thought to break the lipid envelopes of virions or dramatically change the properties of the viral membrane in order to prevent fusion with the cell membrane. A significant advantage of using such an approach is the broadening of the spectrum of antiviral activity and a decrease in the resistance to viral pathogens.

4.1. Disrupting Agents

4.1.1. Photosensitizing Antivirals

Photosensitizers are compounds that can absorb light and generate reactive oxygen species, which, in turn, leads to the peroxidation of membrane lipids and damage to the lipid bilayers of both viral and cellular membranes [464] (Figure 8A). In the absence of virus systems for reparation, the photodamage of the lipid envelope causes a dramatic reduction in the infectivity of virions due to the inactivation of viral fusion. Among the photosensitizers, compounds with absorption in the infrared region are of particular interest in the search for new broad-spectrum antivirals due to their substantially higher tissue transparency for the radiation of this spectrum [465].

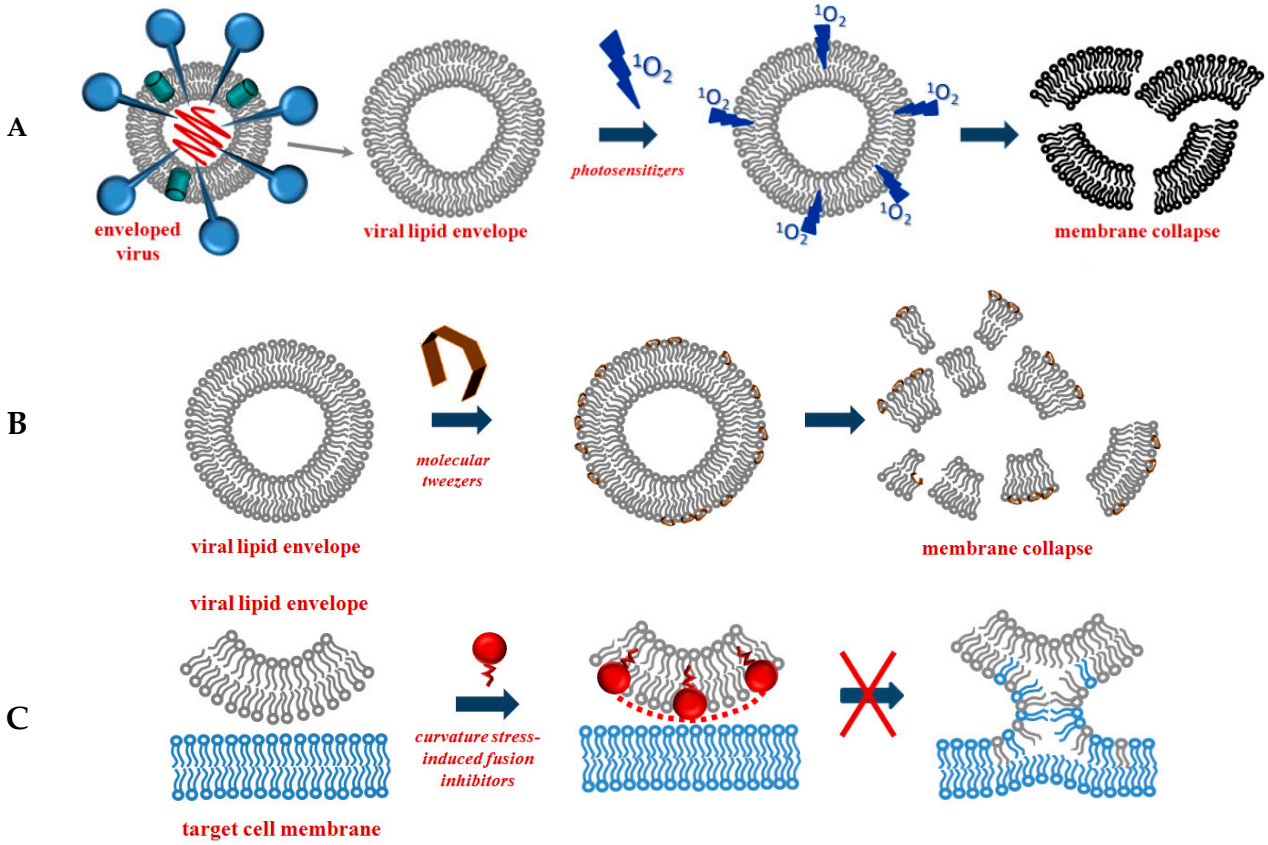

Figure 8. Modes of action of lipid-targeting antivirals: photosensitizers (**A**); molecular tweezers (**B**); curvature stress-induced fusion inhibitors (**C**).

Hypericin, a plant-occurring polycyclic quinone, demonstrated broad-spectrum activity against enveloped viruses such as human immunodeficiency virus type 1 (HIV-1), Moloney murine leukemia virus, equine infectious anemia virus, vesicular stomatitis virus (VSV), herpes simplex virus types 1 (HSV-1) and 2 (HSV-2), parainfluenza virus (PIV), vaccinia virus, murine cytomegalovirus (mCMV), and Sindbis virus (SINV) [466–471] (Table 7). *Hypericin* did not alter non-enveloped viruses [467]. Halogen derivatives of hypericin were shown to be effective against HSV-1 [472,473]. *Gymnochromes* isolated from *Gymnocrinus richer* were shown to be highly potent antiviral agents against dengue virus, HSV-1, and influenza virus type A (IVA) [474,475] (Table 7). *Hypocrellins* from *Hypocrella bambuase* also demonstrated light-dependent anti-HIV, anti-mCMV, anti-HSV-1, anti-VSV, and anti-IVA efficacy [469,476–478] (Table 7), while the non-enveloped virus was not inactivated [477].

Initially, *rigid amphipathic perylene-containing nucleoside derivatives*, particularly 5- (perylen-3-yl)ethynyl-2′-deoxy-uridine (*dUY11*) and 5-(perylen-3-yl)ethynyl-arabino-uridine (aUY11), having considerable activity against IVA, hepatitis C (HCV), HSV-1, HSV-2, mCMV, VSV, SINV, tick-borne encephalitis virus (TBEV), yellow fever virus (YFV), Chikungunya virus (CHIKV), African swine fever virus, PIV, and human respiratory syncytial virus (RSV) (Table 7), were believed to inhibit viral fusion by affecting membrane curvature stress (Section 3.2) [479–481]; however, later, their action through the photosensitization of viruses was postulated [482–487]. No activity or the non-specific activity of perylene derivatives against non-enveloped viruses was found [480,488]. Non-nucleoside perylene derivatives also showed promising antiviral activity [489].

BODIPY-based photosensitizer 2,6-diiodo-1,3,5,7-tetramethyl-8-(N-methyl-4-pyridyl)-4,4′-difluoroboradiazaindacene (*DIMPy-BODIPY*) exhibited the photodynamic inactivation of dengue virus and VSV at nanomolar concentrations [490].

A class of thiazolidine-based lipophilic inhibitors of *LJ* and *JL* series demonstrating high activity against a variety of enveloped viruses (Table 7), with no effect on the infection

of non-enveloped viruses, was also originally described as curvature-induced antivirals (Section 3.2), but it was later shown that the compounds act as membrane-targeted photosensitizers [491–493].

Cationic *imidazolyl* and *pyridyl porphyrins* were characterized as promising photosensitizing antivirals against SARS-CoV-2 and HSV-1 [494,495]. A natural *chlorine* photosensitizer, pheophorbide a, inactivates HSV-1, HSV-2, MERS-CoV, SARS-CoV-2, YFV, HCV, and SINV, by targeting the lipid envelope [496,497] (Table 7).

Table 7. Photosensitizers and their antiviral activity.

Photosensitizer	Structure	Virus	IC_{50}, μM	Reference
hypericin	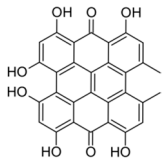	HIV-1	0.44	[466]
		HSV-1	0.006	[469]
gymnochrome B	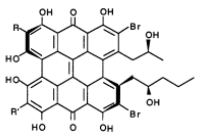	dengue	0.029	[475]
hypocrellin A	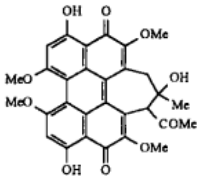	HSV-1	0.015	[469]
hypocrellin B	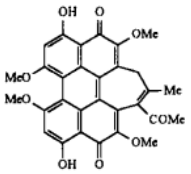	HSV-1	0.025	[469]
5-(perylen-3-yl)ethynyl-2′-deoxy-uridine (dUY11)	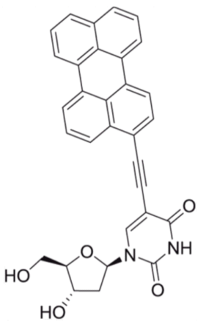	IVA	0.097–2.7	[480,498]
		HSV-1	0.048–0.131	[479]
		HSV-2	0.031–0.055	[479,480]
		HCV	0.183–0.187	[479,480]
		mCMV	0.037 ± 0.016	[480]
		SINV	0.006 ± 0.001	[480]
		TBEV	0.024 ± 0.013	[483,499]
		PIV	2.2 ± 0.5	[498]
		RSV	1.8 ± 0.2	[498]
		SARS-CoV-2	0.2564	[487]

Table 7. *Cont.*

Photosensitizer	Structure	Virus	IC_{50}, μM	Reference
5-(perylen-3-yl)ethynyl-arabino-uridine (aUY11)	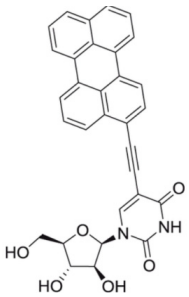	IVA	0.078–5.2	[480,498]
		HSV-1	0.048 ± 0.012	[479]
		HSV-2	0.052 ± 0.003	[480]
		HCV	0.107 ± 0.041	[480]
		mCMV	0.013 ± 0.004	[480]
		SINV	0.011 ± 0.005	[479]
		TBEV	0.018 ± 0.010	[483]
		YFV	0.0086 ± 0.0007	[484]
		CHIKV	<0.78	[484]
		PIV	1.3 ± 0.3	[498]
		RSV	2.3 ± 0.1	[498]
		SARS-CoV-2	0.4058	[487]
(5Z)-5-[(5-phenylfuran-2-yl)methylidene]-3-prop-2-enyl-2-sulfanylidene-1,3-thiazolidin-4-one (LJ-001)	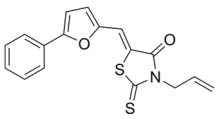	HIV	0.133	[492]
		Newcastle disease virus	0.095	[492]
		Ebola virus	0.9	[492]
		IVA	0.026	[492]
		Nipah virus	0.048	[492]
		Hendra virus	0.018	[492]
		Rift valley fever virus	0.02	[492]
		Semliki forest virus	0.537	[492]
		HSV-1	0.02	[492]
		hCMV	0.13	[492]
		VSV	0.298	[492]
(Z) 3-ethyl-5-[5-(2-methoxyphenyl)-furan-2-ylmethylene]oxazolid-ine-2,4-dithione (JL-103)	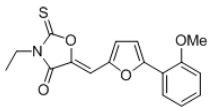	HIV	0.013	[492]
		Newcastle disease virus	0.004	[492]
		Ebola virus	0.185	[492]
		IVA	0.002	[492]
		Nipah virus	0.004	[492]
		Hendra viru	0.0005	[492]
		Rift valley fever virus	0.003	[492]
		Semliki forest virus	0.044	[492]
		HSV-1	0.002	[492]
		hCMV	0.004	[492]
		VSV	0.011	[492]

Table 7. *Cont.*

Photosensitizer	Structure	Virus	IC_{50}, μM	Reference
5,15-bis(1,3-dimethylimidazol-2-yl)chlorin (ICH-Me2+)	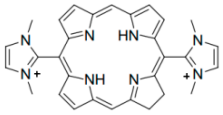	SARS-CoV-2	0.12	[494]
pheophorbide a	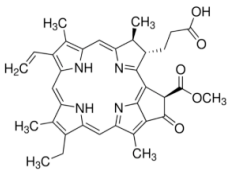	SARS-CoV-2	0.18	[497]
		MERS-CoV	0.18	[497]

IC_{50} is determined at photoactivation.

4.1.2. Tweezers

Molecular tweezers are membrane-destabilizing agents that can disrupt the virus lipid envelope and can be used as broad-spectrum antivirals against influenza A virus, respiratory syncytial virus, human immunodeficiency virus, herpes simplex viruses, human cytomegalovirus, Ebola and Marburg viruses, SARS-CoV, SARS-CoV-2, MERS-CoV, and other enveloped viruses. These small molecules act as pincers that bind lipid head groups and disrupt lipid ordering and packing in the virus lipid envelope, which results in the virions being unable to infect the cells [500] (Figure 8B).

A basing compound, *CLR01*, was shown to inhibit HIV-1, Ebola, Zika, herpes simplex (HSV-1, HSV-2), measles, influenza virus, and SARS-CoV-2 infection by directly targeting the viral membrane [501–503] (Table 8). Its close analog, *CLR05*, also possessed broad-spectrum antiviral activity [500]. *CLR01* and *CLR05* did not reduce infection by the non-enveloped adenovirus and encephalomyocarditis virus [500]. The membrane-disrupting and, consequently, the antiviral activity of *CLR01* might be substantially potentiated by the introduction of C_4, C_7, or aromatic radicals to each phosphate group [500,503] (Table 8).

Table 8. Molecular tweezers and their antiviral activity.

Molecular Tweezer	Structure	Virus	IC_{50}, μM	Reference
CLR01	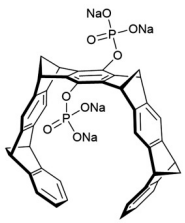	HIV-1	13.7–20.1	[501]
		Ebola	25.8	[502]
		Zika	8.2	[502]
		HSV-1	19.3	[500]
		HSV-2		
		measles		
		IVA		
		SARS-CoV-2	76.7	[503]
CLR05	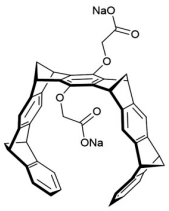	Zika	38.1	[500]
		HSV-1		
		HSV-2		
		measles		
		influenza		
		SARS-CoV-2	167.3	[503]

Table 8. *Cont.*

Molecular Tweezer	Structure	Virus	IC_{50}, μM	Reference
CLR01e	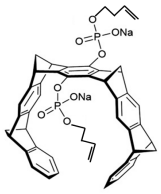	HIV-1	~10	[500]
CLR01f	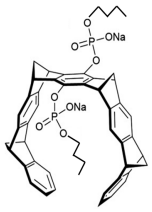	HIV-1	~7	[500]
CP006	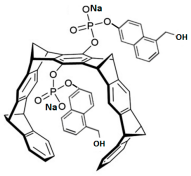	SARS-CoV-2	0.3	[503]
CP020	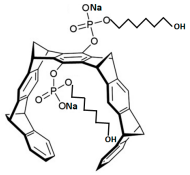	SARS-CoV-2	0.4	[503]
CP025	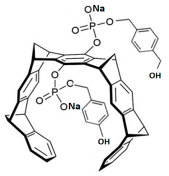	SARS-CoV-2	0.6	[503]
CP036	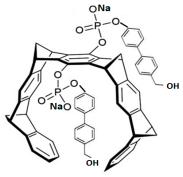	SARS-CoV-2	0.2	[503]

4.1.3. Antimicrobial Peptides

Although many antimicrobial peptides, especially *defensins* and *cathelicidins*, have been shown to possess antiviral effects [273,504,505], the mechanisms of antiviral action are highly pleiotropic and involve more than simply a direct effect on the viral membrane. Regarding the focus of this section, *bomidin*, a naturally occurring antimicrobial peptide that is active against a variety of enveloped viruses, including SARS-CoV-2, HSV, dengue virus, and CHIKV, was supposed to disrupt the viral membrane [506]. *Plantaricin NC8 αβ*, a two-peptide bacteriocin produced by *Lactobacillus plantarum* strains, was shown to inhibit SARS-CoV-2, IVA, flaviviruses Langat and Kunjin, and HIV-1, via permeabilizing and destroying their envelopes [507] (Table 9). It was demonstrated that the anti-HIV activity of a cyclic peptide from plants, *kalata B1*, resulted from the disruption of the membranes of HIV particles due to their raft-like lipid density and enrichment with PE [508].

Table 9. Antimicrobial peptides with direct antiviral action through lipid envelope disruption.

Antimicrobial Peptide	Structure	Virus	IC_{50}, μM	Reference
D-plantaricin NC8 α	Asp – Leu – Thr – Thr – Lys – Leu – Trp – Ser – Ser Trp – Gly – Tyr – Tyr – Leu – Gly – Lys – Lys – Ala Arg – Trp – Asn – Leu – Lys – His – Pro – Tyr – Val	SARS-CoV-2	~0.001	[507]
		IVA	~0.1	[507]
kalata B1	Gly – Leu – Pro – Val – Cys – Gly – Glu – Thr – Cys – Val – Gly – Gly – Thr – Cys – Asn – Thr – Pro – Gly – Cys – Thr – Cys – Ser – Trp – Pro – Val – Cys – Thr – Arg – Asn	HIV	~2–5	[508]

4.2. Fusion Inhibitors Affecting Membrane Fluidity and/or Curvature Stress

An essential step in the fusion of an enveloped virus with a cell is the fusion of their lipid membranes. It is believed that this occurs in several successive stages, one of which includes the assembly of the contiguous outer lipid leaflets of the membranes to constitute an intermediate stalk. The stalk is characterized by a negative spontaneous curvature, corresponding to this formation via the cone-shaped lipids of an inverted hexagonal phase (H_{II}) [509,510]. The induction of positive curvature stress by putative antiviral agents is believed to prevent the generation of fusion intermediates of negative curvature (Figure 8C).

Lipophosphoglycan dramatically reduced the fusion of Sendai virus and IVA with host cells [511,512], while it raised the bilayer-to-H_{II}-phase transition temperature of phosphatidyletanolamine, indicating the elevation of positive curvature stress by lipophosphoglycan [511].

Naturally occurring and synthetic lipopeptides appear to be the most promising candidates when taking into account their amphiphilicity and cone shape, which suggests the induction of positive curvature when incorporated into a lipid monolayer. A simple lipopeptide sequence, myr-WD, was shown to successfully combat IVA and murine coronavirus infections by modulating the membrane lipid packing and surface potential [513]. *Surfactin*, a cyclic lipopeptide from *B. subtilis*, was found to inhibit porcine epidemic diarrhea virus and transmissible gastroenteritis virus infections via affecting curvature stress [514]. The dependence of the efficiency of surfactins to inhibit VSV, HSV-1, and Semliki forest virus on the length of the hydrocarbon "tail" was in good agreement with their membrane targeting [515]. Recently, the ability of several lipopeptides to successfully inhibit SARS-CoV-2 fusion with *Vero* cells was shown [516] (Table 10). The most effective compounds were also characterized by their marked ability to increase the transition temperature of phosphatidylethanolamine from the lamellar to H_{II} phase, i.e., induce a positive curvature stress [516]. Interestingly, simpler molecules, such as black pepper alkaloid piperine, show a similar ability to suppress SARS-CoV-2 infection [517].

Table 10. Fusion inhibitors affecting membrane curvature stress and their antiviral activity.

Inhibitor	Structure	Virus	IC_{50}, μM	Reference
aculeacin A	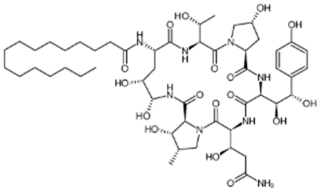	SARS-CoV-2	1.3 ± 0.3	[517]

Table 10. *Cont.*

Inhibitor	Structure	Virus	IC_{50}, μM	Reference
anidulafungin	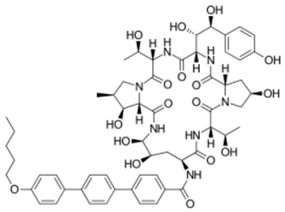	SARS-CoV-2	4.7 ± 0.9	[517]
iturin A	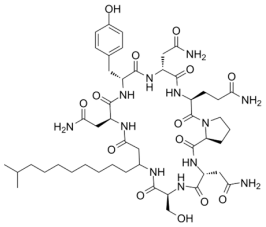	SARS-CoV-2	10.9 ± 2.0	[517]
mycosubtilin	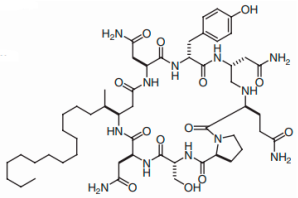	SARS-CoV-2	2.3 ± 0.3	[517]

5. Conclusions

(i) Due to principal differences in the organization of fatty acid synthase systems in bacteria and mammals, the specific inhibitors of bacterial key enzymes, especially the acetyl-CoA-carboxylase complex, various β-ketoacyl-ACP synthases, different NADPH-dependent reductases, β-hydroxyacyl-ACP dehydrases, and acyl-phosphate:glycerol-3-phosphate acyltransferase, are attractive targets for the development of low-toxicity antibacterials.

(ii) The pathway for the synthesis of the lipid fatty acid tails in fungi is similar to that in mammalian cells and, therefore, is not very promising in the search for potential antifungals.

(iii) The presence of a single fundamental pathway for the synthesis of the phospholipid heads in both prokaryotes and eukaryotes makes the majority of the involved enzymes poor targets for antibiotic therapy in bacterial and fungal infections.

(iv) Many enzymes of the lipopolysaccharide (Kdo_2-lipid A) biosynthetic pathway in Gram-negative bacteria (UDP-N-acetylglucosamine acyltransferase, UDP-3-*O*-(*R*-3-hydroxyacyl)glucosamine N-acyltransferase, UDP-3-*O*-(*R*-3-hydroxyacyl)-*N*-acetyl-glucosamine deacetylase, and UDP-diacylglucosamine pyrophosphohydrolase) are identified as targets for antibiotic development.

(v) Sphingolipid biosynthetic pathways are conserved from yeast to humans, and the enzymes cannot serve as targets for low-toxicity antifungals. Some inhibitors of inositol-phosphoceramide synthase demonstrate promisingly low effective concentrations.

(vi) The most effective approach when targeting fungal lipid biosynthesis is to search for inhibitors of enzymes in the ergosterol pathway, especially squalene epoxidase, lanosterol 14α-demethylase, and sterol C14-reductase/sterol C8,7-isomerase.

(vii) A preference given to inhibitors that simultaneously act on two enzymes of the lipid biosynthetic pathway or the combination of inhibitors with agents directly affecting the pathogen membrane should reduce the risk of developing antibiotic resistance in pathogenic strains.

(viii) Natural antimicrobial agents exert their defensive activities via pathogen membrane disruption due to pore formation or the disordering of membrane lipids. Due to the high efficiency of naturally occurring antimicrobial agents, their broad-spectrum antibacterial/antifungal/antiviral effect, and their low rate of resistance in pathogen strains, the use of antimicrobial peptides, lipopeptides, and polyenes is a good anti-infective therapeutic strategy.

(ix) The lipid envelope of viruses should be considered as a target for innovative antivirals, disrupting the membranes of virions or inducing curvature stress and inhibiting viral entry.

Author Contributions: Conceptualization, S.S.E. and O.S.O.; formal analysis, S.S.E. and O.S.O.; investigation, S.S.E. and O.S.O.; resources, S.S.E. and O.S.O.; data curation, S.S.E. and O.S.O.; writing—original draft preparation, S.S.E. and O.S.O.; writing—review and editing, O.S.O.; supervision, O.S.O.; project administration, O.S.O.; funding acquisition, O.S.O. All authors have read and agreed to the published version of the manuscript.

Funding: This study was funded by the Russian Foundation of Science # 22-15-00417.

Conflicts of Interest: The authors declare no conflict of interest.

References

1. Kim, D.; Kim, S.; Kwon, Y.; Kim, Y.; Park, H.; Kwak, K.; Lee, H.; Lee, J.H.; Jang, K.M.; Kim, D.; et al. Structural Insights for β-Lactam Antibiotics. *Biomol. Ther.* **2023**, *31*, 141–147. [CrossRef] [PubMed]
2. Dumas, F.; Haanappel, E. Lipids in infectious diseases—The case of AIDS and tuberculosis. *Biochim. Biophys. Acta Biomembr.* **2017**, *1859*, 1636–1647. [CrossRef]
3. Mochalkin, I.; Miller, J.R.; Narasimhan, L.; Thanabal, V.; Erdman, P.; Cox, P.B.; Prasad, J.V.; Lightle, S.; Huband, M.D.; Stover, C.K. Discovery of antibacterial biotin carboxylase inhibitors by virtual screening and fragment-based approaches. *ACS Chem. Biol.* **2009**, *4*, 473–483. [CrossRef]
4. Cheng, C.C.; Shipps, G.W., Jr.; Yang, Z.; Sun, B.; Kawahata, N.; Soucy, K.A.; Soriano, A.; Orth, P.; Xiao, L.; Mann, P.; et al. Discovery and optimization of antibacterial AccC inhibitors. *Bioorg. Med. Chem. Lett.* **2009**, *19*, 6507–6514. [CrossRef]
5. Freiberg, C.; Pohlmann, J.; Nell, P.G.; Endermann, R.; Schuhmacher, J.; Newton, B.; Otteneder, M.; Lampe, T.; Häbich, D.; Ziegelbauer, K. Novel bacterial acetyl coenzyme A carboxylase inhibitors with antibiotic efficacy in vivo. *Antimicrob. Agents Chemother.* **2006**, *50*, 2707–2712. [CrossRef]
6. Khandekar, S.S.; Gentry, D.R.; Van Aller, G.S.; Warren, P.; Xiang, H.; Silverman, C.; Doyle, M.L.; Chambers, P.A.; Konstantinidis, A.K.; Brandt, M.; et al. Identification, substrate specificity, and inhibition of the *Streptococcus pneumoniae* beta-ketoacyl-acyl carrier protein synthase III (FabH). *J. Biol. Chem.* **2001**, *276*, 30024–30030. [CrossRef]
7. Choi, K.H.; Kremer, L.; Besra, G.S.; Rock, C.O. Identification and substrate specificity of beta -ketoacyl (acyl carrier protein) synthase III (mtFabH) from *Mycobacterium tuberculosis*. *J. Biol. Chem.* **2000**, *275*, 28201–28207. [CrossRef] [PubMed]
8. Price, A.C.; Choi, K.H.; Heath, R.J.; Li, Z.; White, S.W.; Rock, C.O. Inhibition of beta-ketoacyl-acyl carrier protein synthases by thiolactomycin and cerulenin. Structure and mechanism. *J. Biol. Chem.* **2001**, *276*, 6551–6559. [CrossRef] [PubMed]
9. Tsay, J.T.; Rock, C.O.; Jackowski, S. Overproduction of beta-ketoacyl-acyl carrier protein synthase I imparts thiolactomycin resistance to *Escherichia coli* K-12. *J. Bacteriol.* **1992**, *174*, 508–513. [CrossRef]
10. Wang, J.; Kodali, S.; Lee, S.H.; Galgoci, A.; Painter, R.; Dorso, K.; Racine, F.; Motyl, M.; Hernandez, L.; Tinney, E.; et al. Discovery of platencin, a dual FabF and FabH inhibitor with in vivo antibiotic properties. *Proc. Natl. Acad. Sci. USA* **2007**, *104*, 7612–7616. [CrossRef] [PubMed]
11. Jayasuriya, H.; Herath, K.B.; Zhang, C.; Zink, D.L.; Basilio, A.; Genilloud, O.; Diez, M.T.; Vicente, F.; Gonzalez, I.; Salazar, O.; et al. Isolation and structure of platencin: A FabH and FabF dual inhibitor with potent broad-spectrum antibiotic activity. *Angew. Chem. Int. Ed. Engl.* **2007**, *46*, 4684–4688. [CrossRef]
12. Wang, J.; Soisson, S.M.; Young, K.; Shoop, W.; Kodali, S.; Galgoci, A.; Painter, R.; Parthasarathy, G.; Tang, Y.S.; Cummings, R.; et al. Platensimycin is a selective FabF inhibitor with potent antibiotic properties. *Nature* **2006**, *441*, 358–361. [CrossRef]
13. Zhang, Y.M.; Rock, C.O. Evaluation of epigallocatechin gallate and related plant polyphenols as inhibitors of the FabG and FabI reductases of bacterial type II fatty-acid synthase. *J. Biol. Chem.* **2004**, *279*, 30994–31001. [CrossRef]
14. Tasdemir, D.; Lack, G.; Brun, R.; Rüedi, P.; Scapozza, L.; Perozzo, R. Inhibition of *Plasmodium falciparum* fatty acid biosynthesis: Evaluation of FabG, FabZ, and FabI as drug targets for flavonoids. *J. Med. Chem.* **2006**, *49*, 3345–3353. [CrossRef] [PubMed]
15. Belluti, F.; Perozzo, R.; Lauciello, L.; Colizzi, F.; Kostrewa, D.; Bisi, A.; Gobbi, S.; Rampa, A.; Bolognesi, M.L.; Recanatini, M.; et al. Design, synthesis, and biological and crystallographic evaluation of novel inhibitors of *Plasmodium falciparum* enoyl-ACP-reductase (PfFabI). *J. Med. Chem.* **2013**, *56*, 7516–7526. [CrossRef] [PubMed]

16. Kirmizibekmez, H.; Calis, I.; Perozzo, R.; Brun, R.; Dönmez, A.A.; Linden, A.; Rüedi, P.; Tasdemir, D. Inhibiting activities of the secondary metabolites of Phlomis brunneogaleata against parasitic protozoa and plasmodial enoyl-ACP Reductase, a crucial enzyme in fatty acid biosynthesis. *Planta Med.* **2004**, *70*, 711–717. [CrossRef]
17. Sohn, M.J.; Zheng, C.J.; Kim, W.G. Macrolactin S, a new antibacterial agent with FabG-inhibitory activity from *Bacillus* sp. AT28. *J. Antibiot.* **2008**, *61*, 687–691. [CrossRef] [PubMed]
18. Bhowruth, V.; Brown, A.K.; Besra, G.S. Synthesis and biological evaluation of NAS-21 and NAS-91 analogues as potential inhibitors of the mycobacterial FAS-II dehydratase enzyme Rv0636. *Microbiology* **2008**, *154*, 1866–1875. [CrossRef]
19. McGillick, B.E.; Kumaran, D.; Vieni, C.; Swaminathan, S. β-Hydroxyacyl-acyl Carrier Protein Dehydratase (FabZ) from *Francisella tularensis* and *Yersinia pestis*: Structure Determination, Enzymatic Characterization, and Cross-Inhibition Studies. *Biochemistry* **2016**, *55*, 1091–1099. [CrossRef]
20. Chen, J.; Zhang, L.; Zhang, Y.; Zhang, H.; Du, J.; Ding, J.; Guo, Y.; Jiang, H.; Shen, X. Emodin targets the beta-hydroxyacyl-acyl carrier protein dehydratase from *Helicobacter pylori*: Enzymatic inhibition assay with crystal structural and thermodynamic characterization. *BMC Microbiol.* **2009**, *9*, 91. [CrossRef]
21. Kumar, V.; Sharma, A.; Pratap, S.; Kumar, P. Biochemical and biophysical characterization of 1,4-naphthoquinone as a dual inhibitor of two key enzymes of type II fatty acid biosynthesis from *Moraxella catarrhalis*. *Biochim. Biophys. Acta Proteins Proteom.* **2018**, *1866*, 1131–1142. [CrossRef] [PubMed]
22. Kong, Y.H.; Zhang, L.; Yang, Z.Y.; Han, C.; Hu, L.H.; Jiang, H.L.; Shen, X. Natural product juglone targets three key enzymes from *Helicobacter pylori*: Inhibition assay with crystal structure characterization. *Acta Pharmacol. Sin.* **2008**, *29*, 870–876. [CrossRef] [PubMed]
23. Zheng, C.J.; Sohn, M.J.; Lee, S.; Kim, W.G. Meleagrin, a new FabI inhibitor from *Penicillium chryosogenum* with at least one additional mode of action. *PLoS ONE* **2013**, *8*, e78922. [CrossRef] [PubMed]
24. Kim, Y.G.; Seo, J.H.; Kwak, J.H.; Shin, K.J. Discovery of a potent enoyl-acyl carrier protein reductase (FabI) inhibitor suitable for antistaphylococcal agent. *Bioorg. Med. Chem. Lett.* **2015**, *25*, 4481–4486. [CrossRef] [PubMed]
25. Kwon, Y.J.; Kim, H.J.; Kim, W.G. Complestatin exerts antibacterial activity by the inhibition of fatty acid synthesis. *Biol. Pharm. Bull.* **2015**, *38*, 715–721. [CrossRef]
26. Surolia, N.; Surolia, A. Triclosan offers protection against blood stages of malaria by inhibiting enoyl-ACP reductase of *Plasmodium falciparum*. *Nat. Med.* **2001**, *7*, 167–173. [CrossRef]
27. Yao, J.; Abdelrahman, Y.M.; Robertson, R.M.; Cox, J.V.; Belland, R.J.; White, S.W.; Rock, C.O. Type II fatty acid synthesis is essential for the replication of *Chlamydia trachomatis*. *J. Biol. Chem.* **2014**, *289*, 22365–22376. [CrossRef]
28. Yogiara; Mordukhova, E.A.; Kim, D.; Kim, W.G.; Hwang, J.K.; Pan, J.G. The food-grade antimicrobial xanthorrhizol targets the enoyl-ACP reductase (FabI) in *Escherichia coli*. *Bioorg. Med. Chem. Lett.* **2020**, *30*, 127651. [CrossRef]
29. Cho, J.Y.; Kwon, Y.J.; Sohn, M.J.; Seok, S.J.; Kim, W.G. Phellinstatin, a new inhibitor of enoyl-ACP reductase produced by the medicinal fungus *Phellinus linteus*. *Bioorg. Med. Chem. Lett.* **2011**, *21*, 1716–1718. [CrossRef]
30. Kim, Y.J.; Sohn, M.J.; Kim, W.G. Chalcomoracin and moracin C, new inhibitors of *Staphylococcus aureus* enoyl-acyl carrier protein reductase from Morus alba. *Biol. Pharm. Bull.* **2012**, *35*, 791–795. [CrossRef]
31. Kwon, Y.J.; Fang, Y.; Xu, G.H.; Kim, W.G. Aquastatin A, a new inhibitor of enoyl-acyl carrier protein reductase from *Sporothrix* sp. FN611. *Biol. Pharm. Bull.* **2009**, *32*, 2061–2064. [CrossRef]
32. Zheng, C.J.; Sohn, M.J.; Kim, W.G. Atromentin and leucomelone, the first inhibitors specific to enoyl-ACP reductase (FabK) of *Streptococcus pneumoniae*. *J. Antibiot.* **2006**, *59*, 808–812. [CrossRef] [PubMed]
33. Grimes, K.D.; Lu, Y.J.; Zhang, Y.M.; Luna, V.A.; Hurdle, J.G.; Carson, E.I.; Qi, J.; Kudrimoti, S.; Rock, C.O.; Lee, R.E. Novel acyl phosphate mimics that target PlsY, an essential acyltransferase in gram-positive bacteria. *ChemMedChem* **2008**, *3*, 1936–1945. [CrossRef] [PubMed]
34. Cherian, P.T.; Yao, J.; Leonardi, R.; Maddox, M.M.; Luna, V.A.; Rock, C.O.; Lee, R.E. Acyl-sulfamates target the essential glycerol-phosphate acyltransferase (PlsY) in Gram-positive bacteria. *Bioorg. Med. Chem.* **2012**, *20*, 4985–4994. [CrossRef] [PubMed]
35. Jiang, X.; Duan, Y.; Zhou, B.; Guo, Q.; Wang, H.; Hang, X.; Zeng, L.; Jia, J.; Bi, H. The Cyclopropane Fatty Acid Synthase Mediates Antibiotic Resistance and Gastric Colonization of *Helicobacter pylori*. *J. Bacteriol.* **2019**, *201*, e00374-19. [CrossRef]
36. Parsons, J.B.; Rock, C.O. Bacterial lipids: Metabolism and membrane homeostasis. *Prog. Lipid Res.* **2013**, *52*, 249–276. [CrossRef]
37. Larson, E.C.; Lim, A.L.; Pond, C.D.; Craft, M.; Čavužić, M.; Waldrop, G.L.; Schmidt, E.W.; Barrows, L.R. Pyrrolocin C and equisetin inhibit bacterial acetyl-CoA carboxylase. *PLoS ONE* **2020**, *15*, e0233485. [CrossRef] [PubMed]
38. Freiberg, C.; Brunner, N.A.; Schiffer, G.; Lampe, T.; Pohlmann, J.; Brands, M.; Raabe, M.; Häbich, D.; Ziegelbauer, K. Identification and characterization of the first class of potent bacterial acetyl-CoA carboxylase inhibitors with antibacterial activity. *J. Biol. Chem.* **2004**, *279*, 26066–26073. [CrossRef] [PubMed]
39. Freiberg, C.; Fischer, H.P.; Brunner, N.A. Discovering the mechanism of action of novel antibacterial agents through transcriptional profiling of conditional mutants. *Antimicrob. Agents Chemother.* **2005**, *49*, 749–759. [CrossRef]
40. Pohlmann, J.; Lampe, T.; Shimada, M.; Nell, P.G.; Pernerstorfer, J.; Svenstrup, N.; Brunner, N.A.; Schiffer, G.; Freiberg, C. Pyrrolidinedione derivatives as antibacterial agents with a novel mode of action. *Bioorg. Med. Chem. Lett.* **2005**, *15*, 1189–1192. [CrossRef]

41. Toor, H.G.; Banerjee, D.I.; Chauhan, J.B. In Silico Evaluation of Human Cathelicidin LL-37 as a Novel Therapeutic Inhibitor of Panton-Valentine Leukocidin Toxin of Methicillin-Resistant *Staphylococcus aureus*. *Microb. Drug Resist.* **2021**, *27*, 602–615. [CrossRef]
42. Liu, X.; Fortin, P.D.; Walsh, C.T. Andrimid producers encode an acetyl-CoA carboxyltransferase subunit resistant to the action of the antibiotic. *Proc. Natl. Acad. Sci. USA* **2008**, *105*, 13321–13326. [CrossRef]
43. Silvers, M.A.; Robertson, G.T.; Taylor, C.M.; Waldrop, G.L. Design, synthesis, and antibacterial properties of dual-ligand inhibitors of acetyl-CoA carboxylase. *J. Med. Chem.* **2014**, *57*, 8947–8959. [CrossRef] [PubMed]
44. Zhang, W.; Wei, S.; Wu, W. Preliminary studies on the antibacterial mechanism of Yanglingmycin. *Pestic. Biochem. Physiol.* **2018**, *147*, 27–31. [CrossRef] [PubMed]
45. Kuldeep, J.; Sharma, S.K.; Singh, B.N.; Siddiqi, M.I. Computational exploration and anti-mycobacterial activity of potential inhibitors of *Mycobacterium tuberculosis* acetyl coenzyme A carboxylase as anti-tubercular agents. *SAR QSAR Environ. Res.* **2021**, *32*, 191–205. [CrossRef] [PubMed]
46. Kumar, V.; Sharma, A.; Pratap, S.; Kumar, P. Biophysical and in silico interaction studies of aporphine alkaloids with Malonyl-CoA: ACP transacylase (FabD) from drug resistant *Moraxella catarrhalis*. *Biochimie* **2018**, *149*, 18–33. [CrossRef] [PubMed]
47. Heath, R.J.; Rock, C.O. Inhibition of beta-ketoacyl-acyl carrier protein synthase III (FabH) by acyl-acyl carrier protein in *Escherichia coli*. *J. Biol. Chem.* **1996**, *271*, 10996–11000. [CrossRef] [PubMed]
48. Choi, K.H.; Heath, R.J.; Rock, C.O. Beta-ketoacyl-acyl carrier protein synthase III (FabH) is a determining factor in branched-chain fatty acid biosynthesis. *J. Bacteriol.* **2000**, *182*, 365–370. [CrossRef] [PubMed]
49. Qiu, X.; Choudhry, A.E.; Janson, C.A.; Grooms, M.; Daines, R.A.; Lonsdale, J.T.; Khandekar, S.S. Crystal structure and substrate specificity of the beta-ketoacyl-acyl carrier protein synthase III (FabH) from *Staphylococcus aureus*. *Protein Sci.* **2005**, *14*, 2087–2094. [CrossRef]
50. Musayev, F.; Sachdeva, S.; Scarsdale, J.N.; Reynolds, K.A.; Wright, H.T. Crystal structure of a substrate complex of *Mycobacterium tuberculosis* beta-ketoacyl-acyl carrier protein synthase III (FabH) with lauroyl-coenzyme A. *J. Mol. Biol.* **2005**, *346*, 1313–1321. [CrossRef]
51. Luo, Y.; Yang, Y.S.; Fu, J.; Zhu, H.L. Novel FabH inhibitors: A patent and article literature review (2000—2012). *Expert. Opin. Ther. Pat.* **2012**, *22*, 1325–1336. [CrossRef]
52. Wallace, K.K.; Lobo, S.; Han, L.; McArthur, H.A.; Reynolds, K.A. In vivo and In vitro effects of thiolactomycin on fatty acid biosynthesis in *Streptomyces collinus*. *J. Bacteriol.* **1997**, *179*, 3884–3891. [CrossRef]
53. Han, L.; Lobo, S.; Reynolds, K.A. Characterization of beta-ketoacyl-acyl carrier protein synthase III from *Streptomyces glaucescens* and its role in initiation of fatty acid biosynthesis. *J. Bacteriol.* **1998**, *180*, 4481–4486. [CrossRef]
54. Alhamadsheh, M.M.; Waters, N.C.; Huddler, D.P.; Kreishman-Deitrick, M.; Florova, G.; Reynolds, K.A. Synthesis and biological evaluation of thiazolidine-2-one 1,1-dioxide as inhibitors of *Escherichia coli* beta-ketoacyl-ACP-synthase III (FabH). *Bioorg. Med. Chem. Lett.* **2007**, *17*, 879–883. [CrossRef]
55. Li, H.Q.; Shi, L.; Li, Q.S.; Liu, P.G.; Luo, Y.; Zhao, J.; Zhu, H.L. Synthesis of C(7) modified chrysin derivatives designing to inhibit beta-ketoacyl-acyl carrier protein synthase III (FabH) as antibiotics. *Bioorg. Med. Chem.* **2009**, *17*, 6264–6269. [CrossRef] [PubMed]
56. Lv, P.C.; Wang, K.R.; Yang, Y.; Mao, W.J.; Chen, J.; Xiong, J.; Zhu, H.L. Design, synthesis and biological evaluation of novel thiazole derivatives as potent FabH inhibitors. *Bioorg. Med. Chem. Lett.* **2009**, *19*, 6750–6754. [CrossRef] [PubMed]
57. Li, H.Q.; Luo, Y.; Lv, P.C.; Shi, L.; Liu, C.H.; Zhu, H.L. Design and synthesis of novel deoxybenzoin derivatives as FabH inhibitors and anti-inflammatory agents. *Bioorg. Med. Chem. Lett.* **2010**, *20*, 2025–2028. [CrossRef] [PubMed]
58. Cheng, K.; Zheng, Q.Z.; Qian, Y.; Shi, L.; Zhao, J.; Zhu, H.L. Synthesis, antibacterial activities and molecular docking studies of peptide and Schiff bases as targeted antibiotics. *Bioorg. Med. Chem.* **2009**, *17*, 7861–7871. [CrossRef] [PubMed]
59. Shi, L.; Fang, R.Q.; Zhu, Z.W.; Yang, Y.; Cheng, K.; Zhong, W.Q.; Zhu, H.L. Design and synthesis of potent inhibitors of beta-ketoacyl-acyl carrier protein synthase III (FabH) as potential antibacterial agents. *Eur. J. Med. Chem.* **2010**, *45*, 4358–4364. [CrossRef] [PubMed]
60. Cheng, K.; Zheng, Q.Z.; Hou, J.; Zhou, Y.; Liu, C.H.; Zhao, J.; Zhu, H.L. Synthesis, molecular modeling and biological evaluation of PSB as targeted antibiotics. *Bioorg. Med. Chem.* **2010**, *18*, 2447–2455. [CrossRef] [PubMed]
61. Lv, P.C.; Sun, J.; Luo, Y.; Yang, Y.; Zhu, H.L. Design, synthesis, and structure-activity relationships of pyrazole derivatives as potential FabH inhibitors. *Bioorg. Med. Chem. Lett.* **2010**, *20*, 4657–4660. [CrossRef]
62. Zhang, H.J.; Zhu, D.D.; Li, Z.L.; Sun, J.; Zhu, H.L. Synthesis, molecular modeling and biological evaluation of β-ketoacyl-acyl carrier protein synthase III (FabH) as novel antibacterial agents. *Bioorg. Med. Chem.* **2011**, *19*, 4513–4519. [CrossRef]
63. Li, H.Q.; Luo, Y.; Zhu, H.L. Discovery of vinylogous carbamates as a novel class of β-ketoacyl-acyl carrier protein synthase III (FabH) inhibitors. *Bioorg. Med. Chem.* **2011**, *19*, 4454–4459. [CrossRef]
64. Li, Z.L.; Li, Q.S.; Zhang, H.J.; Hu, Y.; Zhu, D.D.; Zhu, H.L. Design, synthesis and biological evaluation of urea derivatives from o-hydroxybenzylamines and phenylisocyanate as potential FabH inhibitors. *Bioorg. Med. Chem.* **2011**, *19*, 4413–4420. [CrossRef]
65. Luo, Y.; Zhang, L.R.; Hu, Y.; Zhang, S.; Fu, J.; Wang, X.M.; Zhu, H.L. Synthesis and antimicrobial activities of oximes derived from O-benzylhydroxylamine as FabH inhibitors. *ChemMedChem* **2012**, *7*, 1587–1593. [CrossRef] [PubMed]
66. Zhou, Y.; Du, Q.R.; Sun, J.; Li, J.R.; Fang, F.; Li, D.D.; Qian, Y.; Gong, H.B.; Zhao, J.; Zhu, H.L. Novel Schiff-base-derived FabH inhibitors with dioxygenated rings as antibiotic agents. *ChemMedChem* **2013**, *8*, 433–441. [CrossRef] [PubMed]

67. Wang, X.L.; Zhang, Y.B.; Tang, J.F.; Yang, Y.S.; Chen, R.Q.; Zhang, F.; Zhu, H.L. Design, synthesis and antibacterial activities of vanillic acylhydrazone derivatives as potential β-ketoacyl-acyl carrier protein synthase III (FabH) inhibitors. *Eur. J. Med. Chem.* **2012**, *57*, 373–382. [CrossRef] [PubMed]
68. Li, Y.; Luo, Y.; Hu, Y.; Zhu, D.D.; Zhang, S.; Liu, Z.J.; Gong, H.B.; Zhu, H.L. Design, synthesis and antimicrobial activities of nitroimidazole derivatives containing 1,3,4-oxadiazole scaffold as FabH inhibitors. *Bioorg. Med. Chem.* **2012**, *20*, 4316–4322. [CrossRef] [PubMed]
69. Yang, Y.S.; Zhang, F.; Gao, C.; Zhang, Y.B.; Wang, X.L.; Tang, J.F.; Sun, J.; Gong, H.B.; Zhu, H.L. Discovery and modification of sulfur-containing heterocyclic pyrazoline derivatives as potential novel class of β-ketoacyl-acyl carrier protein synthase III (FabH) inhibitors. *Bioorg. Med. Chem. Lett.* **2012**, *22*, 4619–4624. [CrossRef]
70. Li, Y.; Zhao, C.P.; Ma, H.P.; Zhao, M.Y.; Xue, Y.R.; Wang, X.M.; Zhu, H.L. Design, synthesis and antimicrobial activities evaluation of Schiff base derived from secnidazole derivatives as potential FabH inhibitors. *Bioorg. Med. Chem.* **2013**, *21*, 3120–3126. [CrossRef] [PubMed]
71. Li, J.R.; Li, D.D.; Wang, R.R.; Sun, J.; Dong, J.J.; Du, Q.R.; Fang, F.; Zhang, W.M.; Zhu, H.L. Design and synthesis of thiazole derivatives as potent FabH inhibitors with antibacterial activity. *Eur. J. Med. Chem.* **2014**, *75*, 438–447. [CrossRef] [PubMed]
72. Duan, Y.T.; Wang, Z.C.; Sang, Y.L.; Tao, X.X.; Teraiya, S.B.; Wang, P.F.; Wen, Q.; Zhou, X.J.; Ding, L.; Yang, Y.H.; et al. Design and synthesis of 2-styryl of 5-Nitroimidazole derivatives and antimicrobial activities as FabH inhibitors. *Eur. J. Med. Chem.* **2014**, *76*, 387–396. [CrossRef] [PubMed]
73. Song, X.; Yang, Y.; Zhao, J.; Chen, Y. Synthesis and antibacterial activity of cinnamaldehyde acylhydrazone with a 1,4-benzodioxan fragment as a novel class of potent β-ketoacyl-acyl carrier protein synthase III (FabH) inhibitor. *Chem. Pharm. Bull.* **2014**, *62*, 1110–1118. [CrossRef]
74. Segretti, N.D.; Serafim, R.A.; Segretti, M.C.; Miyata, M.; Coelho, F.R.; Augusto, O.; Ferreira, E.I. New antibacterial agents: Hybrid bioisoster derivatives as potential *E. coli* FabH inhibitors. *Bioorg. Med. Chem. Lett.* **2016**, *26*, 3988–3993. [CrossRef]
75. Zhou, Y.; Yang, Y.S.; Song, X.D.; Lu, L.; Zhu, H.L. Study of Schiff-Base-Derived with Dioxygenated Rings and Nitrogen Heterocycle as Potential β-Ketoacyl-acyl Carrier Protein Synthase III (FabH) Inhibitors. *Chem. Pharm. Bull.* **2017**, *65*, 178–185. [CrossRef] [PubMed]
76. He, X.; Reynolds, K.A. Purification, characterization, and identification of novel inhibitors of the beta-ketoacyl-acyl carrier protein synthase III (FabH) from *Staphylococcus aureus*. *Antimicrob. Agents Chemother.* **2002**, *46*, 1310–1318. [CrossRef]
77. He, X.; Reeve, A.M.; Desai, U.R.; Kellogg, G.E.; Reynolds, K.A. 1,2-dithiole-3-ones as potent inhibitors of the bacterial 3-ketoacyl acyl carrier protein synthase III (FabH). *Antimicrob. Agents Chemother.* **2004**, *48*, 3093–3102. [CrossRef]
78. Pishchany, G.; Mevers, E.; Ndousse-Fetter, S.; Horvath, D.J., Jr.; Paludo, C.R.; Silva-Junior, E.A.; Koren, S.; Skaar, E.P.; Clardy, J.; Kolter, R. Amycomicin is a potent and specific antibiotic discovered with a targeted interaction screen. *Proc. Natl. Acad. Sci. USA* **2018**, *115*, 10124–10129. [CrossRef]
79. Singh, S.; Soni, L.K.; Gupta, M.K.; Prabhakar, Y.S.; Kaskhedikar, S.G. QSAR studies on benzoylaminobenzoic acid derivatives as inhibitors of beta-ketoacyl-acyl carrier protein synthase III. *Eur. J. Med. Chem.* **2008**, *43*, 1071–1080. [CrossRef]
80. Nie, Z.; Perretta, C.; Lu, J.; Su, Y.; Margosiak, S.; Gajiwala, K.S.; Cortez, J.; Nikulin, V.; Yager, K.M.; Appelt, K.; et al. Structure-based design, synthesis, and study of potent inhibitors of beta-ketoacyl-acyl carrier protein synthase III as potential antimicrobial agents. *J. Med. Chem.* **2005**, *48*, 1596–1609. [CrossRef]
81. Ashek, A.; Cho, S.J. A combined approach of docking and 3D QSAR study of beta-ketoacyl-acyl carrier protein synthase III (FabH) inhibitors. *Bioorg. Med. Chem.* **2006**, *14*, 1474–1482. [CrossRef]
82. Jones, P.B.; Parrish, N.M.; Houston, T.A.; Stapon, A.; Bansal, N.P.; Dick, J.D.; Townsend, C.A. A new class of antituberculosis agents. *J. Med. Chem.* **2000**, *43*, 3304–3314. [CrossRef] [PubMed]
83. Alhamadsheh, M.M.; Musayev, F.; Komissarov, A.A.; Sachdeva, S.; Wright, H.T.; Scarsdale, N.; Florova, G.; Reynolds, K.A. Alkyl-CoA disulfides as inhibitors and mechanistic probes for FabH enzymes. *Chem. Biol.* **2007**, *14*, 513–524. [CrossRef] [PubMed]
84. Liu, Y.; Zhong, W.; Li, R.J.; Li, S. Synthesis of potent inhibitors of β-ketoacyl-acyl carrier protein synthase III as potential antimicrobial agents. *Molecules* **2012**, *17*, 4770–4781. [CrossRef]
85. Borgaro, J.G.; Chang, A.; Machutta, C.A.; Zhang, X.; Tonge, P.J. Substrate recognition by β-ketoacyl-ACP synthases. *Biochemistry* **2011**, *50*, 10678–10686. [CrossRef] [PubMed]
86. Huang, W.; Jia, J.; Edwards, P.; Dehesh, K.; Schneider, G.; Lindqvist, Y. Crystal structure of beta-ketoacyl-acyl carrier protein synthase II from *E.coli* reveals the molecular architecture of condensing enzymes. *EMBO J.* **1998**, *17*, 1183–1191. [CrossRef]
87. Qiu, X.; Janson, C.A.; Konstantinidis, A.K.; Nwagwu, S.; Silverman, C.; Smith, W.W.; Khandekar, S.; Lonsdale, J.; Abdel-Meguid, S.S. Crystal structure of beta-ketoacyl-acyl carrier protein synthase III. A key condensing enzyme in bacterial fatty acid biosynthesis. *J. Biol. Chem.* **1999**, *274*, 36465–36471. [CrossRef]
88. Olsen, J.G.; Kadziola, A.; von Wettstein-Knowles, P.; Siggaard-Andersen, M.; Lindquist, Y.; Larsen, S. The X-ray crystal structure of beta-ketoacyl [acyl carrier protein] synthase I. *FEBS Lett.* **1999**, *460*, 46–52. [CrossRef]
89. Davies, C.; Heath, R.J.; White, S.W.; Rock, C.O. The 1.8 A crystal structure and active-site architecture of beta-ketoacyl-acyl carrier protein synthase III (FabH) from *Escherichia coli*. *Structure* **2000**, *8*, 185–195. [CrossRef]
90. Heath, R.J.; White, S.W.; Rock, C.O. Inhibitors of fatty acid synthesis as antimicrobial chemotherapeutics. *Appl. Microbiol. Biotechnol.* **2002**, *58*, 695–703. [CrossRef]

91. Bommineni, G.R.; Kapilashrami, K.; Cummings, J.E.; Lu, Y.; Knudson, S.E.; Gu, C.; Walker, S.G.; Slayden, R.A.; Tonge, P.J. Thiolactomycin-Based Inhibitors of Bacterial β-Ketoacyl-ACP Synthases with in Vivo Activity. *J. Med. Chem.* **2016**, *59*, 5377–5390. [CrossRef] [PubMed]
92. Rudolf, J.D.; Dong, L.B.; Manoogian, K.; Shen, B. Biosynthetic Origin of the Ether Ring in Platensimycin. *J. Am. Chem. Soc.* **2016**, *138*, 16711–16721. [CrossRef] [PubMed]
93. Manallack, D.T.; Crosby, I.T.; Khakham, Y.; Capuano, B. Platensimycin: A promising antimicrobial targeting fatty acid synthesis. *Curr. Med. Chem.* **2008**, *15*, 705–710. [CrossRef] [PubMed]
94. Moustafa, G.A.I.; Nojima, S.; Yamano, Y.; Aono, A.; Arai, M.; Mitarai, S.; Tanaka, T.; Yoshimitsu, T. Potent growth inhibitory activity of (±)-platencin towards multi-drug-resistant and extensively drug-resistant *Mycobacterium tuberculosis*. *Med. Chem. Commun.* **2013**, *4*, 720–723. [CrossRef]
95. Brown, A.K.; Taylor, R.C.; Bhatt, A.; Fütterer, K.; Besra, G.S. Platensimycin activity against mycobacterial beta-ketoacyl-ACP synthases. *PLoS ONE* **2009**, *4*, e6306. [CrossRef] [PubMed]
96. Das, M.; Sakha Ghosh, P.; Manna, K. A Review on Platensimycin: A Selective FabF Inhibitor. *Int. J. Med. Chem.* **2016**, *2016*, 9706753. [CrossRef] [PubMed]
97. Martens, E.; Demain, A.L. Platensimycin and platencin: Promising antibiotics for future application in human medicine. *J. Antibiot.* **2011**, *64*, 705–710. [CrossRef]
98. Shang, R.; Liang, J.; Yi, Y.; Liu, Y.; Wang, J. Review of Platensimycin and Platencin: Inhibitors of β-Ketoacyl-acyl Carrier Protein (ACP) Synthase III (FabH). *Molecules* **2015**, *20*, 16127–16141. [CrossRef]
99. Su, M.; Qiu, L.; Deng, Y.; Ruiz, C.H.; Rudolf, J.D.; Dong, L.B.; Feng, X.; Cameron, M.D.; Shen, B.; Duan, Y.; et al. Evaluation of Platensimycin and Platensimycin-Inspired Thioether Analogues against Methicillin-Resistant *Staphylococcus aureus* in Topical and Systemic Infection Mouse Models. *Mol. Pharm.* **2019**, *16*, 3065–3071. [CrossRef]
100. Deng, Y.; Weng, X.; Li, Y.; Su, M.; Wen, Z.; Ji, X.; Ren, N.; Shen, B.; Duan, Y.; Huang, Y. Late-Stage Functionalization of Platensimycin Leading to Multiple Analogues with Improved Antibacterial Activity In vitro and in Vivo. *J. Med. Chem.* **2019**, *62*, 6682–6693. [CrossRef]
101. Feng, Z.; Chakraborty, D.; Dewell, S.B.; Reddy, B.V.; Brady, S.F. Environmental DNA-encoded antibiotics fasamycins A and B inhibit FabF in type II fatty acid biosynthesis. *J. Am. Chem. Soc.* **2012**, *134*, 2981–2987. [CrossRef]
102. Zheng, Z.; Parsons, J.B.; Tangallapally, R.; Zhang, W.; Rock, C.O.; Lee, R.E. Discovery of novel bacterial elongation condensing enzyme inhibitors by virtual screening. *Bioorg. Med. Chem. Lett.* **2014**, *24*, 2585–2588. [CrossRef]
103. Wickramasinghe, S.R.; Inglis, K.A.; Urch, J.E.; Müller, S.; van Aalten, D.M.; Fairlamb, A.H. Kinetic, inhibition and structural studies on 3-oxoacyl-ACP reductase from *Plasmodium falciparum*, a key enzyme in fatty acid biosynthesis. *Biochem. J.* **2006**, *393*, 447–457. [CrossRef]
104. Kristan, K.; Bratkovic, T.; Sova, M.; Gobec, S.; Prezelj, A.; Urleb, U. Novel inhibitors of beta-ketoacyl-ACP reductase from *Escherichia coli*. *Chem. Biol. Interact.* **2009**, *178*, 310–316. [CrossRef] [PubMed]
105. Vella, P.; Rudraraju, R.S.; Lundbäck, T.; Axelsson, H.; Almqvist, H.; Vallin, M.; Schneider, G.; Schnell, R. A FabG inhibitor targeting an allosteric binding site inhibits several orthologs from Gram-negative ESKAPE pathogens. *Bioorg. Med. Chem.* **2021**, *30*, 115898. [CrossRef] [PubMed]
106. Cukier, C.D.; Hope, A.G.; Elamin, A.A.; Moynie, L.; Schnell, R.; Schach, S.; Kneuper, H.; Singh, M.; Naismith, J.H.; Lindqvist, Y.; et al. Discovery of an allosteric inhibitor binding site in 3-Oxo-acyl-ACP reductase from *Pseudomonas aeruginosa*. *ACS Chem. Biol.* **2013**, *8*, 2518–2527. [CrossRef]
107. Hu, J.; Webster, D.; Cao, J.; Shao, A. The safety of green tea and green tea extract consumption in adults—Results of a systematic review. *Regul. Toxicol. Pharmacol.* **2018**, *95*, 412–433. [CrossRef] [PubMed]
108. Zakharova, A.A.; Efimova, S.S.; Ostroumova, O.S. Lipid Microenvironment Modulates the Pore-Forming Ability of Polymyxin B. *Antibiotics* **2022**, *11*, 1445. [CrossRef]
109. Chernyshova, D.N.; Tyulin, A.A.; Ostroumova, O.S.; Efimova, S.S. Discovery of the Potentiator of the Pore-Forming Ability of Lantibiotic Nisin: Perspectives for Anticancer Therapy. *Membranes* **2022**, *12*, 1166. [CrossRef] [PubMed]
110. Efimova, S.S.; Malykhina, A.I.; Ostroumova, O.S. Triggering the Amphotericin B Pore-Forming Activity by Phytochemicals. *Membranes* **2023**, *13*, 670. [CrossRef]
111. Sharma, S.K.; Kapoor, M.; Ramya, T.N.; Kumar, S.; Kumar, G.; Modak, R.; Sharma, S.; Surolia, N.; Surolia, A. Identification, characterization, and inhibition of Plasmodium falciparum beta-hydroxyacyl-acyl carrier protein dehydratase (FabZ). *J. Biol. Chem.* **2003**, *278*, 45661–45671. [CrossRef]
112. He, L.; Zhang, L.; Liu, X.; Li, X.; Zheng, M.; Li, H.; Yu, K.; Chen, K.; Shen, X.; Jiang, H.; et al. Discovering potent inhibitors against the beta-hydroxyacyl-acyl carrier protein dehydratase (FabZ) of *Helicobacter pylori*: Structure-based design, synthesis, bioassay, and crystal structure determination. *J. Med. Chem.* **2009**, *52*, 2465–2481. [CrossRef]
113. Saling, S.C.; Comar, J.F.; Mito, M.S.; Peralta, R.M.; Bracht, A. Actions of juglone on energy metabolism in the rat liver. *Toxicol. Appl. Pharmacol.* **2011**, *257*, 319–327. [CrossRef]
114. Zhu, K.; Choi, K.H.; Schweizer, H.P.; Rock, C.O.; Zhang, Y.M. Two aerobic pathways for the formation of unsaturated fatty acids in *Pseudomonas aeruginosa*. *Mol. Microbiol.* **2006**, *60*, 260–273. [CrossRef] [PubMed]

115. Leesong, M.; Henderson, B.S.; Gillig, J.R.; Schwab, J.M.; Smith, J.L. Structure of a dehydratase-isomerase from the bacterial pathway for biosynthesis of unsaturated fatty acids: Two catalytic activities in one active site. *Structure* **1996**, *4*, 253–264. [CrossRef] [PubMed]
116. Clark, D.P.; DeMendoza, D.; Polacco, M.L.; Cronan, J.E., Jr. Beta-hydroxydecanoyl thio ester dehydrase does not catalyze a rate-limiting step in *Escherichia coli* unsaturated fatty acid synthesis. *Biochemistry* **1983**, *22*, 5897–5902. [CrossRef] [PubMed]
117. Marrakchi, H.; Choi, K.H.; Rock, C.O. A new mechanism for anaerobic unsaturated fatty acid formation in *Streptococcus pneumoniae*. *J. Biol. Chem.* **2002**, *277*, 44809–44816. [CrossRef]
118. Fozo, E.M.; Quivey, R.G., Jr. The *fabM* gene product of *Streptococcus mutans* is responsible for the synthesis of monounsaturated fatty acids and is necessary for survival at low pH. *J. Bacteriol.* **2004**, *186*, 4152–4158. [CrossRef]
119. Wang, H.; Cronan, J.E. Functional replacement of the FabA and FabB proteins of *Escherichia coli* fatty acid synthesis by *Enterococcus faecalis* FabZ and FabF homologues. *J. Biol. Chem.* **2004**, *279*, 34489–34495. [CrossRef]
120. Bi, H.; Wang, H.; Cronan, J.E. FabQ, a dual-function dehydratase/isomerase, circumvents the last step of the classical fatty acid synthesis cycle. *Chem. Biol.* **2013**, *20*, 1157–1167. [CrossRef]
121. Altabe, S.G.; Aguilar, P.; Caballero, G.M.; de Mendoza, D. The *Bacillus subtilis* acyl lipid desaturase is a delta5 desaturase. *J. Bacteriol.* **2003**, *185*, 3228–3231. [CrossRef]
122. Moynié, L.; Leckie, S.M.; McMahon, S.A.; Duthie, F.G.; Koehnke, A.; Taylor, J.W.; Alphey, M.S.; Brenk, R.; Smith, A.D.; Naismith, J.H. Structural insights into the mechanism and inhibition of the β-hydroxydecanoyl-acyl carrier protein dehydratase from *Pseudomonas aeruginosa*. *J. Mol. Biol.* **2013**, *425*, 365–377. [CrossRef]
123. Moynié, L.; Hope, A.G.; Finzel, K.; Schmidberger, J.; Leckie, S.M.; Schneider, G.; Burkart, M.D.; Smith, A.D.; Gray, D.W.; Naismith, J.H. A Substrate Mimic Allows High-Throughput Assay of the FabA Protein and Consequently the Identification of a Novel Inhibitor of Pseudomonas aeruginosa FabA. *J. Mol. Biol.* **2016**, *428*, 108–120. [CrossRef] [PubMed]
124. McMurry, L.M.; Oethinger, M.; Levy, S.B. Triclosan targets lipid synthesis. *Nature* **1998**, *394*, 531–532. [CrossRef] [PubMed]
125. Perozzo, R.; Kuo, M.; Sidhu, A.; Valiyaveettil, J.T.; Bittman, R.; Jacobs, W.R., Jr.; Fidock, D.A.; Sacchettini, J.C. Structural elucidation of the specificity of the antibacterial agent triclosan for malarial enoyl acyl carrier protein reductase. *J. Biol. Chem.* **2002**, *277*, 13106–13114. [CrossRef] [PubMed]
126. Sivaraman, S.; Sullivan, T.J.; Johnson, F.; Novichenok, P.; Cui, G.; Simmerling, C.; Tonge, P.J. Inhibition of the bacterial enoyl reductase FabI by triclosan: A structure-reactivity analysis of FabI inhibition by triclosan analogues. *J. Med. Chem.* **2004**, *47*, 509–518. [CrossRef] [PubMed]
127. Park, H.S.; Yoon, Y.M.; Jung, S.J.; Yun, I.N.; Kim, C.M.; Kim, J.M.; Kwak, J.H. CG400462, a new bacterial enoyl-acyl carrier protein reductase (FabI) inhibitor. *Int. J. Antimicrob. Agents* **2007**, *30*, 446–451. [CrossRef]
128. Park, H.S.; Yoon, Y.M.; Jung, S.J.; Kim, C.M.; Kim, J.M.; Kwak, J.H. Antistaphylococcal activities of CG400549, a new bacterial enoyl-acyl carrier protein reductase (FabI) inhibitor. *J. Antimicrob. Chemother.* **2007**, *60*, 568–574. [CrossRef]
129. Sampson, P.B.; Picard, C.; Handerson, S.; McGrath, T.E.; Domagala, M.; Leeson, A.; Romanov, V.; Awrey, D.E.; Thambipillai, D.; Bardouniotis, E.; et al. Spiro-naphthyridinone piperidines as inhibitors of *S. aureus* and *E. coli* enoyl-ACP reductase (FabI). *Bioorg. Med. Chem. Lett.* **2009**, *19*, 5355–5358. [CrossRef]
130. Ramnauth, J.; Surman, M.D.; Sampson, P.B.; Forrest, B.; Wilson, J.; Freeman, E.; Manning, D.D.; Martin, F.; Toro, A.; Domagala, M.; et al. 2,3,4,5-Tetrahydro-1H-pyrido[2,3-b and e][1,4]diazepines as inhibitors of the bacterial enoyl ACP reductase, FabI. *Bioorg. Med. Chem. Lett.* **2009**, *19*, 5359–5362. [CrossRef]
131. Escaich, S.; Prouvensier, L.; Saccomani, M.; Durant, L.; Oxoby, M.; Gerusz, V.; Moreau, F.; Vongsouthi, V.; Maher, K.; Morrissey, I.; et al. The MUT056399 inhibitor of FabI is a new antistaphylococcal compound. *Antimicrob. Agents Chemother.* **2011**, *55*, 4692–4697. [CrossRef]
132. Banevicius, M.A.; Kaplan, N.; Hafkin, B.; Nicolau, D.P. Pharmacokinetics, pharmacodynamics and efficacy of novel FabI inhibitor AFN-1252 against MSSA and MRSA in the murine thigh infection model. *J. Chemother.* **2013**, *25*, 26–31. [CrossRef]
133. Schiebel, J.; Chang, A.; Shah, S.; Lu, Y.; Liu, L.; Pan, P.; Hirschbeck, M.W.; Tareilus, M.; Eltschkner, S.; Yu, W.; et al. Rational design of broad spectrum antibacterial activity based on a clinically relevant enoyl-acyl carrier protein (ACP) reductase inhibitor. *J. Biol. Chem.* **2014**, *289*, 15987–16005. [CrossRef]
134. Mandal, S.; Parish, T. A Novel Benzoxaborole Is Active against *Escherichia coli* and Binds to FabI. *Antimicrob. Agents Chemother.* **2021**, *65*, e0262220. [CrossRef] [PubMed]
135. Yao, J.; Maxwell, J.B.; Rock, C.O. Resistance to AFN-1252 arises from missense mutations in *Staphylococcus aureus* enoyl-acyl carrier protein reductase (FabI). *J. Biol. Chem.* **2013**, *288*, 36261–36271. [CrossRef]
136. Mehboob, S.; Song, J.; Hevener, K.E.; Su, P.C.; Boci, T.; Brubaker, L.; Truong, L.; Mistry, T.; Deng, J.; Cook, J.L.; et al. Structural and biological evaluation of a novel series of benzimidazole inhibitors of Francisella tularensis enoyl-ACP reductase (FabI). *Bioorg. Med. Chem. Lett.* **2015**, *25*, 1292–1296. [CrossRef] [PubMed]
137. Takahata, S.; Iida, M.; Yoshida, T.; Kumura, K.; Kitagawa, H.; Hoshiko, S. Discovery of 4-Pyridone derivatives as specific inhibitors of enoyl-acyl carrier protein reductase (FabI) with antibacterial activity against *Staphylococcus aureus*. *J. Antibiot.* **2007**, *60*, 123–128. [CrossRef]
138. Wang, S.F.; Yin, Y.; Wu, X.; Qiao, F.; Sha, S.; Lv, P.C.; Zhao, J.; Zhu, H.L. Synthesis, molecular docking and biological evaluation of coumarin derivatives containing piperazine skeleton as potential antibacterial agents. *Bioorg. Med. Chem.* **2014**, *22*, 5727–5737. [CrossRef]

139. Hu, Y.; Shen, Y.; Wu, X.; Tu, X.; Wang, G.X. Synthesis and biological evaluation of coumarin derivatives containing imidazole skeleton as potential antibacterial agents. *Eur. J. Med. Chem.* **2018**, *143*, 958–969. [CrossRef] [PubMed]
140. Kwon, J.; Mistry, T.; Ren, J.; Johnson, M.E.; Mehboob, S. A novel series of enoyl reductase inhibitors targeting the ESKAPE pathogens, *Staphylococcus aureus* and *Acinetobacter baumannii*. *Bioorg. Med. Chem.* **2018**, *26*, 65–76. [CrossRef]
141. Davis, M.C.; Franzblau, S.G.; Martin, A.R. Syntheses and evaluation of benzodiazaborine compounds against *M. tuberculosis* H37Rv In vitro. *Bioorg. Med. Chem. Lett.* **1998**, *8*, 843–846. [CrossRef] [PubMed]
142. Rodriguez, F.; Saffon, N.; Sammartino, J.C.; Degiacomi, G.; Pasca, M.R.; Lherbet, C. First triclosan-based macrocyclic inhibitors of InhA enzyme. *Bioorg. Chem.* **2020**, *95*, 103498. [CrossRef] [PubMed]
143. Manjunatha, U.H.; Rao, S.P.S.; Kondreddi, R.R.; Noble, C.G.; Camacho, L.R.; Tan, B.H.; Ng, S.H.; Ng, P.S.; Ma, N.L.; Lakshminarayana, S.B.; et al. Direct inhibitors of InhA are active against *Mycobacterium tuberculosis*. *Sci. Transl. Med.* **2015**, *7*, 269ra3. [CrossRef] [PubMed]
144. Shirude, P.S.; Madhavapeddi, P.; Naik, M.; Murugan, K.; Shinde, V.; Nandishaiah, R.; Bhat, J.; Kumar, A.; Hameed, S.; Holdgate, G.; et al. Methyl-thiazoles: A novel mode of inhibition with the potential to develop novel inhibitors targeting InhA in *Mycobacterium tuberculosis*. *J. Med. Chem.* **2013**, *56*, 8533–8542. [CrossRef]
145. Šink, R.; Sosič, I.; Živec, M.; Fernandez-Menendez, R.; Turk, S.; Pajk, S.; Alvarez-Gomez, D.; Lopez-Roman, E.M.; Gonzales-Cortez, C.; Rullas-Triconado, J.; et al. Design, synthesis, and evaluation of new thiadiazole-based direct inhibitors of enoyl acyl carrier protein reductase (InhA) for the treatment of tuberculosis. *J. Med. Chem.* **2015**, *58*, 613–624. [CrossRef] [PubMed]
146. Joshi, S.D.; Dixit, S.R.; Kulkarni, V.H.; Lherbet, C.; Nadagouda, M.N.; Aminabhavi, T.M. Synthesis, biological evaluation and in silico molecular modeling of pyrrolyl benzohydrazide derivatives as enoyl ACP reductase inhibitors. *Eur. J. Med. Chem.* **2017**, *126*, 286–297. [CrossRef]
147. Rotta, M.; Pissinate, K.; Villela, A.D.; Back, D.F.; Timmers, L.F.; Bachega, J.F.; de Souza, O.N.; Santos, D.S.; Basso, L.A.; Machado, P. Piperazine derivatives: Synthesis, inhibition of the *Mycobacterium tuberculosis* enoyl-acyl carrier protein reductase and SAR studies. *Eur. J. Med. Chem.* **2015**, *90*, 436–447. [CrossRef]
148. Chollet, A.; Mori, G.; Menendez, C.; Rodriguez, F.; Fabing, I.; Pasca, M.R.; Madacki, J.; Korduláková, J.; Constant, P.; Quémard, A.; et al. Design, synthesis and evaluation of new GEQ derivatives as inhibitors of InhA enzyme and *Mycobacterium tuberculosis* growth. *Eur. J. Med. Chem.* **2015**, *101*, 218–235. [CrossRef]
149. Hartkoorn, R.C.; Sala, C.; Neres, J.; Pojer, F.; Magnet, S.; Mukherjee, R.; Uplekar, S.; Boy-Röttger, S.; Altmann, K.H.; Cole, S.T. Towards a new tuberculosis drug: Pyridomycin—Nature's isoniazid. *EMBO Mol. Med.* **2012**, *4*, 1032–1042. [CrossRef]
150. Karioti, A.; Skaltsa, H.; Zhang, X.; Tonge, P.J.; Perozzo, R.; Kaiser, M.; Franzblau, S.G.; Tasdemir, D. Inhibiting enoyl-ACP reductase (FabI) across pathogenic microorganisms by linear sesquiterpene lactones from *Anthemis auriculata*. *Phytomedicine* **2008**, *15*, 1125–1129. [CrossRef]
151. Brenwald, N.P.; Fraise, A.P. Triclosan resistance in methicillin-resistant *Staphylococcus aureus* (MRSA). *J. Hosp. Infect.* **2003**, *55*, 141–144. [CrossRef] [PubMed]
152. Yu, B.J.; Kim, J.A.; Pan, J.G. Signature gene expression profile of triclosan-resistant *Escherichia coli*. *J. Antimicrob. Chemother.* **2010**, *65*, 1171–1177. [CrossRef] [PubMed]
153. Ciusa, M.L.; Furi, L.; Knight, D.; Decorosi, F.; Fondi, M.; Raggi, C.; Coelho, J.R.; Aragones, L.; Moce, L.; Visa, P.; et al. A novel resistance mechanism to triclosan that suggests horizontal gene transfer and demonstrates a potential selective pressure for reduced biocide susceptibility in clinical strains of *Staphylococcus aureus*. *Int. J. Antimicrob. Agents* **2012**, *40*, 210–220. [CrossRef] [PubMed]
154. Chuanchuen, R.; Beinlich, K.; Hoang, T.T.; Becher, A.; Karkhoff-Schweizer, R.R.; Schweizer, H.P. Cross-resistance between triclosan and antibiotics in *Pseudomonas aeruginosa* is mediated by multidrug efflux pumps: Exposure of a susceptible mutant strain to triclosan selects nfxB mutants overexpressing MexCD-OprJ. *Antimicrob. Agents Chemother.* **2001**, *45*, 428–432. [CrossRef]
155. Wang, L.; Mao, B.; He, H.; Shang, Y.; Zhong, Y.; Yu, Z.; Yang, Y.; Li, H.; An, J. Comparison of hepatotoxicity and mechanisms induced by triclosan (TCS) and methyl-triclosan (MTCS) in human liver hepatocellular HepG2 cells. *Toxicol. Res.* **2018**, *8*, 38–45. [CrossRef]
156. Marrakchi, H.; Dewolf, W.E., Jr.; Quinn, C.; West, J.; Polizzi, B.J.; So, C.Y.; Holmes, D.J.; Reed, S.L.; Heath, R.J.; Payne, D.J.; et al. Characterization of *Streptococcus pneumoniae* enoyl-(acyl-carrier protein) reductase (FabK). *Biochem. J.* **2003**, *370*, 1055–1062. [CrossRef]
157. Heath, R.J.; Rock, C.O. A triclosan-resistant bacterial enzyme. *Nature* **2000**, *406*, 145–146. [CrossRef]
158. Heath, R.J.; Su, N.; Murphy, C.K.; Rock, C.O. The enoyl-[acyl-carrier-protein] reductases FabI and FabL from *Bacillus subtilis*. *J. Biol. Chem.* **2000**, *275*, 40128–40133. [CrossRef]
159. Huang, Y.H.; Lin, J.S.; Ma, J.C.; Wang, H.H. Functional Characterization of Triclosan-Resistant Enoyl-acyl-carrier Protein Reductase (FabV) in *Pseudomonas aeruginosa*. *Front. Microbiol.* **2016**, *7*, 1903. [CrossRef]
160. Kim, S.H.; Khan, R.; Choi, K.; Lee, S.W.; Rhee, S. A triclosan-resistance protein from the soil metagenome is a novel enoyl-acyl carrier protein reductase: Structure-guided functional analysis. *FEBS J.* **2020**, *287*, 4710–4728. [CrossRef]
161. Seefeld, M.A.; Miller, W.H.; Newlander, K.A.; Burgess, W.J.; DeWolf, W.E., Jr.; Elkins, P.A.; Head, M.S.; Jakas, D.R.; Janson, C.A.; Keller, P.M.; et al. Indole naphthyridinones as inhibitors of bacterial enoyl-ACP reductases FabI and FabK. *J. Med. Chem.* **2003**, *46*, 1627–1635. [CrossRef]

162. Takahata, S.; Iida, M.; Osaki, Y.; Saito, J.; Kitagawa, H.; Ozawa, T.; Yoshida, T.; Hoshiko, S. AG205, a novel agent directed against FabK of *Streptococcus pneumoniae*. *Antimicrob. Agents Chemother.* **2006**, *50*, 2869–2871. [CrossRef] [PubMed]
163. Mahfuz, A.M.U.B.; Stambuk Opazo, F.; Aguilar, L.F.; Iqbal, M.N. Carfilzomib as a potential inhibitor of NADH-dependent enoyl-acyl carrier protein reductases of *Klebsiella pneumoniae* and *Mycobacterium tuberculosis* as a drug target enzyme: Insights from molecular docking and molecular dynamics. *J. Biomol. Struct. Dyn.* **2022**, *40*, 4021–4037. [CrossRef] [PubMed]
164. Zhang, Y.M.; Rock, C.O. Thematic review series: Glycerolipids. Acyltransferases in bacterial glycerophospholipid synthesis. *J. Lipid Res.* **2008**, *49*, 1867–1874. [CrossRef] [PubMed]
165. De Mendoza, D.; Klages Ulrich, A.; Cronan, J.E., Jr. Thermal regulation of membrane fluidity in *Escherichia coli*. Effects of overproduction of beta-ketoacyl-acyl carrier protein synthase I. *J. Biol. Chem.* **1983**, *258*, 2098–2101. [CrossRef]
166. Cronan, J.E., Jr.; Weisberg, L.J.; Allen, R.G. Regulation of membrane lipid synthesis in *Escherichia coli*. Accumulation of free fatty acids of abnormal length during inhibition of phospholipid synthesis. *J. Biol. Chem.* **1975**, *250*, 5835–5840. [CrossRef]
167. Bell, R.M. Mutants of *Escherichia coli* defective in membrane phospholipid synthesis. Properties of wild type and Km defective sn-glycerol-3-phosphate acyltransferase activities. *J. Biol. Chem.* **1975**, *250*, 7147–7152. [CrossRef]
168. Lu, Y.J.; Zhang, Y.M.; Grimes, K.D.; Qi, J.; Lee, R.E.; Rock, C.O. Acyl-phosphates initiate membrane phospholipid synthesis in Gram-positive pathogens. *Mol. Cell* **2006**, *23*, 765–772. [CrossRef]
169. Greenway, D.L.; Silbert, D.F. Altered acyltransferase activity in *Escherichia coli* associated with mutations in acyl coenzyme A synthetase. *J. Biol. Chem.* **1983**, *258*, 13034–13042. [CrossRef]
170. Brinster, S.; Lamberet, G.; Staels, B.; Trieu-Cuot, P.; Gruss, A.; Poyart, C. Type II fatty acid synthesis is not a suitable antibiotic target for Gram-positive pathogens. *Nature* **2009**, *458*, 83–86. [CrossRef]
171. Morvan, C.; Halpern, D.; Kénanian, G.; Hays, C.; Anba-Mondoloni, J.; Brinster, S.; Kennedy, S.; Trieu-Cuot, P.; Poyart, C.; Lamberet, G.; et al. Environmental fatty acids enable emergence of infectious *Staphylococcus aureus* resistant to FASII-targeted antimicrobials. *Nat. Commun.* **2016**, *7*, 12944. [CrossRef] [PubMed]
172. Gloux, K.; Guillemet, M.; Soler, C.; Morvan, C.; Halpern, D.; Pourcel, C.; Vu Thien, H.; Lamberet, G.; Gruss, A. Clinical Relevance of Type II Fatty Acid Synthesis Bypass in *Staphylococcus aureus*. *Antimicrob. Agents Chemother.* **2017**, *61*, e02515-16. [CrossRef] [PubMed]
173. Kim, E.J.; Lee, J.K. Effect of changes in the composition of cellular fatty acids on membrane fluidity of *Rhodobacter sphaeroides*. *J. Microbiol. Biotechnol.* **2015**, *25*, 162–173. [CrossRef] [PubMed]
174. Grogan, D.W.; Cronan, J.E., Jr. Characterization of *Escherichia coli* mutants completely defective in synthesis of cyclopropane fatty acids. *J. Bacteriol.* **1986**, *166*, 872–877. [CrossRef]
175. Harley, J.B.; Santangelo, G.M.; Rasmussen, H.; Goldfine, H. Dependence of *Escherichia coli* hyperbaric oxygen toxicity on the lipid acyl chain composition. *J. Bacteriol.* **1978**, *134*, 808–820. [CrossRef]
176. Dufourc, E.J.; Smith, I.C.; Jarrell, H.C. A 2H-NMR analysis of dihydrosterculoyl-containing lipids in model membranes: Structural effects of a cyclopropane ring. *Chem. Phys. Lipids* **1983**, *33*, 153–177. [CrossRef] [PubMed]
177. Choi, T.R.; Park, Y.L.; Song, H.S.; Lee, S.M.; Park, S.L.; Lee, H.S.; Kim, H.J.; Bhatia, S.K.; Gurav, R.; Lee, Y.K.; et al. Effects of a Δ-9-fatty acid desaturase and a cyclopropane-fatty acid synthase from the novel psychrophile *Pseudomonas* sp. B14-6 on bacterial membrane properties. *J. Ind. Microbiol. Biotechnol.* **2020**, *47*, 1045–1057. [CrossRef] [PubMed]
178. Choi, T.R.; Song, H.S.; Han, Y.H.; Park, Y.L.; Park, J.Y.; Yang, S.Y.; Bhatia, S.K.; Gurav, R.; Kim, H.J.; Lee, Y.K.; et al. Enhanced tolerance to inhibitors of *Escherichia coli* by heterologous expression of cyclopropane-fatty acid-acyl-phospholipid synthase (cfa) from Halomonas socia. *Bioprocess Biosyst. Eng.* **2020**, *43*, 909–918. [CrossRef]
179. Wang, A.Y.; Grogan, D.W.; Cronan, J.E., Jr. Cyclopropane fatty acid synthase of *Escherichia coli*: Deduced amino acid sequence, purification, and studies of the enzyme active site. *Biochemistry* **1992**, *31*, 11020–11028. [CrossRef]
180. Barkan, D.; Liu, Z.; Sacchettini, J.C.; Glickman, M.S. Mycolic acid cyclopropanation is essential for viability, drug resistance, and cell wall integrity of *Mycobacterium tuberculosis*. *Chem. Biol.* **2009**, *16*, 499–509. [CrossRef]
181. Barkan, D.; Hedhli, D.; Yan, H.G.; Huygen, K.; Glickman, M.S. *Mycobacterium tuberculosis* lacking all mycolic acid cyclopropanation is viable but highly attenuated and hyperinflammatory in mice. *Infect. Immun.* **2012**, *80*, 1958–1968. [CrossRef]
182. Blunsom, N.J.; Cockcroft, S. CDP-Diacylglycerol Synthases (CDS): Gateway to Phosphatidylinositol and Cardiolipin Synthesis. *Front. Cell Dev. Biol.* **2020**, *8*, 63. [CrossRef]
183. Jennings, W.; Epand, R.M. CDP-diacylglycerol, a critical intermediate in lipid metabolism. *Chem. Phys. Lipids* **2020**, *230*, 104914. [CrossRef] [PubMed]
184. Lu, Y.H.; Guan, Z.; Zhao, J.; Raetz, C.R. Three phosphatidylglycerol-phosphate phosphatases in the inner membrane of *Escherichia coli*. *J. Biol. Chem.* **2011**, *286*, 5506–5518. [CrossRef] [PubMed]
185. Tan, B.K.; Bogdanov, M.; Zhao, J.; Dowhan, W.; Raetz, C.R.; Guan, Z. Discovery of a cardiolipin synthase utilizing phosphatidylethanolamine and phosphatidylglycerol as substrates. *Proc. Natl. Acad. Sci. USA* **2012**, *109*, 16504–16509. [CrossRef] [PubMed]
186. Guo, D.; Tropp, B.E. A second *Escherichia coli* protein with CL synthase activity. *Biochim. Biophys. Acta* **2000**, *1483*, 263–274. [CrossRef]
187. Li, C.; Tan, B.K.; Zhao, J.; Guan, Z. In Vivo and In vitro Synthesis of Phosphatidylglycerol by an *Escherichia coli* Cardiolipin Synthase. *J. Biol. Chem.* **2016**, *291*, 25144–25153. [CrossRef]

188. Tsai, M.; Ohniwa, R.L.; Kato, Y.; Takeshita, S.L.; Ohta, T.; Saito, S.; Hayashi, H.; Morikawa, K. *Staphylococcus aureus* requires cardiolipin for survival under conditions of high salinity. *BMC Microbiol.* **2011**, *11*, 13. [CrossRef]
189. Kawai, F.; Shoda, M.; Harashima, R.; Sadaie, Y.; Hara, H.; Matsumoto, K. Cardiolipin domains in *Bacillus subtilis* marburg membranes. *J. Bacteriol.* **2004**, *186*, 1475–1483. [CrossRef] [PubMed]
190. Sohlenkamp, C.; de Rudder, K.E.; Geiger, O. Phosphatidylethanolamine is not essential for growth of *Sinorhizobium meliloti* on complex culture media. *J. Bacteriol.* **2004**, *186*, 1667–1677. [CrossRef]
191. Sohlenkamp, C.; López-Lara, I.M.; Geiger, O. Biosynthesis of phosphatidylcholine in bacteria. *Prog. Lipid Res.* **2003**, *42*, 115–162. [CrossRef] [PubMed]
192. Jackson, M.; Crick, D.C.; Brennan, P.J. Phosphatidylinositol is an essential phospholipid of mycobacteria. *J. Biol. Chem.* **2000**, *275*, 30092–30099. [CrossRef] [PubMed]
193. Salman, M.; Lonsdale, J.T.; Besra, G.S.; Brennan, P.J. Phosphatidylinositol synthesis in mycobacteria. *Biochim. Biophys. Acta* **1999**, *1436*, 437–450. [CrossRef] [PubMed]
194. Morii, H.; Okauchi, T.; Nomiya, H.; Ogawa, M.; Fukuda, K.; Taniguchi, H. Studies of inositol 1-phosphate analogues as inhibitors of the phosphatidylinositol phosphate synthase in mycobacteria. *J. Biochem.* **2013**, *153*, 257–266. [CrossRef] [PubMed]
195. Roy, H.; Dare, K.; Ibba, M. Adaptation of the bacterial membrane to changing environments using aminoacylated phospholipids. *Mol. Microbiol.* **2009**, *71*, 547–550. [CrossRef] [PubMed]
196. Andrä, J.; Goldmann, T.; Ernst, C.M.; Peschel, A.; Gutsmann, T. Multiple peptide resistance factor (MprF)-mediated Resistance of *Staphylococcus aureus* against antimicrobial peptides coincides with a modulated peptide interaction with artificial membranes comprising lysyl-phosphatidylglycerol. *J. Biol. Chem.* **2011**, *286*, 18692–18700. [CrossRef] [PubMed]
197. Ernst, C.M.; Peschel, A. Broad-spectrum antimicrobial peptide resistance by MprF-mediated aminoacylation and flipping of phospholipids. *Mol. Microbiol.* **2011**, *80*, 290–299. [CrossRef]
198. Slavetinsky, C.J.; Hauser, J.N.; Gekeler, C.; Slavetinsky, J.; Geyer, A.; Kraus, A.; Heilingbrunner, D.; Wagner, S.; Tesar, M.; Krismer, B.; et al. Sensitizing *Staphylococcus aureus* to antibacterial agents by decoding and blocking the lipid flippase MprF. *Elife* **2022**, *11*, e66376. [CrossRef]
199. Dhankhar, P.; Dalal, V.; Kotra, D.G.; Kumar, P. In-silico approach to identify novel potent inhibitors against GraR of *S. aureus*. *Front. Biosci. Landmark Ed.* **2020**, *25*, 1337–1360. [CrossRef]
200. Van Horn, W.D.; Sanders, C.R. Prokaryotic diacylglycerol kinase and undecaprenol kinase. *Annu. Rev. Biophys.* **2012**, *41*, 81–101. [CrossRef]
201. Baker, B.R.; Ives, C.M.; Bray, A.; Caffrey, M.; Cochrane, S.A. Undecaprenol kinase: Function, mechanism and substrate specificity of a potential antibiotic target. *Eur. J. Med. Chem.* **2021**, *210*, 113062. [CrossRef]
202. Yeo, W.S.; Jeong, B.; Ullah, N.; Shah, M.A.; Ali, A.; Kim, K.K.; Bae, T. Ftsh Sensitizes Methicillin-Resistant *Staphylococcus aureus* to β-Lactam Antibiotics by Degrading YpfP, a Lipoteichoic Acid Synthesis Enzyme. *Antibiotics* **2021**, *10*, 1198. [CrossRef] [PubMed]
203. Galloway, S.M.; Raetz, C.R. A mutant of *Escherichia coli* defective in the first step of endotoxin biosynthesis. *J. Biol. Chem.* **1990**, *265*, 6394–6402. [CrossRef]
204. Kelly, T.M.; Stachula, S.A.; Raetz, C.R.; Anderson, M.S. The *firA* gene of *Escherichia coli* encodes UDP-3-O-(R-3-hydroxymyristoyl)-glucosamine N-acyltransferase. The third step of endotoxin biosynthesis. *J. Biol. Chem.* **1993**, *268*, 19866–19874. [CrossRef]
205. Raetz, C.R.; Whitfield, C. Lipopolysaccharide endotoxins. *Annu. Rev. Biochem.* **2002**, *71*, 635–700. [CrossRef] [PubMed]
206. Williams, A.H.; Immormino, R.M.; Gewirth, D.T.; Raetz, C.R. Structure of UDP-N-acetylglucosamine acyltransferase with a bound antibacterial pentadecapeptide. *Proc. Natl. Acad. Sci. USA* **2006**, *103*, 10877–10882. [CrossRef]
207. Jenkins, R.J.; Dotson, G.D. Dual targeting antibacterial peptide inhibitor of early lipid A biosynthesis. *ACS Chem. Biol.* **2012**, *7*, 1170–1177. [CrossRef] [PubMed]
208. Han, W.; Ma, X.; Balibar, C.J.; Baxter Rath, C.M.; Benton, B.; Bermingham, A.; Casey, F.; Chie-Leon, B.; Cho, M.K.; Frank, A.O.; et al. Two Distinct Mechanisms of Inhibition of LpxA Acyltransferase Essential for Lipopolysaccharide Biosynthesis. *J. Am. Chem. Soc.* **2020**, *142*, 4445–4455. [CrossRef]
209. Clements, J.M.; Coignard, F.; Johnson, I.; Chandler, S.; Palan, S.; Waller, A.; Wijkmans, J.; Hunter, M.G. Antibacterial activities and characterization of novel inhibitors of LpxC. *Antimicrob. Agents Chemother.* **2002**, *46*, 1793–1799. [CrossRef]
210. Mdluli, K.E.; Witte, P.R.; Kline, T.; Barb, A.W.; Erwin, A.L.; Mansfield, B.E.; McClerren, A.L.; Pirrung, M.C.; Tumey, L.N.; Warrener, P.; et al. Molecular validation of LpxC as an antibacterial drug target in *Pseudomonas aeruginosa*. *Antimicrob. Agents Chemother.* **2006**, *50*, 2178–2184. [CrossRef]
211. Chen, M.H.; Steiner, M.G.; de Laszlo, S.E.; Patchett, A.A.; Anderson, M.S.; Hyland, S.A.; Onishi, H.R.; Silver, L.L.; Raetz, C.R. Carbohydroxamido-oxazolidines: Antibacterial agents that target lipid A biosynthesis. *Bioorg. Med. Chem. Lett.* **1999**, *9*, 313–318. [CrossRef]
212. McClerren, A.L.; Endsley, S.; Bowman, J.L.; Andersen, N.H.; Guan, Z.; Rudolph, J.; Raetz, C.R. A slow, tight-binding inhibitor of the zinc-dependent deacetylase LpxC of lipid A biosynthesis with antibiotic activity comparable to ciprofloxacin. *Biochemistry* **2005**, *44*, 16574–16583. [CrossRef]
213. Barb, A.W.; McClerren, A.L.; Snehelatha, K.; Reynolds, C.M.; Zhou, P.; Raetz, C.R. Inhibition of lipid A biosynthesis as the primary mechanism of CHIR-090 antibiotic activity in *Escherichia coli*. *Biochemistry* **2007**, *46*, 3793–3802. [CrossRef] [PubMed]

214. Tomaras, A.P.; McPherson, C.J.; Kuhn, M.; Carifa, A.; Mullins, L.; George, D.; Desbonnet, C.; Eidem, T.M.; Montgomery, J.I.; Brown, M.F.; et al. LpxC inhibitors as new antibacterial agents and tools for studying regulation of lipid A biosynthesis in Gram-negative pathogens. *mBio* **2014**, *5*, e01551-14. [CrossRef] [PubMed]
215. Jackman, J.E.; Fierke, C.A.; Tumey, L.N.; Pirrung, M.; Uchiyama, T.; Tahir, S.H.; Hindsgaul, O.; Raetz, C.R. Antibacterial agents that target lipid A biosynthesis in gram-negative bacteria. Inhibition of diverse UDP-3-O-(r-3-hydroxymyristoyl)-n-acetylglucosamine deacetylases by substrate analogs containing zinc binding motifs. *J. Biol. Chem.* **2000**, *275*, 11002–11009. [CrossRef] [PubMed]
216. Ma, X.; Prathapam, R.; Wartchow, C.; Chie-Leon, B.; Ho, C.M.; De Vicente, J.; Han, W.; Li, M.; Lu, Y.; Ramurthy, S.; et al. Structural and Biological Basis of Small Molecule Inhibition of *Escherichia coli* LpxD Acyltransferase Essential for Lipopolysaccharide Biosynthesis. *ACS Infect. Dis.* **2020**, *6*, 1480–1489. [CrossRef] [PubMed]
217. Bohl, H.O.; Ieong, P.; Lee, J.K.; Lee, T.; Kankanala, J.; Shi, K.; Demir, Ö.; Kurahashi, K.; Amaro, R.E.; Wang, Z.; et al. The substrate-binding cap of the UDP-diacylglucosamine pyrophosphatase LpxH is highly flexible, enabling facile substrate binding and product release. *J. Biol. Chem.* **2018**, *293*, 7969–7981. [CrossRef]
218. Cho, J.; Lee, M.; Cochrane, C.S.; Webster, C.G.; Fenton, B.A.; Zhao, J.; Hong, J.; Zhou, P. Structural basis of the UDP-diacylglucosamine pyrophosphohydrolase LpxH inhibition by sulfonyl piperazine antibiotics. *Proc. Natl. Acad. Sci. USA* **2020**, *117*, 4109–4116. [CrossRef] [PubMed]
219. Lee, M.; Zhao, J.; Kwak, S.H.; Cho, J.; Lee, M.; Gillespie, R.A.; Kwon, D.Y.; Lee, H.; Park, H.J.; Wu, Q.; et al. Structure-Activity Relationship of Sulfonyl Piperazine LpxH Inhibitors Analyzed by an LpxE-Coupled Malachite Green Assay. *ACS Infect. Dis.* **2019**, *5*, 641–651. [CrossRef]
220. Raetz, C.R.; Reynolds, C.M.; Trent, M.S.; Bishop, R.E. Lipid A modification systems in gram-negative bacteria. *Annu. Rev. Biochem.* **2007**, *76*, 295–329. [CrossRef]
221. Williams, A.H.; Raetz, C.R. Structural basis for the acyl chain selectivity and mechanism of UDP-N-acetylglucosamine acyltransferase. *Proc. Natl. Acad. Sci. USA* **2007**, *104*, 13543–13550. [CrossRef] [PubMed]
222. Jenkins, R.J.; Heslip, K.A.; Meagher, J.L.; Stuckey, J.A.; Dotson, G.D. Structural basis for the recognition of peptide RJPXD33 by acyltransferases in lipid A biosynthesis. *J. Biol. Chem.* **2014**, *289*, 15527–15535. [CrossRef] [PubMed]
223. Dangkulwanich, M.; Raetz, C.R.H.; Williams, A.H. Structure guided design of an antibacterial peptide that targets UDP-N-acetylglucosamine acyltransferase. *Sci. Rep.* **2019**, *9*, 3947. [CrossRef] [PubMed]
224. Kroeck, K.G.; Sacco, M.D.; Smith, E.W.; Zhang, X.; Shoun, D.; Akhtar, A.; Darch, S.E.; Cohen, F.; Andrews, L.D.; Knox, J.E.; et al. Discovery of dual-activity small-molecule ligands of *Pseudomonas aeruginosa* LpxA and LpxD using SPR and X-ray crystallography. *Sci. Rep.* **2019**, *9*, 15450. [CrossRef]
225. Bhaskar, B.V.; Babu, T.M.C.; Rammohan, A.; Zheng, G.Y.; Zyryanov, G.V.; Gu, W. Structure-Based Virtual Screening of *Pseudomonas aeruginosa* LpxA Inhibitors Using Pharmacophore-Based Approach. *Biomolecules* **2020**, *10*, 266. [CrossRef]
226. Pratap, S.; Kesari, P.; Yadav, R.; Dev, A.; Narwal, M.; Kumar, P. Acyl chain preference and inhibitor identification of *Moraxella catarrhalis* LpxA: Insight through crystal structure and computational studies. *Int. J. Biol. Macromol.* **2017**, *96*, 759–765. [CrossRef]
227. Shapiro, A.B.; Ross, P.L.; Gao, N.; Livchak, S.; Kern, G.; Yang, W.; Andrews, B.; Thresher, J. A high-throughput-compatible fluorescence anisotropy-based assay for competitive inhibitors of *Escherichia coli* UDP-N-acetylglucosamine acyltransferase (LpxA). *J. Biomol. Screen.* **2013**, *18*, 341–347. [CrossRef]
228. Mochalkin, I.; Knafels, J.D.; Lightle, S. Crystal structure of LpxC from *Pseudomonas aeruginosa* complexed with the potent BB-78485 inhibitor. *Protein Sci.* **2008**, *17*, 450–457. [CrossRef]
229. Onishi, H.R.; Pelak, B.A.; Gerckens, L.S.; Silver, L.L.; Kahan, F.M.; Chen, M.H.; Patchett, A.A.; Galloway, S.M.; Hyland, S.A.; Anderson, M.S.; et al. Antibacterial agents that inhibit lipid A biosynthesis. *Science* **1996**, *274*, 980–982. [CrossRef]
230. Coggins, B.E.; McClerren, A.L.; Jiang, L.; Li, X.; Rudolph, J.; Hindsgaul, O.; Raetz, C.R.; Zhou, P. Refined solution structure of the LpxC-TU-514 complex and pKa analysis of an active site histidine: Insights into the mechanism and inhibitor design. *Biochemistry* **2005**, *44*, 1114–1126. [CrossRef]
231. Caughlan, R.E.; Jones, A.K.; Delucia, A.M.; Woods, A.L.; Xie, L.; Ma, B.; Barnes, S.W.; Walker, J.R.; Sprague, E.R.; Yang, X.; et al. Mechanisms decreasing In vitro susceptibility to the LpxC inhibitor CHIR-090 in the gram-negative pathogen *Pseudomonas aeruginosa*. *Antimicrob. Agents Chemother.* **2012**, *56*, 17–27. [CrossRef] [PubMed]
232. Lee, C.J.; Liang, X.; Chen, X.; Zeng, D.; Joo, S.H.; Chung, H.S.; Barb, A.W.; Swanson, S.M.; Nicholas, R.A.; Li, Y.; et al. Species-specific and inhibitor-dependent conformations of LpxC: Implications for antibiotic design. *Chem. Biol.* **2011**, *18*, 38–47. [CrossRef] [PubMed]
233. Liang, X.; Lee, C.J.; Chen, X.; Chung, H.S.; Zeng, D.; Raetz, C.R.; Li, Y.; Zhou, P.; Toone, E.J. Syntheses, structures and antibiotic activities of LpxC inhibitors based on the diacetylene scaffold. *Bioorg. Med. Chem.* **2011**, *19*, 852–860. [CrossRef] [PubMed]
234. Zeng, D.; Zhao, J.; Chung, H.S.; Guan, Z.; Raetz, C.R.; Zhou, P. Mutants resistant to LpxC inhibitors by rebalancing cellular homeostasis. *J. Biol. Chem.* **2013**, *288*, 5475–5486. [CrossRef]
235. Jones, A.K.; Caughlan, R.E.; Woods, A.L.; Uehara, K.; Xie, L.; Barnes, S.W.; Walker, J.R.; Thompson, K.V.; Ranjitkar, S.; Lee, P.S.; et al. Mutations Reducing In vitro Susceptibility to Novel LpxC Inhibitors in *Pseudomonas aeruginosa* and Interplay of Efflux and Nonefflux Mechanisms. *Antimicrob. Agents Chemother.* **2019**, *64*, e01490-19. [CrossRef] [PubMed]
236. Niu, Z.; Lei, P.; Wang, Y.; Wang, J.; Yang, J.; Zhang, J. Small molecule LpxC inhibitors against gram-negative bacteria: Advances and future perspectives. *Eur. J. Med. Chem.* **2023**, *253*, 115326. [CrossRef] [PubMed]

237. Rath, S.N.; Ray, M.; Pattnaik, A.; Pradhan, S.K. Drug Target Identification and Elucidation of Natural Inhibitors for *Bordetella petrii*: An In Silico Study. *Genom. Inform.* **2016**, *14*, 241–254. [CrossRef]
238. Metzger, L.E., 4th; Lee, J.K.; Finer-Moore, J.S.; Raetz, C.R.; Stroud, R.M. LpxI structures reveal how a lipid A precursor is synthesized. *Nat. Struct. Mol. Biol.* **2012**, *19*, 1132–1138. [CrossRef]
239. Metzger, L.E., 4th; Raetz, C.R. An alternative route for UDP-diacylglucosamine hydrolysis in bacterial lipid A biosynthesis. *Biochemistry* **2010**, *49*, 6715–6726. [CrossRef]
240. Young, H.E.; Zhao, J.; Barker, J.R.; Guan, Z.; Valdivia, R.H.; Zhou, P. Discovery of the Elusive UDP-Diacylglucosamine Hydrolase in the Lipid A Biosynthetic Pathway in *Chlamydia trachomatis*. *mBio* **2016**, *7*, e00090. [CrossRef]
241. Nayar, A.S.; Dougherty, T.J.; Ferguson, K.E.; Granger, B.A.; McWilliams, L.; Stacey, C.; Leach, L.J.; Narita, S.; Tokuda, H.; Miller, A.A.; et al. Novel antibacterial targets and compounds revealed by a high-throughput cell wall reporter assay. *J. Bacteriol.* **2015**, *197*, 1726–1734. [CrossRef]
242. Kwak, S.H.; Cochrane, C.S.; Ennis, A.F.; Lim, W.Y.; Webster, C.G.; Cho, J.; Fenton, B.A.; Zhou, P.; Hong, J. Synthesis and evaluation of sulfonyl piperazine LpxH inhibitors. *Bioorg. Chem.* **2020**, *102*, 104055. [CrossRef]
243. Zhou, P.; Hong, J. Structure- and Ligand-Dynamics-Based Design of Novel Antibiotics Targeting Lipid A Enzymes LpxC and LpxH in Gram-Negative Bacteria. *Acc. Chem. Res.* **2021**, *54*, 1623–1634. [CrossRef]
244. Martínez-Guitián, M.; Vázquez-Ucha, J.C.; Álvarez-Fraga, L.; Conde-Pérez, K.; Bou, G.; Poza, M.; Beceiro, A. Antisense inhibition of *lpxB* gene expression in *Acinetobacter baumannii* by peptide-PNA conjugates and synergy with colistin. *J. Antimicrob. Chemother.* **2020**, *75*, 51–59. [CrossRef] [PubMed]
245. Damale, M.G.; Pathan, S.K.; Patil, R.B.; Sangshetti, J.N. Pharmacoinformatics approaches to identify potential hits against tetraacyldisaccharide 4′-kinase (LpxK) of *Pseudomonas aeruginosa*. *RSC Adv.* **2020**, *10*, 32856–32874. [CrossRef] [PubMed]
246. Wang, X.; Quinn, P.J.; Yan, A. Kdo2 -lipid A: Structural diversity and impact on immunopharmacology. *Biol. Rev. Camb. Philos. Soc.* **2015**, *90*, 408–427. [CrossRef]
247. Emiola, A.; George, J.; Andrews, S.S. A Complete Pathway Model for Lipid A Biosynthesis in *Escherichia coli*. *PLoS ONE* **2015**, *10*, e0121216. [CrossRef] [PubMed]
248. Hankins, J.V.; Madsen, J.A.; Giles, D.K.; Childers, B.M.; Klose, K.E.; Brodbelt, J.S.; Trent, M.S. Elucidation of a novel *Vibrio cholerae* lipid A secondary hydroxy-acyltransferase and its role in innate immune recognition. *Mol. Microbiol.* **2011**, *81*, 1313–1329. [CrossRef] [PubMed]
249. Shai, Y.; Makovitzky, A.; Avrahami, D. Host defense peptides and lipopeptides: Modes of action and potential candidates for the treatment of bacterial and fungal infections. *Curr. Protein Pept. Sci.* **2006**, *7*, 479–486. [CrossRef] [PubMed]
250. Radek, K.; Gallo, R. Antimicrobial peptides: Natural effectors of the innate immune system. *Semin. Immunopathol.* **2007**, *29*, 27–43. [CrossRef]
251. Hancock, R.E.; Sahl, H.G. Antimicrobial and host-defense peptides as new anti-infective therapeutic strategies. *Nat. Biotechnol.* **2006**, *24*, 1551–1557. [CrossRef] [PubMed]
252. Wang, J.; Dou, X.; Song, J.; Lyu, Y.; Zhu, X.; Xu, L.; Li, W.; Shan, A. Antimicrobial peptides: Promising alternatives in the post feeding antibiotic era. *Med. Res. Rev.* **2019**, *39*, 831–859. [CrossRef]
253. Ahmed, T.A.E.; Hammami, R. Recent insights into structure-function relationships of antimicrobial peptides. *J. Food Biochem.* **2019**, *43*, e12546. [CrossRef] [PubMed]
254. Antonov, V.F.; Petrov, V.V.; Molnar, A.A.; Predvoditelev, D.A.; Ivanov, A.S. The appearance of single-ion channels in unmodified lipid bilayer membranes at the phase transition temperature. *Nature* **1980**, *283*, 585–586. [CrossRef]
255. Finkelstein, A.; Andersen, O.S. The gramicidin A channel: A review of its permeability characteristics with special reference to the single-file aspect of transport. *J. Membr. Biol.* **1981**, *59*, 155–171. [CrossRef] [PubMed]
256. Andersen, O.S.; Koeppe, R.E., 2nd. Molecular determinants of channel function. *Physiol. Rev.* **1992**, *72* (Suppl. S4), S89–S158. [CrossRef]
257. Fringeli, U.P.; Fringeli, M. Pore formation in lipid membranes by alamethicin. *Proc. Natl. Acad. Sci. USA* **1979**, *76*, 3852–3856. [CrossRef]
258. Shai, Y.; Bach, D.; Yanovsky, A. Channel formation properties of synthetic pardaxin and analogues. *J. Biol. Chem.* **1990**, *265*, 20202–20209. [CrossRef]
259. Capone, R.; Mustata, M.; Jang, H.; Arce, F.T.; Nussinov, R.; Lal, R. Antimicrobial protegrin-1 forms ion channels: Molecular dynamic simulation, atomic force microscopy, and electrical conductance studies. *Biophys. J.* **2010**, *98*, 2644–2652. [CrossRef]
260. Watanabe, H.; Kawano, R. Channel Current Analysis for Pore-forming Properties of an Antimicrobial Peptide, Magainin 1, Using the Droplet Contact Method. *Anal. Sci.* **2016**, *32*, 57–60. [CrossRef]
261. Gallucci, E.; Meleleo, D.; Micelli, S.; Picciarelli, V. Magainin 2 channel formation in planar lipid membranes: The role of lipid polar groups and ergosterol. *Eur. Biophys. J.* **2003**, *32*, 22–32. [CrossRef]
262. Mellor, I.R.; Sansom, M.S. Ion-channel properties of mastoparan, a 14-residue peptide from wasp venom, and of MP3, a 12-residue analogue. *Proc. R. Soc. Lond. B Biol. Sci.* **1990**, *239*, 383–400. [CrossRef]
263. Arbuzova, A.; Schwarz, G. Pore-forming action of mastoparan peptides on liposomes: A quantitative analysis. *Biochim. Biophys. Acta* **1999**, *1420*, 139–152. [CrossRef]
264. Efimova, S.S.; Schagina, L.V.; Ostroumova, O.S. Channel-forming activity of cecropins in lipid bilayers: Effect of agents modifying the membrane dipole potential. *Langmuir* **2014**, *30*, 7884–7892. [CrossRef] [PubMed]

265. Efimova, S.S.; Shekunov, E.V.; Chernyshova, D.N.; Zakharova, A.A.; Ostroumova, O.S. Dependence of the channel-forming ability of lantibiotics on the lipid composition of the membranes. *Biochem. Suppl. Ser. A Membr. Cell Biol.* **2022**, *16*, 144–150. [CrossRef]
266. Sheth, T.R.; Henderson, R.M.; Hladky, S.B.; Cuthbert, A.W. Ion channel formation by duramycin. *Biochim. Biophys. Acta* **1992**, *1107*, 179–185. [CrossRef] [PubMed]
267. Sansom, M.S. Alamethicin and related peptaibols—Model ion channels. *Eur. Biophys. J.* **1993**, *22*, 105–124. [CrossRef]
268. Gordon, L.G.; Haydon, D.A. The unit conductance channel of alamethicin. *Biochim. Biophys. Acta* **1972**, *255*, 1014–1018. [CrossRef] [PubMed]
269. Christensen, B.; Fink, J.; Merrifield, R.B.; Mauzerall, D. Channel-forming properties of cecropins and related model compounds incorporated into planar lipid membranes. *Proc. Natl. Acad. Sci. USA* **1988**, *85*, 5072–5076. [CrossRef] [PubMed]
270. Sokolov, Y.; Mirzabekov, T.; Martin, D.W.; Lehrer, R.I.; Kagan, B.L. Membrane channel formation by antimicrobial protegrins. *Biochim. Biophys. Acta* **1999**, *1420*, 23–29. [CrossRef]
271. Saint, N.; Marri, L.; Marchini, D.; Molle, G. The antibacterial peptide ceratotoxin A displays alamethicin-like behavior in lipid bilayers. *Peptides* **2003**, *24*, 1779–1784. [CrossRef]
272. Mayer, S.F.; Ducrey, J.; Dupasquier, J.; Haeni, L.; Rothen-Rutishauser, B.; Yang, J.; Fennouri, A.; Mayer, M. Targeting specific membranes with an azide derivative of the pore-forming peptide ceratotoxin A. *Biochim. Biophys. Acta Biomembr.* **2019**, *1861*, 183023. [CrossRef] [PubMed]
273. Wang, G. Human antimicrobial peptides and proteins. *Pharmaceuticals* **2014**, *7*, 545–594. [CrossRef]
274. Henzler Wildman, K.A.; Lee, D.K.; Ramamoorthy, A. Mechanism of lipid bilayer disruption by the human antimicrobial peptide, LL-37. *Biochemistry* **2003**, *42*, 6545–6558. [CrossRef]
275. Khondker, A.; Rheinstädter, M.C. How do bacterial membranes resist polymyxin antibiotics? *Commun. Biol.* **2020**, *3*, 77. [CrossRef] [PubMed]
276. Sabnis, A.; Hagart, K.L.; Klöckner, A.; Becce, M.; Evans, L.E.; Furniss, R.C.D.; Mavridou, D.A.; Murphy, R.; Stevens, M.M.; Davies, J.C.; et al. Colistin kills bacteria by targeting lipopolysaccharide in the cytoplasmic membrane. *Elife* **2021**, *10*, e65836. [CrossRef]
277. Taylor, R.; Beriashvili, D.; Taylor, S.; Palmer, M. Daptomycin Pore Formation Is Restricted by Lipid Acyl Chain Composition. *ACS Infect. Dis.* **2017**, *3*, 797–801. [CrossRef] [PubMed]
278. Beriashvili, D.; Taylor, R.; Kralt, B.; Abu Mazen, N.; Taylor, S.D.; Palmer, M. Mechanistic studies on the effect of membrane lipid acyl chain composition on daptomycin pore formation. *Chem. Phys. Lipids* **2018**, *216*, 73–79. [CrossRef] [PubMed]
279. Tyurin, A.P.; Alferova, V.A.; Paramonov, A.S.; Shuvalov, M.V.; Kudryakova, G.K.; Rogozhin, E.A.; Zherebker, A.Y.; Brylev, V.A.; Chistov, A.A.; Baranova, A.A.; et al. Gausemycins-A,B: Cyclic Lipoglycopeptides from *Streptomyces* sp. *Angew. Chem. Int. Ed. Engl.* **2021**, *60*, 18694–18703. [CrossRef]
280. Brogden, K.A. Antimicrobial peptides: Pore formers or metabolic inhibitors in bacteria? *Nat. Rev. Microbiol.* **2005**, *3*, 238–250. [CrossRef]
281. Laver, D.R. The barrel-stave model as applied to alamethicin and its analogs reevaluated. *Biophys. J.* **1994**, *66*, 355–359. [CrossRef] [PubMed]
282. Porcelli, F.; Buck, B.; Lee, D.K.; Hallock, K.J.; Ramamoorthy, A.; Veglia, G. Structure and orientation of pardaxin determined by NMR experiments in model membranes. *J. Biol. Chem.* **2004**, *279*, 45815–45823. [CrossRef]
283. Allende, D.; Simon, S.A.; McIntosh, T.J. Melittin-induced bilayer leakage depends on lipid material properties: Evidence for toroidal pores. *Biophys. J.* **2005**, *88*, 1828–1837. [CrossRef]
284. Matsuzaki, K. Magainins as paradigm for the mode of action of pore forming polypeptides. *Biochim. Biophys. Acta* **1998**, *1376*, 391–400. [CrossRef] [PubMed]
285. Murzyn, K.; Pasenkiewicz-Gierula, M. Construction of a toroidal model for the magainin pore. *J. Mol. Model.* **2003**, *9*, 217–224. [CrossRef]
286. Gazit, E.; Boman, A.; Boman, H.G.; Shai, Y. Interaction of the mammalian antibacterial peptide cecropin P1 with phospholipid vesicles. *Biochemistry* **1995**, *34*, 11479–11488. [CrossRef]
287. Fernandez, D.I.; Le Brun, A.P.; Whitwell, T.C.; Sani, M.A.; James, M.; Separovic, F. The antimicrobial peptide aurein 1.2 disrupts model membranes via the carpet mechanism. *Phys. Chem. Chem. Phys.* **2012**, *14*, 15739–15751. [CrossRef]
288. Battista, F.; Oliva, R.; Del Vecchio, P.; Winter, R.; Petraccone, L. Insights into the Action Mechanism of the Antimicrobial Peptide Lasioglossin III. *Int. J. Mol. Sci.* **2021**, *22*, 2857. [CrossRef]
289. Ma, B.; Fang, C.; Lu, L.; Wang, M.; Xue, X.; Zhou, Y.; Li, M.; Hu, Y.; Luo, X.; Hou, Z. The antimicrobial peptide thanatin disrupts the bacterial outer membrane and inactivates the NDM-1 metallo-β-lactamase. *Nat. Commun.* **2019**, *10*, 3517. [CrossRef]
290. Henderson, J.M.; Waring, A.J.; Separovic, F.; Lee, K.Y.C. Antimicrobial Peptides Share a Common Interaction Driven by Membrane Line Tension Reduction. *Biophys. J.* **2016**, *111*, 2176–2189. [CrossRef]
291. Efimova, S.S.; Medvedev, R.Y.; Chulkov, E.G.; Ostroumova, O.S. Regulation of the Pore-Forming Activity of Cecropin A by Local Anesthetics. *Cell Tiss. Biol.* **2018**, *12*, 331–341. [CrossRef]
292. Lee, C.C.; Sun, Y.; Qian, S.; Huang, H.W. Transmembrane pores formed by human antimicrobial peptide LL-37. *Biophys. J.* **2011**, *100*, 1688–1696. [CrossRef]
293. Mak, D.O.; Webb, W.W. Two classes of alamethicin transmembrane channels: Molecular models from single-channel properties. *Biophys. J.* **1995**, *69*, 2323–2336. [CrossRef]

294. Fennouri, A.; Mayer, S.F.; Schroeder, T.B.H.; Mayer, M. Single channel planar lipid bilayer recordings of the melittin variant MelP5. *Biochim. Biophys. Acta Biomembr.* **2017**, *1859*, 2051–2057. [CrossRef]
295. Wiedemann, I.; Benz, R.; Sahl, H.G. Lipid II-mediated pore formation by the peptide antibiotic nisin: A black lipid membrane study. *J. Bacteriol.* **2004**, *186*, 3259–3261. [CrossRef]
296. Kagan, B.L.; Selsted, M.E.; Ganz, T.; Lehrer, R.I. Antimicrobial defensin peptides form voltage-dependent ion-permeable channels in planar lipid bilayer membranes. *Proc. Natl. Acad. Sci. USA* **1990**, *87*, 210–214. [CrossRef]
297. Hristova, K.; Selsted, M.E.; White, S.H. Critical role of lipid composition in membrane permeabilization by rabbit neutrophil defensins. *J. Biol. Chem.* **1997**, *272*, 24224–24233. [CrossRef]
298. Seydlová, G.; Sokol, A.; Lišková, P.; Konopásek, I.; Fišer, R. Daptomycin Pore Formation and Stoichiometry Depend on Membrane Potential of Target Membrane. *Antimicrob. Agents Chemother.* **2018**, *63*, e01589-18. [CrossRef]
299. Peschel, A.; Jack, R.W.; Otto, M.; Collins, L.V.; Staubitz, P.; Nicholson, G.; Kalbacher, H.; Nieuwenhuizen, W.F.; Jung, G.; Tarkowski, A.; et al. *Staphylococcus aureus* resistance to human defensins and evasion of neutrophil killing via the novel virulence factor MprF is based on modification of membrane lipids with l-lysine. *J. Exp. Med.* **2001**, *193*, 1067–1076. [CrossRef]
300. Dorrer, E.; Teuber, M. Induction of polymyxin resistance in *Pseudomonas fluorescens* by phosphate limitation. *Arch. Microbiol.* **1977**, *114*, 87–89. [CrossRef]
301. Breazeale, S.D.; Ribeiro, A.A.; McClerren, A.L.; Raetz, C.R. A formyltransferase required for polymyxin resistance in *Escherichia coli* and the modification of lipid A with 4-Amino-4-deoxy-L-arabinose. Identification and function oF UDP-4-deoxy-4-formamido-L-arabinose. *J. Biol. Chem.* **2005**, *280*, 14154–14167. [CrossRef]
302. Ernst, R.K.; Guina, T.; Miller, S.I. *Salmonella* typhimurium outer membrane remodeling: Role in resistance to host innate immunity. *Microbes Infect.* **2001**, *3*, 1327–1334. [CrossRef]
303. Gunn, J.S.; Lim, K.B.; Krueger, J.; Kim, K.; Guo, L.; Hackett, M.; Miller, S.I. PmrA-PmrB-regulated genes necessary for 4-aminoarabinose lipid A modification and polymyxin resistance. *Mol. Microbiol.* **1998**, *27*, 1171–1182. [CrossRef] [PubMed]
304. Moskowitz, S.M.; Ernst, R.K.; Miller, S.I. PmrAB, a two-component regulatory system of *Pseudomonas aeruginosa* that modulates resistance to cationic antimicrobial peptides and addition of aminoarabinose to lipid A. *J. Bacteriol.* **2004**, *186*, 575–579. [CrossRef]
305. Trent, M.S.; Ribeiro, A.A.; Lin, S.; Cotter, R.J.; Raetz, C.R. An inner membrane enzyme in *Salmonella* and *Escherichia coli* that transfers 4-amino-4-deoxy-L-arabinose to lipid A: Induction on polymyxin-resistant mutants and role of a novel lipid-linked donor. *J. Biol. Chem.* **2001**, *276*, 43122–43131. [CrossRef]
306. Müller, A.; Wenzel, M.; Strahl, H.; Grein, F.; Saaki, T.N.V.; Kohl, B.; Siersma, T.; Bandow, J.E.; Sahl, H.G.; Schneider, T.; et al. Daptomycin inhibits cell envelope synthesis by interfering with fluid membrane microdomains. *Proc. Natl. Acad. Sci. USA* **2016**, *113*, E7077–E7086. [CrossRef]
307. Mishra, N.N.; Tran, T.T.; Seepersaud, R.; Garcia-de-la-Maria, C.; Faull, K.; Yoon, A.; Proctor, R.; Miro, J.M.; Rybak, M.J.; Bayer, A.S.; et al. Perturbations of Phosphatidate Cytidylyltransferase (CdsA) Mediate Daptomycin Resistance in Streptococcus mitis/oralis by a Novel Mechanism. *Antimicrob. Agents Chemother.* **2017**, *61*, e02435-16. [CrossRef]
308. Tran, T.T.; Panesso, D.; Gao, H.; Roh, J.H.; Munita, J.M.; Reyes, J.; Diaz, L.; Lobos, E.A.; Shamoo, Y.; Mishra, N.N.; et al. Whole-genome analysis of a daptomycin-susceptible enterococcus faecium strain and its daptomycin-resistant variant arising during therapy. *Antimicrob. Agents Chemother.* **2013**, *57*, 261–268. [CrossRef]
309. Poshvina, D.V.; Dilbaryan, D.S.; Kasyanov, S.P.; Sadykova, V.S.; Lapchinskaya, O.A.; Rogozhin, E.A.; Vasilchenko, A.S. *Staphylococcus aureus* is able to generate resistance to novel lipoglycopeptide antibiotic gausemycin A. *Front. Microbiol.* **2022**, *13*, 963979. [CrossRef]
310. Boudjemaa, R.; Cabriel, C.; Dubois-Brissonnet, F.; Bourg, N.; Dupuis, G.; Gruss, A.; Lévêque-Fort, S.; Briandet, R.; Fontaine-Aupart, M.P.; Steenkeste, K. Impact of Bacterial Membrane Fatty Acid Composition on the Failure of Daptomycin to Kill *Staphylococcus aureus*. *Antimicrob. Agents Chemother.* **2018**, *62*, e00023-18. [CrossRef]
311. Ming, X.; Daeschel, M.A. Correlation of Cellular Phospholipid Content with Nisin Resistance of Listeria monocytogenes Scott A. *J. Food Prot.* **1995**, *58*, 416–420. [CrossRef]
312. Gow, N.A.R.; Latge, J.P.; Munro, C.A. The Fungal Cell Wall: Structure, Biosynthesis, and Function. *Microbiol. Spectr.* **2017**, *5*, 10–1128. [CrossRef] [PubMed]
313. Sudoh, M.; Yamazaki, T.; Masubuchi, K.; Taniguchi, M.; Shimma, N.; Arisawa, M.; Yamada-Okabe, H. Identification of a novel inhibitor specific to the fungal chitin synthase. Inhibition of chitin synthase 1 arrests the cell growth, but inhibition of chitin synthase 1 and 2 is lethal in the pathogenic fungus *Candida albicans*. *J. Biol. Chem.* **2000**, *275*, 32901–32905. [CrossRef]
314. Garcia-Effron, G.; Park, S.; Perlin, D.S. Correlating echinocandin MIC and kinetic inhibition of fks1 mutant glucan synthases for *Candida albicans*: Implications for interpretive breakpoints. *Antimicrob. Agents Chemother.* **2009**, *53*, 112–122. [CrossRef] [PubMed]
315. Onishi, J.; Meinz, M.; Thompson, J.; Curotto, J.; Dreikorn, S.; Rosenbach, M.; Douglas, C.; Abruzzo, G.; Flattery, A.; Kong, L.; et al. Discovery of novel antifungal (1,3)-beta-D-glucan synthase inhibitors. *Antimicrob. Agents Chemother.* **2000**, *44*, 368–377. [CrossRef] [PubMed]
316. Healey, K.R.; Katiyar, S.K.; Raj, S.; Edlind, T.D. CRS-MIS in *Candida glabrata*: Sphingolipids modulate echinocandin-Fks interaction. *Mol. Microbiol.* **2012**, *86*, 303–313. [CrossRef]
317. Satish, S.; Jiménez-Ortigosa, C.; Zhao, Y.; Lee, M.H.; Dolgov, E.; Krüger, T.; Park, S.; Denning, D.W.; Kniemeyer, O.; Brakhage, A.A.; et al. Stress-Induced Changes in the Lipid Microenvironment of β-(1,3)-d-Glucan Synthase Cause Clinically Important Echinocandin Resistance in *Aspergillus fumigatus*. *mBio* **2019**, *10*, e00779-19. [CrossRef]

318. Ren, Z.; Chhetri, A.; Guan, Z.; Suo, Y.; Yokoyama, K.; Lee, S.Y. Structural basis for inhibition and regulation of a chitin synthase from *Candida albicans*. *Nat. Struct. Mol. Biol.* **2022**, *29*, 653–664. [CrossRef]
319. Hu, X.; Yang, P.; Chai, C.; Liu, J.; Sun, H.; Wu, Y.; Zhang, M.; Zhang, M.; Liu, X.; Yu, H. Structural and mechanistic insights into fungal β-1,3-glucan synthase FKS1. *Nature* **2023**, *616*, 190–198. [CrossRef]
320. Leibundgut, M.; Maier, T.; Jenni, S.; Ban, N. The multienzyme architecture of eukaryotic fatty acid synthases. *Curr. Opin. Struct. Biol.* **2008**, *18*, 714–725. [CrossRef]
321. Maier, T.; Jenni, S.; Ban, N. Architecture of mammalian fatty acid synthase at 4.5 A resolution. *Science* **2006**, *311*, 1258–1262. [CrossRef]
322. Jenni, S.; Leibundgut, M.; Maier, T.; Ban, N. Architecture of a fungal fatty acid synthase at 5 A resolution. *Science* **2006**, *311*, 1263–1267. [CrossRef]
323. Chayakulkeeree, M.; Rude, T.H.; Toffaletti, D.L.; Perfect, J.R. Fatty acid synthesis is essential for survival of *Cryptococcus neoformans* and a potential fungicidal target. *Antimicrob. Agents Chemother.* **2007**, *51*, 3537–3545. [CrossRef]
324. Zhao, X.J.; McElhaney-Feser, G.E.; Bowen, W.H.; Cole, M.F.; Broedel, S.E., Jr.; Cihlar, R.L. Requirement for the *Candida albicans FAS2* gene for infection in a rat model of oropharyngeal candidiasis. *Microbiology* **1996**, *142*, 2509–2514. [CrossRef]
325. Zhao, X.J.; McElhaney-Feser, G.E.; Sheridan, M.J.; Broedel, S.E., Jr.; Cihlar, R.L. Avirulence of *Candida albicans* FAS2 mutants in a mouse model of systemic candidiasis. *Infect. Immun.* **1997**, *65*, 829–832. [CrossRef]
326. Faergeman, N.J.; Black, P.N.; Zhao, X.D.; Knudsen, J.; DiRusso, C.C. The Acyl-CoA synthetases encoded within FAA1 and FAA4 in *Saccharomyces cerevisiae* function as components of the fatty acid transport system linking import, activation, and intracellular Utilization. *J. Biol. Chem.* **2001**, *276*, 37051–37059. [CrossRef] [PubMed]
327. Johansson, P.; Wiltschi, B.; Kumari, P.; Kessler, B.; Vonrhein, C.; Vonck, J.; Oesterhelt, D.; Grininger, M. Inhibition of the fungal fatty acid synthase type I multienzyme complex. *Proc. Natl. Acad. Sci. USA* **2008**, *105*, 12803–12808. [CrossRef]
328. DeJarnette, C.; Meyer, C.J.; Jenner, A.R.; Butts, A.; Peters, T.; Cheramie, M.N.; Phelps, G.A.; Vita, N.A.; Loudon-Hossler, V.C.; Lee, R.E.; et al. Identification of Inhibitors of Fungal Fatty Acid Biosynthesis. *ACS Infect. Dis.* **2021**, *7*, 3210–3223. [CrossRef] [PubMed]
329. Xu, D.; Sillaots, S.; Davison, J.; Hu, W.; Jiang, B.; Kauffman, S.; Martel, N.; Ocampo, P.; Oh, C.; Trosok, S.; et al. Chemical genetic profiling and characterization of small-molecule compounds that affect the biosynthesis of unsaturated fatty acids in *Candida albicans*. *J. Biol. Chem.* **2009**, *284*, 19754–19764. [CrossRef] [PubMed]
330. Sant, D.G.; Tupe, S.G.; Ramana, C.V.; Deshpande, M.V. Fungal cell membrane-promising drug target for antifungal therapy. *J. Appl. Microbiol.* **2016**, *121*, 1498–1510. [CrossRef] [PubMed]
331. Carman, G.M.; Han, G.S. Regulation of phospholipid synthesis in the yeast *Saccharomyces cerevisiae*. *Annu. Rev. Biochem.* **2011**, *80*, 859–883. [CrossRef]
332. Pan, J.; Hu, C.; Yu, J.H. Lipid Biosynthesis as an Antifungal Target. *J. Fungi* **2018**, *4*, 50. [CrossRef] [PubMed]
333. McDonough, V.M.; Buxeda, R.J.; Bruno, M.E.; Ozier-Kalogeropoulos, O.; Adeline, M.T.; McMaster, C.R.; Bell, R.M.; Carman, G.M. Regulation of phospholipid biosynthesis in *Saccharomyces cerevisiae* by CTP. *J. Biol. Chem.* **1995**, *270*, 18774–18780. [CrossRef] [PubMed]
334. Tams, R.N.; Cassilly, C.D.; Anaokar, S.; Brewer, W.T.; Dinsmore, J.T.; Chen, Y.L.; Patton-Vogt, J.; Reynolds, T.B. Overproduction of Phospholipids by the Kennedy Pathway Leads to Hypervirulence in *Candida albicans*. *Front. Microbiol.* **2019**, *10*, 86. [CrossRef] [PubMed]
335. Kim, Y.S.; Oh, J.Y.; Hwang, B.K.; Kim, K.D. Variation in sensitivity of *Magnaporthe oryzae* isolates from Korea to edifenphos and iprobenfos. *Crop Prot.* **2008**, *27*, 1464–1470. [CrossRef]
336. Kennedy, E.P.; Weiss, S.B. The function of cytidine coenzymes in the biosynthesis of phospholipides. *J. Biol. Chem.* **1956**, *222*, 193–214. [CrossRef]
337. Kennedy, E.P. Metabolism of lipides. *Annu. Rev. Biochem.* **1957**, *26*, 119–148. [CrossRef]
338. Nagiec, M.M.; Nagiec, E.E.; Baltisberger, J.A.; Wells, G.B.; Lester, R.L.; Dickson, R.C. Sphingolipid synthesis as a target for antifungal drugs. Complementation of the inositol phosphorylceramide synthase defect in a mutant strain of *Saccharomyces cerevisiae* by the *AUR1* gene. *J. Biol. Chem.* **1997**, *272*, 9809–9817. [CrossRef]
339. Dickson, R.C. Roles for sphingolipids in *Saccharomyces cerevisiae*. *Adv. Exp. Med. Biol.* **2010**, *688*, 217–231. [CrossRef]
340. Obeid, L.M.; Okamoto, Y.; Mao, C. Yeast sphingolipids: Metabolism and biology. *Biochim. Biophys. Acta* **2002**, *1585*, 163–171. [CrossRef]
341. Ren, J.; Snider, J.; Airola, M.V.; Zhong, A.; Rana, N.A.; Obeid, L.M.; Hannun, Y.A. Quantification of 3-ketodihydrosphingosine using HPLC-ESI-MS/MS to study SPT activity in yeast *Saccharomyces cerevisiae*. *J. Lipid Res.* **2018**, *59*, 162–170. [CrossRef]
342. Dickson, R.C.; Lester, R.L. Sphingolipid functions in *Saccharomyces cerevisiae*. *Biochim. Biophys. Acta* **2002**, *1583*, 13–25. [CrossRef]
343. Dickson, R.C.; Sumanasekera, C.; Lester, R.L. Functions and metabolism of sphingolipids in *Saccharomyces cerevisiae*. *Prog. Lipid Res.* **2006**, *45*, 447–465. [CrossRef]
344. Whaley, H.A. The structure of lipoxamycin, a novel antifungal antibiotic. *J. Am. Chem. Soc.* **1971**, *93*, 3767–3769. [CrossRef]
345. Mandala, S.M.; Frommer, B.R.; Thornton, R.A.; Kurtz, M.B.; Young, N.M.; Cabello, M.A.; Genilloud, O.; Liesch, J.M.; Smith, J.L.; Horn, W.S. Inhibition of serine palmitoyl-transferase activity by lipoxamycin. *J. Antibiot.* **1994**, *47*, 376–379. [CrossRef]
346. Kluepfel, D.; Bagli, J.; Baker, H.; Charest, M.P.; Kudelski, A. Myriocin, a new antifungal antibiotic from *Myriococcum albomyces*. *J. Antibiot.* **1972**, *25*, 109–115. [CrossRef] [PubMed]

347. VanMiddlesworth, F.; Giacobbe, R.A.; Lopez, M.; Garrity, G.; Bland, J.A.; Bartizal, K.; Fromtling, R.A.; Polishook, J.; Zweerink, M.; Edison, A.M.; et al. Sphingofungins A, B, C, and D; a new family of antifungal agents. I. Fermentation, isolation, and biological activity. *J. Antibiot.* **1992**, *45*, 861–867. [CrossRef]
348. Mandala, S.M.; Thornton, R.A.; Frommer, B.R.; Curotto, J.E.; Rozdilsky, W.; Kurtz, M.B.; Giacobbe, R.A.; Bills, G.F.; Cabello, M.A.; Martín, I.; et al. The discovery of australifungin, a novel inhibitor of sphinganine N-acyltransferase from *Sporormiella australis*. Producing organism, fermentation, isolation, and biological activity. *J. Antibiot.* **1995**, *48*, 349–356. [CrossRef] [PubMed]
349. Raguž, L.; Peng, C.C.; Kaiser, M.; Görls, H.; Beemelmanns, C. A Modular Approach to the Antifungal Sphingofungin Family: Concise Total Synthesis of Sphingofungin A and C. *Angew. Chem. Int. Ed. Engl.* **2022**, *61*, e202112616. [CrossRef] [PubMed]
350. Mandala, S.M.; Thornton, R.A.; Frommer, B.R.; Dreikorn, S.; Kurtz, M.B. Viridiofungins, novel inhibitors of sphingolipid synthesis. *J. Antibiot.* **1997**, *50*, 339–343. [CrossRef]
351. Delgado, A.; Casas, J.; Llebaria, A.; Abad, J.L.; Fabrias, G. Inhibitors of sphingolipid metabolism enzymes. *Biochim. Biophys. Acta* **2006**, *1758*, 1957–1977. [CrossRef]
352. Gable, K.; Slife, H.; Bacikova, D.; Monaghan, E.; Dunn, T.M. Tsc3p is an 80-amino acid protein associated with serine palmitoyltransferase and required for optimal enzyme activity. *J. Biol. Chem.* **2000**, *275*, 7597–7603. [CrossRef]
353. Yoo, H.S.; Norred, W.P.; Wang, E.; Merrill, A.H., Jr.; Riley, R.T. Fumonisin inhibition of de novo sphingolipid biosynthesis and cytotoxicity are correlated in LLC-PK1 cells. *Toxicol. Appl. Pharmacol.* **1992**, *114*, 9–15. [CrossRef] [PubMed]
354. McEvoy, K.; Normile, T.G.; Del Poeta, M. Antifungal Drug Development: Targeting the Fungal Sphingolipid Pathway. *J. Fungi* **2020**, *6*, 142. [CrossRef] [PubMed]
355. Heidler, S.A.; Radding, J.A. The *AUR1* gene in *Saccharomyces cerevisiae* encodes dominant resistance to the antifungal agent aureobasidin A (LY295337). *Antimicrob. Agents Chemother.* **1995**, *39*, 2765–2769. [CrossRef]
356. Mandala, S.M.; Thornton, R.A.; Rosenbach, M.; Milligan, J.; Garcia-Calvo, M.; Bull, H.G.; Kurtz, M.B. Khafrefungin, a novel inhibitor of sphingolipid synthesis. *J. Biol. Chem.* **1997**, *272*, 32709–32714. [CrossRef]
357. Ohnuki, T.; Yano, T.; Ono, Y.; Kozuma, S.; Suzuki, T.; Ogawa, Y.; Takatsu, T. Haplofungins, novel inositol phosphorylceramide synthase inhibitors, from *Lauriomyces bellulus* SANK 26899 I. Taxonomy, fermentation, isolation and biological activities. *J. Antibiot.* **2009**, *62*, 545–549. [CrossRef] [PubMed]
358. Yano, T.; Aoyagi, A.; Kozuma, S.; Kawamura, Y.; Tanaka, I.; Suzuki, Y.; Takamatsu, Y.; Takatsu, T.; Inukai, M. Pleofungins, novel inositol phosphorylceramide synthase inhibitors, from Phoma sp. SANK 13899. I. Taxonomy, fermentation, isolation, and biological activities. *J. Antibiot.* **2007**, *60*, 136–142. [CrossRef]
359. Mandala, S.M.; Thornton, R.A.; Milligan, J.; Rosenbach, M.; Garcia-Calvo, M.; Bull, H.G.; Harris, G.; Abruzzo, G.K.; Flattery, A.M.; Gill, C.J.; et al. Rustmicin, a potent antifungal agent, inhibits sphingolipid synthesis at inositol phosphoceramide synthase. *J. Biol. Chem.* **1998**, *273*, 14942–14949. [CrossRef]
360. Harris, G.H.; Shafiee, A.; Cabello, M.A.; Curotto, J.E.; Genilloud, O.; Göklen, K.E.; Kurtz, M.B.; Rosenbach, M.; Salmon, P.M.; Thornton, R.A.; et al. Inhibition of fungal sphingolipid biosynthesis by rustmicin, galbonolide B and their new 21-hydroxy analogs. *J. Antibiot.* **1998**, *51*, 837–844. [CrossRef]
361. Fauth, U.; Zähner, H.; Mühlenfeld, A.; Achenbach, H. Galbonolides A and B--two non-glycosidic antifungal macrolides. *J. Antibiot.* **1986**, *39*, 1760–1764. [CrossRef] [PubMed]
362. Nakamura, M.; Mori, Y.; Okuyama, K.; Tanikawa, K.; Yasuda, S.; Hanada, K.; Kobayashi, S. Chemistry and biology of khafrefungin. Large-scale synthesis, design, and structure-activity relationship of khafrefungin, an antifungal agent. *Org. Biomol. Chem.* **2003**, *1*, 3362–3376. [CrossRef] [PubMed]
363. Zhong, W.; Jeffries, M.W.; Georgopapadakou, N.H. Inhibition of inositol phosphorylceramide synthase by aureobasidin A in *Candida* and *Aspergillus* species. *Antimicrob. Agents Chemother.* **2000**, *44*, 651–653. [CrossRef] [PubMed]
364. Dupont, S.; Lemetais, G.; Ferreira, T.; Cayot, P.; Gervais, P.; Beney, L. Ergosterol biosynthesis: A fungal pathway for life on land? *Evolution* **2012**, *66*, 2961–2968. [CrossRef]
365. Jordá, T.; Puig, S. Regulation of Ergosterol Biosynthesis in *Saccharomyces cerevisiae*. *Genes* **2020**, *11*, 795. [CrossRef]
366. Hu, Z.; He, B.; Ma, L.; Sun, Y.; Niu, Y.; Zeng, B. Recent Advances in Ergosterol Biosynthesis and Regulation Mechanisms in *Saccharomyces cerevisiae*. *Indian J. Microbiol.* **2017**, *57*, 270–277. [CrossRef]
367. Miziorko, H.M. Enzymes of the mevalonate pathway of isoprenoid biosynthesis. *Arch. Biochem. Biophys.* **2011**, *505*, 131–143. [CrossRef]
368. Tavakkoli, A.; Johnston, T.P.; Sahebkar, A. Antifungal effects of statins. *Pharmacol. Ther.* **2020**, *208*, 107483. [CrossRef]
369. Ting, M.; Whitaker, E.J.; Albandar, J.M. Systematic review of the In vitro effects of statins on oral and perioral microorganisms. *Eur. J. Oral Sci.* **2016**, *124*, 4–10. [CrossRef]
370. Westermeyer, C.; Macreadie, I.G. Simvastatin reduces ergosterol levels, inhibits growth and causes loss of mtDNA in *Candida glabrata*. *FEMS Yeast Res.* **2007**, *7*, 436–441. [CrossRef]
371. Gyetvai, A.; Emri, T.; Takács, K.; Dergez, T.; Fekete, A.; Pesti, M.; Pócsi, I.; Lenkey, B. Lovastatin possesses a fungistatic effect against *Candida albicans*, but does not trigger apoptosis in this opportunistic human pathogen. *FEMS Yeast Res.* **2006**, *6*, 1140–1148. [CrossRef]
372. Liu, G.; Vellucci, V.F.; Kyc, S.; Hostetter, M.K. Simvastatin inhibits *Candida albicans* biofilm In vitro. *Pediatr. Res.* **2009**, *66*, 600–604. [CrossRef]

373. Rosales-Acosta, B.; Mendieta, A.; Zúñiga, C.; Tamariz, J.; Hernández Rodríguez, C.; Ibarra-García, J.A.; Villa-Tanaca, L. Simvastatin and other inhibitors of the enzyme 3-hydroxy-3-methylglutaryl coenzyme A reductase of *Ustilago maydis* (Um-Hmgr) affect the viability of the fungus, its synthesis of sterols and mating. *Rev. Iberoam. Micol.* **2019**, *36*, 1–8. [CrossRef] [PubMed]
374. Florin-Christensen, M.; Florin-Christensen, J.; Garin, C.; Isola, E.; Brenner, R.R.; Rasmussen, L. Inhibition of *Trypanosoma cruzi* growth and sterol biosynthesis by lovastatin. *Biochem. Biophys. Res. Commun.* **1990**, *166*, 1441–1445. [CrossRef] [PubMed]
375. Callegari, S.; McKinnon, R.A.; Andrews, S.; de Barros Lopes, M.A. Atorvastatin-induced cell toxicity in yeast is linked to disruption of protein isoprenylation. *FEMS Yeast Res.* **2010**, *10*, 1881–1898. [CrossRef] [PubMed]
376. Qiao, J.; Kontoyiannis, D.P.; Wan, Z.; Li, R.; Liu, W. Antifungal activity of statins against *Aspergillus species*. *Med. Mycol.* **2007**, *45*, 589–593. [CrossRef] [PubMed]
377. Macreadie, I.G.; Johnson, G.; Schlosser, T.; Macreadie, P.I. Growth inhibition of *Candida species* and *Aspergillus fumigatus* by statins. *FEMS Microbiol. Lett.* **2006**, *262*, 9–13. [CrossRef]
378. Chin, N.X.; Weitzman, I.; Della-Latta, P. In vitro activity of fluvastatin, a cholesterol-lowering agent, and synergy with flucanazole and itraconazole against *Candida species* and *Cryptococcus neoformans*. *Antimicrob. Agents Chemother.* **1997**, *41*, 850–852. [CrossRef] [PubMed]
379. Chamilos, G.; Lewis, R.E.; Kontoyiannis, D.P. Lovastatin has significant activity against zygomycetes and interacts synergistically with voriconazole. *Antimicrob. Agents Chemother.* **2006**, *50*, 96–103. [CrossRef]
380. Madrigal-Aguilar, D.A.; Gonzalez-Silva, A.; Rosales-Acosta, B.; Bautista-Crescencio, C.; Ortiz-Álvarez, J.; Escalante, C.H.; Sánchez-Navarrete, J.; Hernández-Rodríguez, C.; Chamorro-Cevallos, G.; Tamariz, J.; et al. Antifungal Activity of Fibrate-Based Compounds and Substituted Pyrroles That Inhibit the Enzyme 3-Hydroxy-methyl-glutaryl-CoA Reductase of *Candida glabrata* (CgHMGR), Thus Decreasing Yeast Viability and Ergosterol Synthesis. *Microbiol. Spectr.* **2022**, *10*, e0164221. [CrossRef]
381. Brilhante, R.S.N.; Fonseca, X.M.Q.C.; Pereira, V.S.; Araújo, G.D.S.; Oliveira, J.S.; Garcia, L.G.S.; Rodrigues, A.M.; Camargo, Z.P.; Pereira-Neto, W.A.; Castelo-Branco, D.S.C.M.; et al. In vitro inhibitory effect of statins on planktonic cells and biofilms of the *Sporothrix schenckii* species complex. *J. Med. Microbiol.* **2020**, *69*, 838–843. [CrossRef]
382. Darwazeh, A.; Al-Shorman, H.; Mrayan, B. Effect of statin therapy on oral *Candida* carriage in hyperlipidemia patients: A pioneer study. *Dent. Med. Probl.* **2022**, *59*, 93–97. [CrossRef] [PubMed]
383. Bellanger, A.P.; Tatara, A.M.; Shirazi, F.; Gebremariam, T.; Albert, N.D.; Lewis, R.E.; Ibrahim, A.S.; Kontoyiannis, D.P. Statin Concentrations Below the Minimum Inhibitory Concentration Attenuate the Virulence of *Rhizopus oryzae*. *J. Infect. Dis.* **2016**, *214*, 114–121. [CrossRef] [PubMed]
384. Tavakkoli, A.; Johnston, T.P.; Sahebkar, A. Fluvastatin: A choice for COVID-19 associated mucormycosis management. *Curr. Med. Chem.* **2023**, *6*. *E-pub Ahead of Print*. [CrossRef]
385. Hussain, M.K.; Ahmed, S.; Khan, A.; Siddiqui, A.J.; Khatoon, S.; Jahan, S. Mucormycosis: A hidden mystery of fungal infection, possible diagnosis, treatment and development of new therapeutic agents. *Eur. J. Med. Chem.* **2023**, *246*, 115010. [CrossRef] [PubMed]
386. Klug, L.; Daum, G. Yeast lipid metabolism at a glance. *FEMS Yeast Res.* **2014**, *14*, 369–388. [CrossRef]
387. Plochocka, D.; Karst, F.; Swiezewska, E.; Szkopińska, A. The role of *ERG20* gene (encoding yeast farnesyl diphosphate synthase) mutation in long dolichol formation. Molecular modeling of FPP synthase. *Biochimie* **2000**, *82*, 733–738. [CrossRef]
388. Bergstrom, J.D.; Dufresne, C.; Bills, G.F.; Nallin-Omstead, M.; Byrne, K. Discovery, biosynthesis, and mechanism of action of the zaragozic acids: Potent inhibitors of squalene synthase. *Annu. Rev. Microbiol.* **1995**, *49*, 607–639. [CrossRef]
389. Pospiech, M.; Owens, S.E.; Miller, D.J.; Austin-Muttitt, K.; Mullins, J.G.L.; Cronin, J.G.; Allemann, R.K.; Sheldon, I.M. Bisphosphonate inhibitors of squalene synthase protect cells against cholesterol-dependent cytolysins. *FASEB J.* **2021**, *35*, e21640. [CrossRef]
390. Ryder, N.S. Inhibition of squalene epoxidase and sterol side-chain methylation by allylamines. *Biochem. Soc. Trans.* **1990**, *18*, 45–46. [CrossRef]
391. Birnbaum, J.E. Pharmacology of the allylamines. *J. Am. Acad. Dermatol.* **1990**, *23*, 782–785. [CrossRef]
392. Favre, B.; Ryder, N.S. Characterization of squalene epoxidase activity from the dermatophyte *Trichophyton rubrum* and its inhibition by terbinafine and other antimycotic agents. *Antimicrob. Agents Chemother.* **1996**, *40*, 443–447. [CrossRef]
393. Astvad, K.M.T.; Hare, R.K.; Jørgensen, K.M.; Saunte, D.M.L.; Thomsen, P.K.; Arendrup, M.C. Increasing Terbinafine Resistance in Danish *Trichophyton* Isolates 2019–2020. *J. Fungi* **2022**, *8*, 150. [CrossRef] [PubMed]
394. Moreno-Sabater, A.; Normand, A.C.; Bidaud, A.L.; Cremer, G.; Foulet, F.; Brun, S.; Bonnal, C.; Aït-Ammar, N.; Jabet, A.; Ayachi, A.; et al. Terbinafine Resistance in Dermatophytes: A French Multicenter Prospective Study. *J. Fungi* **2022**, *8*, 220. [CrossRef]
395. Gaurav, V.; Bhattacharya, S.N.; Sharma, N.; Datt, S.; Kumar, P.; Rai, G.; Singh, P.K.; Taneja, B.; Das, S. Terbinafine resistance in dermatophytes: Time to revisit alternate antifungal therapy. *J. Mycol. Med.* **2021**, *31*, 101087. [CrossRef] [PubMed]
396. Ajit, C.; Suvannasankha, A.; Zaeri, N.; Munoz, S.J. Terbinafine-associated hepatotoxicity. *Am. J. Med. Sci.* **2003**, *325*, 292–295. [CrossRef] [PubMed]
397. Trösken, E.R.; Adamska, M.; Arand, M.; Zarn, J.A.; Patten, C.; Völkel, W.; Lutz, W.K. Comparison of lanosterol-14 alpha-demethylase (CYP51) of human and *Candida albicans* for inhibition by different antifungal azoles. *Toxicology* **2006**, *228*, 24–32. [CrossRef] [PubMed]

398. Singh, A.; Singh, K.; Sharma, A.; Kaur, K.; Chadha, R.; Bedi, P.M.S. Recent advances in antifungal drug development targeting lanosterol 14α-demethylase (CYP51): A comprehensive review with structural and molecular insights. *Chem. Biol. Drug Des.* **2023**, *102*, 606–639. [CrossRef]
399. Sabatelli, F.; Patel, R.; Mann, P.A.; Mendrick, C.A.; Norris, C.C.; Hare, R.; Loebenberg, D.; Black, T.A.; McNicholas, P.M. In vitro activities of posaconazole, fluconazole, itraconazole, voriconazole, and amphotericin B against a large collection of clinically important molds and yeasts. *Antimicrob. Agents Chemother.* **2006**, *50*, 2009–2015. [CrossRef]
400. Shafiei, M.; Peyton, L.; Hashemzadeh, M.; Foroumadi, A. History of the development of antifungal azoles: A review on structures, SAR, and mechanism of action. *Bioorg. Chem.* **2020**, *104*, 104240. [CrossRef]
401. Khan, A.; Iqbal, A.; Ahmedi, S.; Manzoor, N.; Siddiqui, T. Synthesis, Anti-Fungal Potency and In silico Studies of Novel Steroidal 1,4-Dihydropyridines. *Chem. Biodivers.* **2023**, *20*, e202300096. [CrossRef]
402. Pristov, K.E.; Ghannoum, M.A. Resistance of *Candida* to azoles and echinocandins worldwide. *Clin. Microbiol. Infect.* **2019**, *25*, 792–798. [CrossRef] [PubMed]
403. Paul, S.; Shaw, D.; Joshi, H.; Singh, S.; Chakrabarti, A.; Rudramurthy, S.M.; Ghosh, A.K. Mechanisms of azole antifungal resistance in clinical isolates of *Candida tropicalis*. *PLoS ONE* **2022**, *17*, e0269721. [CrossRef]
404. Husselstein, T.; Schaller, H.; Gachotte, D.; Benveniste, P. Delta7-sterol-C5-desaturase: Molecular characterization and functional expression of wild-type and mutant alleles. *Plant Mol. Biol.* **1999**, *39*, 891–906. [CrossRef] [PubMed]
405. Ganapathy, K.; Jones, C.W.; Stephens, C.M.; Vatsyayan, R.; Marshall, J.A.; Nes, W.D. Molecular probing of the *Saccharomyces cerevisiae* sterol 24-C methyltransferase reveals multiple amino acid residues involved with C2-transfer activity. *Biochim. Biophys. Acta* **2008**, *1781*, 344–351. [CrossRef] [PubMed]
406. Kaneshiro, E.S.; Johnston, L.Q.; Nkinin, S.W.; Romero, B.I.; Giner, J.L. Sterols of *Saccharomyces cerevisiae* erg6 Knockout Mutant Expressing the Pneumocystis carinii S-Adenosylmethionine:Sterol C-24 Methyltransferase. *J. Eukaryot. Microbiol.* **2015**, *62*, 298–306. [CrossRef] [PubMed]
407. Krauß, J.; Müller, C.; Klimt, M.; Valero, L.J.; Martínez, J.F.; Müller, M.; Bartel, K.; Binder, U.; Bracher, F. Synthesis, Biological Evaluation, and Structure-Activity Relationships of 4-Aminopiperidines as Novel Antifungal Agents Targeting Ergosterol Biosynthesis. *Molecules* **2021**, *26*, 7208. [CrossRef] [PubMed]
408. Jachak, G.R.; Ramesh, R.; Sant, D.G.; Jorwekar, S.U.; Jadhav, M.R.; Tupe, S.G.; Deshpande, M.V.; Reddy, D.S. Silicon Incorporated Morpholine Antifungals: Design, Synthesis, and Biological Evaluation. *ACS Med. Chem. Lett.* **2015**, *6*, 1111–1116. [CrossRef]
409. Hata, M.; Yoshida, K.; Ishii, C.; Otani, T.; Ando, A. In vitro and in vivo antifungal activities of aminopiperidine derivatives, novel ergosterol synthesis inhibitors. *Biol. Pharm. Bull.* **2010**, *33*, 473–476. [CrossRef]
410. Mitsche, M.A.; McDonald, J.G.; Hobbs, H.H.; Cohen, J.C. Flux analysis of cholesterol biosynthesis in vivo reveals multiple tissue and cell-type specific pathways. *Elife* **2015**, *4*, e07999. [CrossRef]
411. Benveniste, P. Sterol metabolism. *Arab. Book* **2002**, *1*, e0004. [CrossRef] [PubMed]
412. Warrilow, A.G.; Parker, J.E.; Kelly, D.E.; Kelly, S.L. Azole affinity of sterol 14α-demethylase (CYP51) enzymes from *Candida albicans* and *Homo sapiens*. *Antimicrob. Agents Chemother.* **2013**, *57*, 1352–1360. [CrossRef] [PubMed]
413. Warrilow, A.G.; Parker, J.E.; Price, C.L.; Nes, W.D.; Garvey, E.P.; Hoekstra, W.J.; Schotzinger, R.J.; Kelly, D.E.; Kelly, S.L. The Investigational Drug VT-1129 Is a Highly Potent Inhibitor of Cryptococcus Species CYP51 but Only Weakly Inhibits the Human Enzyme. *Antimicrob. Agents Chemother.* **2016**, *60*, 4530–4538. [CrossRef] [PubMed]
414. Warrilow, A.G.; Price, C.L.; Parker, J.E.; Rolley, N.J.; Smyrniotis, C.J.; Hughes, D.D.; Thoss, V.; Nes, W.D.; Kelly, D.E.; Holman, T.R.; et al. Azole Antifungal Sensitivity of Sterol 14α-Demethylase (CYP51) and CYP5218 from *Malassezia globosa*. *Sci. Rep.* **2016**, *6*, 27690. [CrossRef]
415. Hata, M.; Ishii, Y.; Watanabe, E.; Uoto, K.; Kobayashi, S.; Yoshida, K.; Otani, T.; Ando, A. Inhibition of ergosterol synthesis by novel antifungal compounds targeting C-14 reductase. *Med. Mycol.* **2010**, *48*, 613–621. [CrossRef] [PubMed]
416. Agner, G.; Kaulin, Y.A.; Gurnev, P.A.; Szabo, Z.; Schagina, L.V.; Takemoto, J.Y.; Blasko, K. Membrane-permeabilizing activities of cyclic lipodepsipeptides, syringopeptin 22A and syringomycin E from *Pseudomonas syringae* pv. *syringae* in human red blood cells and in bilayer lipid membranes. *Bioelectrochemistry* **2000**, *52*, 161–167.
417. Hutchison, M.L.; Gross, D.C. Lipopeptide phytotoxins produced by *Pseudomonas syringae* pv. *syringae*: Comparison of the biosurfactant and ion channel-forming activities of syringopeptin and syringomycin. *Mol. Plant Microbe Interact.* **1997**, *10*, 347–354. [CrossRef]
418. Bensaci, M.F.; Gurnev, P.A.; Bezrukov, S.M.; Takemoto, J.Y. Fungicidal Activities and Mechanisms of Action of *Pseudomonas syringae* pv. *syringae* Lipodepsipeptide Syringopeptins 22A and 25A. *Front. Microbiol.* **2011**, *2*, 216. [CrossRef]
419. Falardeau, J.; Wise, C.; Novitsky, L.; Avis, T.J. Ecological and mechanistic insights into the direct and indirect antimicrobial properties of *Bacillus subtilis* lipopeptides on plant pathogens. *J. Chem. Ecol.* **2013**, *39*, 869–878. [CrossRef]
420. Hutchison, M.L.; Tester, M.A.; Gross, D.C. Role of biosurfactant and ion channel-forming activities of syringomycin in transmembrane ion flux: A model for the mechanism of action in the plant-pathogen interaction. *Mol. Plant Microbe Interact.* **1995**, *8*, 610–620. [CrossRef]
421. Maget-Dana, R.; Heitz, F.; Ptak, M.; Peypoux, F.; Guinand, M. Bacterial lipopeptides induce ion-conducting pores in planar bilayers. *Biochem. Biophys. Res. Commun.* **1985**, *129*, 965–971. [CrossRef]
422. Malev, V.V.; Schagina, L.V.; Gurnev, P.A.; Takemoto, J.Y.; Nestorovich, E.M.; Bezrukov, S.M. Syringomycin E channel: A lipidic pore stabilized by lipopeptide? *Biophys. J.* **2002**, *82*, 1985–1994. [CrossRef]

423. Ostroumova, O.S.; Gurnev, P.A.; Schagina, L.V.; Bezrukov, S.M. Asymmetry of syringomycin E channel studied by polymer partitioning. *FEBS Lett.* **2007**, *581*, 804–808. [CrossRef] [PubMed]
424. Ostroumova, O.S.; Malev, V.V.; Ilin, M.G.; Schagina, L.V. Surfactin activity depends on the membrane dipole potential. *Langmuir* **2010**, *26*, 15092–15097. [CrossRef] [PubMed]
425. Zakharova, A.A.; Efimova, S.S.; Malev, V.V.; Ostroumova, O.S. Fengycin induces ion channels in lipid bilayers mimicking target fungal cell membranes. *Sci. Rep.* **2019**, *9*, 16034. [CrossRef] [PubMed]
426. Sheppard, J.D.; Jumarie, C.; Cooper, D.G.; Laprade, R. Ionic channels induced by surfactin in planar lipid bilayer membranes. *Biochim. Biophys. Acta* **1991**, *1064*, 13–23. [CrossRef] [PubMed]
427. Maget-Dana, R.; Peypoux, F. Iturins, a special class of pore-forming lipopeptides: Biological and physicochemical properties. *Toxicology* **1994**, *87*, 151–174. [CrossRef]
428. Dalla Serra, M.; Bernhart, I.; Nordera, P.; Di Giorgio, D.; Ballio, A.; Menestrina, G. Conductive properties and gating of channels formed by syringopeptin 25A, a bioactive lipodepsipeptide from *Pseudomonas syringae* pv. *syringae*, in planar lipid membranes. *Mol. Plant Microbe Interact.* **1999**, *12*, 401–409. [CrossRef]
429. Maget-Dana, R.; Ptak, M.; Peypoux, F.; Michel, G. Pore-forming properties of iturin A, a lipopeptide antibiotic. *Biochim. Biophys. Acta* **1985**, *815*, 405–409. [CrossRef]
430. Maget-Dana, R.; Ptak, M. Iturin lipopeptides: Interactions of mycosubtilin with lipids in planar membranes and mixed monolayers. *Biochim. Biophys. Acta* **1990**, *1023*, 34–40. [CrossRef] [PubMed]
431. Ermishkin, L.N.; Kasumov, K.M.; Potzeluyev, V.M. Single ionic channels induced in lipid bilayers by polyene antibiotics amphotericin B and nystatine. *Nature* **1976**, *262*, 698–699. [CrossRef]
432. Ostroumova, O.S.; Efimova, S.S.; Schagina, L.V. Probing amphotericin B single channel activity by membrane dipole modifiers. *PLoS ONE* **2012**, *7*, e30261. [CrossRef] [PubMed]
433. Tevyashova, A.; Efimova, S.; Alexandrov, A.; Omelchuk, O.; Ghazy, E.; Bychkova, E.; Zatonsky, G.; Grammatikova, N.; Dezhenkova, L.; Solovieva, S.; et al. Semisynthetic Amides of Amphotericin B and Nystatin A_1: A Comparative Study of In vitro Activity/Toxicity Ratio in Relation to Selectivity to Ergosterol Membranes. *Antibiotics* **2023**, *12*, 151. [CrossRef] [PubMed]
434. Samedova, A.A.; Kasumov, K.M. Mechanism of action of macrolide antibiotic filipin on cell and lipid membranes. *Antibiot. Khimioter.* **2009**, *54*, 44–52. [PubMed]
435. Ostroumova, O.S.; Efimova, S.S.; Chulkov, E.G.; Schagina, L.V. The interaction of dipole modifiers with polyene-sterol complexes. *PLoS ONE* **2012**, *7*, e45135. [CrossRef]
436. Campagna, S.; Saint, N.; Molle, G.; Aumelas, A. Structure and mechanism of action of the antimicrobial peptide piscidin. *Biochemistry* **2007**, *46*, 1771–1778. [CrossRef]
437. Tevyashova, A.N.; Efimova, S.S.; Alexandrov, A.I.; Ghazy, E.S.M.O.; Bychkova, E.N.; Solovieva, S.E.; Zatonsky, G.B.; Grammatikova, N.E.; Dezhenkova, L.G.; Pereverzeva, E.R.; et al. Semisynthetic Amides of Polyene Antibiotic Natamycin. *ACS Infect. Dis.* **2023**, *9*, 42–55. [CrossRef]
438. Andreoli, T.E. The structure and function of amphotericin B-cholesterol pores in lipid bilayer membranes. *Ann. N. Y. Acad. Sci.* **1974**, *235*, 448–468. [CrossRef]
439. De Kruijff, B.; Gerritsen, W.J.; Oerlemans, A.; Demel, R.A.; van Deenen, L.L. Polyene antibiotic-sterol interactions in membranes of *Acholeplasma laidlawii* cells and lecithin liposomes. I. Specificity of the membrane permeability changes induced by the polyene antibiotics. *Biochim. Biophys. Acta* **1974**, *339*, 30–43. [CrossRef]
440. Cohen, B.E. Amphotericin B membrane action: Role for two types of ion channels in eliciting cell survival and lethal effects. *J. Membr. Biol.* **2010**, *238*, 1–20. [CrossRef]
441. Dos Santos, A.G.; Marquês, J.T.; Carreira, A.C.; Castro, I.R.; Viana, A.S.; Mingeot-Leclercq, M.P.; de Almeida, R.F.M.; Silva, L.C. The molecular mechanism of Nystatin action is dependent on the membrane biophysical properties and lipid composition. *Phys. Chem. Chem. Phys.* **2017**, *19*, 30078–30088. [CrossRef] [PubMed]
442. Baghirova, A.A.; Kasumov, K.M. Antifungal Macrocycle Antibiotic Amphotericin B-Its Present and Future. Multidisciplinary Perspective for the Use in the Medical Practice. *Biochem. Mosc. Suppl. B Biomed. Chem.* **2022**, *16*, 1–12. [CrossRef] [PubMed]
443. Chulkov, E.G.; Schagina, L.V.; Ostroumova, O.S. Membrane dipole modifiers modulate single-length nystatin channels via reducing elastic stress in the vicinity of the lipid mouth of a pore. *Biochim. Biophys. Acta* **2015**, *1848*, 192–199. [CrossRef] [PubMed]
444. Umegawa, Y.; Yamamoto, T.; Dixit, M.; Funahashi, K.; Seo, S.; Nakagawa, Y.; Suzuki, T.; Matsuoka, S.; Tsuchikawa, H.; Hanashima, S.; et al. Amphotericin B assembles into seven-molecule ion channels: An NMR and molecular dynamics study. *Sci. Adv.* **2022**, *8*, eabo2658. [CrossRef]
445. Akkerman, V.; Scheidt, H.A.; Reinholdt, P.; Bashawat, M.; Szomek, M.; Lehmann, M.; Wessig, P.; Covey, D.F.; Kongsted, J.; Müller, P.; et al. Natamycin interferes with ergosterol-dependent lipid phases in model membranes. *BBA Adv.* **2023**, *4*, 100102. [CrossRef] [PubMed]
446. Iwamoto, M.; Sumino, A.; Shimada, E.; Kinoshita, M.; Matsumori, N.; Oiki, S. Channel Formation and Membrane Deformation via Sterol-Aided Polymorphism of Amphidinol 3. *Sci. Rep.* **2017**, *7*, 10782. [CrossRef] [PubMed]
447. Sung, W.S.; Lee, J.; Lee, D.G. Fungicidal effect of piscidin on *Candida albicans*: Pore formation in lipid vesicles and activity in fungal membranes. *Biol. Pharm. Bull.* **2008**, *31*, 1906–1910. [CrossRef]

448. Gomes, I.P.; Santos, T.L.; de Souza, A.N.; Nunes, L.O.; Cardoso, G.A.; Matos, C.O.; Costa, L.M.F.; Lião, L.M.; Resende, J.M.; Verly, R.M. Membrane interactions of the anuran antimicrobial peptide HSP1-NH_2: Different aspects of the association to anionic and zwitterionic biomimetic systems. *Biochim. Biophys. Acta Biomembr.* **2021**, *1863*, 183449. [CrossRef]
449. Stock, S.D.; Hama, H.; Radding, J.A.; Young, D.A.; Takemoto, J.Y. Syringomycin E inhibition of *Saccharomyces cerevisiae*: Requirement for biosynthesis of sphingolipids with very-long-chain fatty acids and mannose- and phosphoinositol-containing head groups. *Antimicrob. Agents Chemother.* **2000**, *44*, 1174–1180. [CrossRef]
450. Grilley, M.M.; Stock, S.D.; Dickson, R.C.; Lester, R.L.; Takemoto, J.Y. Syringomycin action gene *SYR2* is essential for sphingolipid 4-hydroxylation in *Saccharomyces cerevisiae*. *J. Biol. Chem.* **1998**, *273*, 11062–11068. [CrossRef]
451. Bento-Oliveira, A.; Santos, F.C.; Marquês, J.T.; Paulo, P.M.R.; Korte, T.; Herrmann, A.; Marinho, H.S.; de Almeida, R.F.M. Yeast Sphingolipid-Enriched Domains and Membrane Compartments in the Absence of Mannosyldiinositolphosphorylceramide. *Biomolecules* **2020**, *10*, 871. [CrossRef] [PubMed]
452. Idkowiak-Baldys, J.; Grilley, M.M.; Takemoto, J.Y. Sphingolipid C4 hydroxylation influences properties of yeast detergent-insoluble glycolipid-enriched membranes. *FEBS Lett.* **2004**, *569*, 272–276. [CrossRef]
453. Kaulin, Y.A.; Takemoto, J.Y.; Schagina, L.V.; Ostroumova, O.S.; Wangspa, R.; Teeter, J.H.; Brand, J.G. Sphingolipids influence the sensitivity of lipid bilayers to fungicide, syringomycin E. *J. Bioenerg. Biomembr.* **2005**, *37*, 339–348. [CrossRef]
454. Efimova, S.S.; Zakharova, A.A.; Schagina, L.V.; Ostroumova, O.S. Two types of syringomycin E channels in sphingomyelin-containing bilayers. *Eur. Biophys. J.* **2016**, *45*, 91–98. [CrossRef]
455. Mbongo, N.; Loiseau, P.M.; Billion, M.A.; Robert-Gero, M. Mechanism of amphotericin B resistance in *Leishmania donovani* promastigotes. *Antimicrob. Agents Chemother.* **1998**, *42*, 352–357. [CrossRef]
456. Young, L.Y.; Hull, C.M.; Heitman, J. Disruption of ergosterol biosynthesis confers resistance to amphotericin B in *Candida lusitaniae*. *Antimicrob. Agents Chemother.* **2003**, *47*, 2717–2724. [CrossRef]
457. Aloia, R.C.; Jensen, F.C.; Curtain, C.C.; Mobley, P.W.; Gordon, L.M. Lipid composition and fluidity of the human immunodeficiency virus. *Proc. Natl. Acad. Sci. USA* **1988**, *85*, 900–904. [CrossRef]
458. Kalvodova, L.; Sampaio, J.L.; Cordo, S.; Ejsing, C.S.; Shevchenko, A.; Simons, K. The lipidomes of vesicular stomatitis virus, semliki forest virus, and the host plasma membrane analyzed by quantitative shotgun mass spectrometry. *J. Virol.* **2009**, *83*, 7996–8003. [CrossRef]
459. Merz, A.; Long, G.; Hiet, M.S.; Brügger, B.; Chlanda, P.; Andre, P.; Wieland, F.; Krijnse-Locker, J.; Bartenschlager, R. Biochemical and morphological properties of hepatitis C virus particles and determination of their lipidome. *J. Biol. Chem.* **2011**, *286*, 3018–3032. [CrossRef]
460. Gerl, M.J.; Sampaio, J.L.; Urban, S.; Kalvodova, L.; Verbavatz, J.M.; Binnington, B.; Lindemann, D.; Lingwood, C.A.; Shevchenko, A.; Schroeder, C.; et al. Quantitative analysis of the lipidomes of the influenza virus envelope and MDCK cell apical membrane. *J. Cell Biol.* **2012**, *196*, 213–221. [CrossRef]
461. Martín-Acebes, M.A.; Merino-Ramos, T.; Blázquez, A.B.; Casas, J.; Escribano-Romero, E.; Sobrino, F.; Saiz, J.C. The composition of West Nile virus lipid envelope unveils a role of sphingolipid metabolism in flavivirus biogenesis. *J. Virol.* **2014**, *88*, 12041–12054. [CrossRef]
462. Hofmann, S.; Krajewski, M.; Scherer, C.; Scholz, V.; Mordhorst, V.; Truschow, P.; Schöbel, A.; Reimer, R.; Schwudke, D.; Herker, E. Complex lipid metabolic remodeling is required for efficient hepatitis C virus replication. *Biochim. Biophys. Acta Mol. Cell Biol. Lipids* **2018**, *1863*, 1041–1056. [CrossRef] [PubMed]
463. Martín-Acebes, M.A.; Vázquez-Calvo, Á.; Saiz, J.C. Lipids and flaviviruses, present and future perspectives for the control of dengue, Zika, and West Nile viruses. *Prog. Lipid Res.* **2016**, *64*, 123–137. [CrossRef] [PubMed]
464. Mariewskaya, K.A.; Tyurin, A.P.; Chistov, A.A.; Korshun, V.A.; Alferova, V.A.; Ustinov, A.V. Photosensitizing Antivirals. *Molecules* **2021**, *26*, 3971. [CrossRef]
465. Mariewskaya, K.A.; Krasilnikov, M.S.; Korshun, V.A.; Ustinov, A.V.; Alferova, V.A. Near-Infrared Dyes: Towards Broad-Spectrum Antivirals. *Int. J. Mol. Sci.* **2022**, *24*, 188. [CrossRef] [PubMed]
466. Schinazi, R.F.; Chu, C.K.; Babu, J.R.; Oswald, B.J.; Saalmann, V.; Cannon, D.L.; Eriksson, B.F.; Nasr, M. Anthraquinones as a new class of antiviral agents against human immunodeficiency virus. *Antivir. Res.* **1990**, *13*, 265–272. [CrossRef]
467. Tang, J.; Colacino, J.M.; Larsen, S.H.; Spitzer, W. Virucidal activity of hypericin against enveloped and non-enveloped DNA and RNA viruses. *Antivir. Res.* **1990**, *13*, 313–325. [CrossRef]
468. Kraus, G.A.; Pratt, D.; Tossberg, J.; Carpenter, S. Antiretroviral activity of synthetic hypericin and related analogs. *Biochem. Biophys. Res. Commun.* **1990**, *172*, 149–153. [CrossRef]
469. Hudson, J.B.; Imperial, V.; Haugland, R.P.; Diwu, Z. Antiviral activities of photoactive perylenequinones. *Photochem. Photobiol.* **1997**, *65*, 352–354. [CrossRef]
470. Andersen, D.O.; Weber, N.D.; Wood, S.G.; Hughes, B.G.; Murray, B.K.; North, J.A. In vitro virucidal activity of selected anthraquinones and anthraquinone derivatives. *Antivir. Res.* **1991**, *16*, 185–196. [CrossRef]
471. Hudson, J.B.; Lopez-Bazzocchi, I.; Towers, G.H. Antiviral activities of hypericin. *Antivir. Res.* **1991**, *15*, 101–112. [CrossRef]
472. Cohen, P.A.; Hudson, J.B.; Towers, G.H. Antiviral activities of anthraquinones, bianthrones and hypericin derivatives from lichens. *Experientia* **1996**, *52*, 180–183. [CrossRef]
473. Hudson, J.B.; Delaey, E.; de Witte, P.A. Bromohypericins Are Potent Photoactive Antiviral Agents. *Photochem. Photobiol.* **1999**, *70*, 820–822. [CrossRef]

474. Laille, M.; Gerald, F.; Debitus, C. In vitro antiviral activity on dengue virus of marine natural products. *Cell. Mol. Life Sci.* **1998**, *54*, 167–170. [CrossRef]
475. Laurent, D.; Baumann, F.; Benoit, A.G.; Mortelecqe, A.; Nitatpattana, N.; Desvignes, I.; Debitus, C.; Laille, M.; Gonzalez, J.P.; Chungue, E. Structure-activity relationships of dengue antiviral polycyclic quinones. *Southeast Asian J. Trop. Med. Public Health* **2005**, *36*, 901–905.
476. Hudson, J.B.; Zhou, J.; Chen, J.; Harris, L.; Yip, L.; Towers, G.H. Hypocrellin, from *Hypocrella bambuase*, is phototoxic to human immunodeficiency virus. *Photochem. Photobiol.* **1994**, *60*, 253–255. [CrossRef]
477. Hirayama, J.; Ikebuchi, K.; Abe, H.; Kwon, K.W.; Ohnishi, Y.; Horiuchi, M.; Shinagawa, M.; Ikuta, K.; Kamo, N.; Sekiguchi, S. Photoinactivation of virus infectivity by hypocrellin A. *Photochem. Photobiol.* **1997**, *66*, 697–700. [CrossRef]
478. Sun, Y.; Chen, Y.L.; Xu, C.P.; Gao, J.; Feng, Y.; Wu, Q.F. Disinfection of influenza a viruses by Hypocrellin a-mediated photodynamic inactivation. *Photodiagnosis Photodyn. Ther.* **2023**, *43*, 103674. [CrossRef]
479. St Vincent, M.R.; Colpitts, C.C.; Ustinov, A.V.; Muqadas, M.; Joyce, M.A.; Barsby, N.L.; Epand, R.F.; Epand, R.M.; Khramyshev, S.A.; Valueva, O.A.; et al. Rigid amphipathic fusion inhibitors, small molecule antiviral compounds against enveloped viruses. *Proc. Natl. Acad. Sci. USA* **2010**, *107*, 17339–17344. [CrossRef]
480. Colpitts, C.C.; Ustinov, A.V.; Epand, R.F.; Epand, R.M.; Korshun, V.A.; Schang, L.M. 5-(Perylen-3-yl)ethynyl-arabino-uridine (aUY11), an arabino-based rigid amphipathic fusion inhibitor, targets virion envelope lipids to inhibit fusion of influenza virus, hepatitis C virus, and other enveloped viruses. *J. Virol.* **2013**, *87*, 3640–3654. [CrossRef]
481. Speerstra, S.; Chistov, A.A.; Proskurin, G.V.; Aralov, A.V.; Ulashchik, E.A.; Streshnev, P.P.; Shmanai, V.V.; Korshun, V.A.; Schang, L.M. Antivirals acting on viral envelopes via biophysical mechanisms of action. *Antivir. Res.* **2018**, *149*, 164–173. [CrossRef] [PubMed]
482. Vigant, F.; Hollmann, A.; Lee, J.; Santos, N.C.; Jung, M.E.; Lee, B. The rigid amphipathic fusion inhibitor dUY11 acts through photosensitization of viruses. *J. Virol.* **2014**, *88*, 1849–1853. [CrossRef]
483. Orlov, A.A.; Chistov, A.A.; Kozlovskaya, L.I.; Ustinov, A.V.; Korshun, V.A.; Karganova, G.G.; Osolodkin, D.I. Rigid amphipathic nucleosides suppress reproduction of the tick-borne encephalitis virus. *Med. Chem. Commun.* **2016**, *7*, 495–499. [CrossRef]
484. Chistov, A.A.; Chumakov, S.P.; Mikhnovets, I.E.; Nikitin, T.D.; Slesarchuk, N.A.; Uvarova, V.I.; Rubekina, A.A.; Nikolaeva, Y.V.; Radchenko, E.V.; Khvatov, E.V.; et al. 5-(Perylen-3-ylethynyl)uracil as an antiviral scaffold: Potent suppression of enveloped virus reproduction by 3-methyl derivatives In vitro. *Antivir. Res.* **2023**, *209*, 105508. [CrossRef]
485. Hakobyan, A.; Galindo, I.; Nañez, A.; Arabyan, E.; Karalyan, Z.; Chistov, A.A.; Streshnev, P.P.; Korshun, V.A.; Alonso, C.; Zakaryan, H. Rigid amphipathic fusion inhibitors demonstrate antiviral activity against African swine fever virus. *J. Gen. Virol.* **2018**, *99*, 148–156. [CrossRef] [PubMed]
486. Wiehe, A.; O'Brien, J.M.; Senge, M.O. Trends and targets in antiviral phototherapy. *Photochem. Photobiol. Sci.* **2019**, *18*, 2565–2612. [CrossRef] [PubMed]
487. Straková, P.; Bednář, P.; Kotouček, J.; Holoubek, J.; Fořtová, A.; Svoboda, P.; Štefánik, M.; Huvarová, I.; Šimečková, P.; Mašek, J.; et al. Antiviral activity of singlet oxygen-photogenerating perylene compounds against SARS-CoV-2: Interaction with the viral envelope and photodynamic virion inactivation. *Virus Res.* **2023**, *334*, 199158. [CrossRef]
488. Chistov, A.A.; Orlov, A.A.; Streshnev, P.P.; Slesarchuk, N.A.; Aparin, I.O.; Rathi, B.; Brylev, V.A.; Kutyakov, S.V.; Mikhura, I.V.; Ustinov, A.V.; et al. Compounds based on 5-(perylen-3-ylethynyl)uracil scaffold: High activity against tick-borne encephalitis virus and non-specific activity against enterovirus A. *Eur. J. Med. Chem.* **2019**, *171*, 93–103. [CrossRef]
489. Mariewskaya, K.A.; Gvozdev, D.A.; Chistov, A.A.; Straková, P.; Huvarová, I.; Svoboda, P.; Kotouček, J.; Ivanov, N.M.; Krasilnikov, M.S.; Zhitlov, M.Y.; et al. Membrane-Targeting Perylenylethynylphenols Inactivate Medically Important Coronaviruses via the Singlet Oxygen Photogeneration Mechanism. *Molecules* **2023**, *28*, 6278. [CrossRef]
490. Carpenter, B.L.; Situ, X.; Scholle, F.; Bartelmess, J.; Weare, W.W.; Ghiladi, R.A. Antiviral, Antifungal and Antibacterial Activities of a BODIPY-Based Photosensitizer. *Molecules* **2015**, *20*, 10604–10621. [CrossRef]
491. Wolf, M.C.; Freiberg, A.N.; Zhang, T.; Akyol-Ataman, Z.; Grock, A.; Hong, P.W.; Li, J.; Watson, N.F.; Fang, A.Q.; Aguilar, H.C.; et al. A broad-spectrum antiviral targeting entry of enveloped viruses. *Proc. Natl. Acad. Sci. USA* **2010**, *107*, 3157–3162. [CrossRef]
492. Vigant, F.; Lee, J.; Hollmann, A.; Tanner, L.B.; Akyol Ataman, Z.; Yun, T.; Shui, G.; Aguilar, H.C.; Zhang, D.; Meriwether, D.; et al. A mechanistic paradigm for broad-spectrum antivirals that target virus-cell fusion. *PLoS Pathog.* **2013**, *9*, e1003297. [CrossRef]
493. Hollmann, A.; Gonçalves, S.; Augusto, M.T.; Castanho, M.A.; Lee, B.; Santos, N.C. Effects of singlet oxygen generated by a broad-spectrum viral fusion inhibitor on membrane nanoarchitecture. *Nanomedicine* **2015**, *11*, 1163–1167. [CrossRef]
494. Arnaut, Z.A.; Pinto, S.M.A.; Aroso, R.T.; Amorim, A.S.; Lobo, C.S.; Schaberle, F.A.; Pereira, D.; Núñez, J.; Nunes, S.C.C.; Pais, A.A.C.C.; et al. Selective, broad-spectrum antiviral photodynamic disinfection with dicationic imidazolyl chlorin photosensitizers. *Photochem. Photobiol. Sci.* **2023**, *22*, 2607–2620. [CrossRef] [PubMed]
495. Jurak, I.; Cokarić Brdovčak, M.; Djaković, L.; Bertović, I.; Knežević, K.; Lončarić, M.; Jurak Begonja, A.; Malatesti, N. Photodynamic Inhibition of Herpes Simplex Virus 1 Infection by Tricationic Amphiphilic Porphyrin with a Long Alkyl Chain. *Pharmaceutics* **2023**, *15*, 956. [CrossRef]
496. Monjo, A.L.; Pringle, E.S.; Thornbury, M.; Duguay, B.A.; Monro, S.M.A.; Hetu, M.; Knight, D.; Cameron, C.G.; McFarland, S.A.; McCormick, C. Photodynamic Inactivation of Herpes Simplex Viruses. *Viruses* **2018**, *10*, 532. [CrossRef] [PubMed]

497. Meunier, T.; Desmarets, L.; Bordage, S.; Bamba, M.; Hervouet, K.; Rouillé, Y.; François, N.; Decossas, M.; Sencio, V.; Trottein, F.; et al. A Photoactivable Natural Product with Broad Antiviral Activity against Enveloped Viruses, Including Highly Pathogenic Coronaviruses. *Antimicrob. Agents Chemother.* **2022**, *66*, e0158121. [CrossRef] [PubMed]
498. Nikolayeva, Y.V.; Ulashchik, E.A.; Chekerda, E.V.; Galochkina, A.V.; Slesarchuk, N.A.; Chistov, A.A.; Nikitin, T.D.; Korshun, V.A.; Shmanai, V.V.; Ustinov, A.V.; et al. 5-(Perylen-3-ylethynyl)uracil Derivatives Inhibit Reproduction of Respiratory Viruses. *Russ. J. Bioorg. Chem.* **2020**, *46*, 315–320. [CrossRef] [PubMed]
499. Proskurin, G.V.; Orlov, A.A.; Brylev, V.A.; Kozlovskaya, L.I.; Chistov, A.A.; Karganova, G.G.; Palyulin, V.A.; Osolodkin, D.I.; Korshun, V.A.; Aralov, A.V. 3′-O-Substituted 5-(perylen-3-ylethynyl)-2′-deoxyuridines as tick-borne encephalitis virus reproduction inhibitors. *Eur. J. Med. Chem.* **2018**, *155*, 77–83. [CrossRef]
500. Weil, T.; Groß, R.; Röcker, A.; Bravo-Rodriguez, K.; Heid, C.; Sowislok, A.; Le, M.H.; Erwin, N.; Dwivedi, M.; Bart, S.M.; et al. Supramolecular Mechanism of Viral Envelope Disruption by Molecular Tweezers. *J. Am. Chem. Soc.* **2020**, *142*, 17024–17038. [CrossRef]
501. Lump, E.; Castellano, L.M.; Meier, C.; Seeliger, J.; Erwin, N.; Sperlich, B.; Stürzel, C.M.; Usmani, S.; Hammond, R.M.; von Einem, J.; et al. A molecular tweezer antagonizes seminal amyloids and HIV infection. *Elife* **2015**, *4*, e05397. [CrossRef]
502. Röcker, A.E.; Müller, J.A.; Dietzel, E.; Harms, M.; Krüger, F.; Heid, C.; Sowislok, A.; Riber, C.F.; Kupke, A.; Lippold, S.; et al. The molecular tweezer CLR01 inhibits Ebola and Zika virus infection. *Antivir. Res.* **2018**, *152*, 26–35. [CrossRef] [PubMed]
503. Weil, T.; Kirupakaran, A.; Le, M.H.; Rebmann, P.; Mieres-Perez, J.; Issmail, L.; Conzelmann, C.; Müller, J.A.; Rauch, L.; Gilg, A.; et al. Advanced Molecular Tweezers with Lipid Anchors against SARS-CoV-2 and Other Respiratory Viruses. *JACS Au* **2022**, *2*, 2187–2202. [CrossRef]
504. Wang, G.; Watson, K.M.; Buckheit, R.W., Jr. Anti-human immunodeficiency virus type 1 activities of antimicrobial peptides derived from human and bovine cathelicidins. *Antimicrob. Agents Chemother.* **2008**, *52*, 3438–3440. [CrossRef]
505. Kagan, B.L.; Ganz, T.; Lehrer, R.I. Defensins: A family of antimicrobial and cytotoxic peptides. *Toxicology* **1994**, *87*, 131–149. [CrossRef] [PubMed]
506. Liu, R.; Liu, Z.; Peng, H.; Lv, Y.; Feng, Y.; Kang, J.; Lu, N.; Ma, R.; Hou, S.; Sun, W.; et al. Bomidin: An Optimized Antimicrobial Peptide with Broad Antiviral Activity Against Enveloped Viruses. *Front. Immunol.* **2022**, *13*, 851642. [CrossRef] [PubMed]
507. Omer, A.A.M.; Hinkula, J.; Tran, P.T.; Melik, W.; Zattarin, E.; Aili, D.; Selegård, R.; Bengtsson, T.; Khalaf, H. Plantaricin NC8 αβ rapidly and efficiently inhibits flaviviruses and SARS-CoV-2 by disrupting their envelopes. *PLoS ONE* **2022**, *17*, e0278419. [CrossRef] [PubMed]
508. Henriques, S.T.; Huang, Y.H.; Rosengren, K.J.; Franquelim, H.G.; Carvalho, F.A.; Johnson, A.; Sonza, S.; Tachedjian, G.; Castanho, M.A.; Daly, N.L.; et al. Decoding the membrane activity of the cyclotide kalata B1: The importance of phosphatidylethanolamine phospholipids and lipid organization on hemolytic and anti-HIV activities. *J. Biol. Chem.* **2011**, *286*, 24231–24241. [CrossRef]
509. Kozlov, M.M.; Leikin, S.L.; Chernomordik, L.V.; Markin, V.S.; Chizmadzhev, Y.A. Stalk mechanism of vesicle fusion. Intermixing of aqueous contents. *Eur. Biophys. J.* **1989**, *17*, 121–129. [CrossRef]
510. Cooke, I.R.; Deserno, M. Coupling between lipid shape and membrane curvature. *Biophys. J.* **2006**, *91*, 487–495. [CrossRef]
511. Miao, L.; Stafford, A.; Nir, S.; Turco, S.J.; Flanagan, T.D.; Epand, R.M. Potent inhibition of viral fusion by the lipophosphoglycan of Leishmania donovani. *Biochemistry* **1995**, *34*, 4676–4683. [CrossRef] [PubMed]
512. Rasmusson, B.J.; Flanagan, T.D.; Turco, S.J.; Epand, R.M.; Petersen, N.O. Fusion of Sendai virus and individual host cells and inhibition of fusion by lipophosphoglycan measured with image correlation spectroscopy. *Biochim. Biophys. Acta* **1998**, *1404*, 338–352. [CrossRef] [PubMed]
513. Sardar, A.; Lahiri, A.; Kamble, M.; Mallick, A.I.; Tarafdar, P.K. Translation of Mycobacterium Survival Strategy to Develop a Lipo-peptide based Fusion Inhibitor. *Angew. Chem. Int. Ed. Engl.* **2021**, *60*, 6101–6106. [CrossRef] [PubMed]
514. Yuan, L.; Zhang, S.; Wang, Y.; Li, Y.; Wang, X.; Yang, Q. Surfactin Inhibits Membrane Fusion during Invasion of Epithelial Cells by Enveloped Viruses. *J. Virol.* **2018**, *92*, e00809-18. [CrossRef]
515. Kracht, M.; Rokos, H.; Ozel, M.; Kowall, M.; Pauli, G.; Vater, J. Antiviral and hemolytic activities of surfactin isoforms and their methyl ester derivatives. *J. Antibiot.* **1999**, *52*, 613–619. [CrossRef]
516. Shekunov, E.V.; Zlodeeva, P.D.; Efimova, S.S.; Muryleva, A.A.; Zarubaev, V.V.; Slita, A.V.; Ostroumova, O.S. Cyclic lipopeptides as membrane fusion inhibitors against SARS-CoV-2: New tricks for old dogs. *Antivir. Res.* **2023**, *212*, 105575. [CrossRef]
517. Shekunov, E.V.; Efimova, S.S.; Yudintceva, N.M.; Muryleva, A.A.; Zarubaev, V.V.; Slita, A.V.; Ostroumova, O.S. Plant Alkaloids Inhibit Membrane Fusion Mediated by Calcium and Fragments of MERS-CoV and SARS-CoV/SARS-CoV-2 Fusion Peptides. *Biomedicines* **2021**, *9*, 1434. [CrossRef]